UNIVERSIDADE NOVA DE LISBOA

Faculdade de Ciências e Tecnologia

Departamento de Física

Modulation of electrical stimulation applied to human physiology and clinical diagnostic

Tiago Sérgio Santos Rodrigues Araújo

Thesis submitted in the fulfillment of the requirements for the Degree of Doctor in Biomedical Engineering, under the scientific guidance of Professor Hugo Gamboa.

June, 2015

Modulation of electrical stimulation applied to human physiology and clinical diagnostic

To my parents: For your unconditional love.
To my godson Martim: As today your personality inspires me, I hope that one day this work inspires you.

Acknowledgements

The course of events for pursuing my PhD degree allowed truly meaningful academic, professional and personal growth. During this learning experience, I had the opportunity to count on exceptional people, who deserve my profound acknowledgment for their active collaboration and constant support. In the following lines I express my gratitude to some people that made all of this possible.

My first acknowledgment words go to my academic supervisor Professor Hugo Gamboa for his guidance, support and friendship. I also thank him for giving me intellectual freedom in this exploratory process and inspiration to move forward. Thank you for showing me the path for rigor, clarity, motivation and, above all, the ability to question. These last years under your guidance gave me tools, virtues and capabilities that I will use for the rest of my life.

My second word of acknowledgment goes to Professor Alberto Cliquet, my internship coordinator at UNICAMP - Brasil. Thank you for being kind enough to welcome me with open arms and also provide the most intense research experience that I had. Thank you for the wisdom, the friendship and the sense of contribution that you always passed me. Working with the patients from *Laboratório de Marcha e Reabilitação do Aparelho Locomotor, Hospital de Clinicas, UNICAMP*, was the most enriching process of this PhD. Although thinking that I would transmit strength and motivation to highly disabled people, it was them who gave me all the motivation and strength to follow my way. To all of them a big thank you. I also thank my co-workers from the rehabilitation wing, namely Karina, Elize (she was tireless with me!), Carolina, Janaina and Paola.

I thank Professor Pedro Costa from FCM-UNL with whom I spent several work hours and had long discussions that gave me solid bases on human electrophysiology, supporting this work. I equally thank Professor Ana Fred from IST and Professor Paulo Armada from FMH, with whom I developed two important curricular components of this PhD.

A thank you to Professor Pedro Mil-Homens, from FMH, for the prompt availability of a laboratory and the Biodex system, without which the study described in Chapter 7 would not be possible, and for the external accompaniment to my doctoral course. I also equally thank Professor Mamede de Carvalho, FML-UL, who promoted and followed the study depicted in Chapter 6 of this document and the validation study of the electrical stimulator device.

I acknowledge Professor Adelaide Jesus, coordinator of the doctoral plan, for the quick and efficient answer given to all necessary components and also for the critic inputs to

this work.

To the funding sources that allowed me the financial support necessary to the accomplishment of this project: Fundação para a Ciência e Tecnologia, PLUX - Wireless Biosignals, S.A. and FCT-UNL- CEFITEC.

I thank Plux - Wireless Biosignals, S.A., the company that welcomed me during most of my PhD, that fully funded the technical developments necessary and that provided me a deep professional enrichment in varied areas. Plux is the people that work there and because of that I thank all collaborators in general with relevance to those who actively helped me in the developments. To Filipe Silva, working with him is a unique experience because of his technological knowledge and logic reasoning well above average. I will always look to each and every teaching and time-sharing moment with fascination. When no one else knows how to solve it, he will! I also thank Fernando Cardoso and Filipe Carvalho who accompanied my hardware developments. A special thanks to Paulo Aires and Dário Bento, great friends, and that besides all the technical support knew how to rejoice every day, every hour. And what is life without joy?

Thanks also to my friends, Nuno Santos, Nídia Batista, Madalena Serra, Carina Morais, Ana Raquel and David Pires for the excellent inputs they gave to this thesis.

To all my master students that I had the pleasure to coordinate and also my students from Applied Electronics. I taught to learn and learned from teaching.

To my dear friends: Rogério Rocha, Eliana Rocha for their constant presence, care, help, assertiveness and motivation and for the "two little things" that they put in this world that I love from the deep of my heart, Gonçalo and Martim, for all the fun, hugs and affection. To Padre Jorge for the spiritual purity that you provide me. To Carlos Amorim and Daniele Pereira, Daniel Garrudo, João Fonseca, Luís Galvão, Pedro Benvindo, João Mendes, you are family to me =).

To my Mom and Dad for their unconditional love. The good things that I do in my life is with you and for you. I love you more than anything. To them and to my godson Martim I dedicate this work.

My last word and my biggest thank you goes to my best friend, Neuza Nunes, she was a partner, a friend and an excellent co-worker. Because you execute when I think but cannot translate into words, because you solve when I block, because you guide when I am adrift, because you could write the whole world in Python code! Because we make a powerful team and you motivated me when nothing would... Working with you on a daily basis and overcome all the technical, scientific, mathematical and all other challenges was deeply rewarding... Your mind is brilliant and fascinating. My biggest thank you!!!!

"The two most important days in your life are the day you are born and the day you find out why." - Mark Twain

ABSTRACT

The use, manipulation and application of electrical currents, as a controlled interference mechanism in the human body system, is currently a strong source of motivation to researchers in areas such as clinical, sports, neuroscience, amongst others. In electrical stimulation (ES), the current applied to tissue is traditionally controlled concerning stimulation amplitude, frequency and pulse-width. The main drawbacks of the transcutaneous ES are the rapid fatigue induction and the high discomfort induced by the non-selective activation of nervous fibers.

There are, however, electrophysiological parameters whose response, like the response to different stimulation waveforms, polarity or a personalized charge control, is still unknown. The study of the following questions is of great importance:

- What is the physiological effect of the electric pulse parametrization concerning charge, waveform and polarity? Does the effect change with the clinical condition of the subjects?
- The parametrization influence on muscle recruitment can retard fatigue onset?
- Can parametrization enable fiber selectivity, optimizing the motor fibers recruitment rather than the nervous fibers, reducing contraction discomfort?

Current hardware solutions lack flexibility at the level of stimulation control and physiological response assessment. To answer these questions, a miniaturized, portable and wireless controlled device with ES functions and full integration with a generic biosignals acquisition platform has been created. Hardware was also developed to provide complete freedom for controlling the applied current with respect to the waveform, polarity, frequency, amplitude, pulse-width and duration.

The impact of the methodologies developed is successfully applied and evaluated in the contexts of fundamental electrophysiology, psycho-motor rehabilitation and neuromuscular disorders diagnosis.

This PhD project was carried out in the Physics Department of Faculty of Sciences and Technology (FCT-UNL), in straight collaboration with PLUX - Wireless Biosignals S.A. company and co-funded by the Foundation for Science and Technology.

Keywords: Electrical Stimulator, Neuromuscular Electrical Stimulation (NMES), Peripheral Nerve Stimulation (PNS), Functional Electrical Stimulation (FES), Single Pulse Waveform, Single Pulse Charge, Excitability, Human Electrophysiology.

RESUMO

O uso, manipulação e aplicação de correntes eléctricas no corpo humano como um mecanismo de interferência controlado motiva, actualmente, um grande número de investigadores do contexto clínico, desportivo, das neurociências, entre muitos outros. A corrente aplicada no tecido é tradicionalmente controlada ao nível da frequência, amplitude e largura de pulso. Os maiores inconvenientes da estimulação eléctrica transcutânea residem numa rápida indução de fadiga muscular e elevada activação de fibras de dor.

Existem, no entanto, parâmetros cuja resposta electrofisiológica é pouco abordada, como a forma de onda do estímulo eléctrico, a polaridade e a carga total do impulso, tornando-se relevante o levantamento das seguintes questões:

- Qual o efeito fisiológico da parameterização do estímulo eléctrico ao nível da forma de onda, carga e polaridade? Esse efeito difere com a condição clínica do sujeito?
- A influência que a parameterização do estímulo eléctrico provoca no recrutamento muscular pode retardar o efeito de fadiga?
- Poderá a parameterização possibilitar uma selectividade das fibras activadas, optimizando o recrutamento das fibras motoras e consequentemente reduzindo o disconforto de contracção?

As soluções de hardware disponíveis actualmente para estimulação eléctrica são pouco flexíveis e deficitárias no âmbito da investigação. Para dar resposta a estas questões, foi desenvolvido um dispositivo miniaturizado, portátil e wireless com funções de electroestimulação e de sincronização com dispositivo genérico de aquisição de biossinais. O hardware foi desenvolvido visando a total liberdade no controlo da corrente aplicada tendo em consideração a forma de onda, polaridade, frequência, amplitude, largura de pulso e duração.

O impacto das soluções desenvolvidas foi avaliado no contexto da electrofisiologia geral e em contexto clínico, especificamente, na reabilitação psicomotora e no diagnóstico de patologias neuromusculares.

Este projecto de doutoramento foi inserido no Departamento de Física da Faculdade de Ciências e Tecnologia (FCT-UNL), em colaboração com a empresa PLUX – Wireless Biosignals S.A. e co-financiado pela Fundação para a Ciência e Tecnologia.

Palavras-chave: Electrostimulador, Estimulação muscular, Estimulação do nervo periférico, Electroestimulação funcional, Excitabilidade, Forma de onda, Electrofisiologia Humana.

Contents

Contents **xv**

List of Figures **xix**

List of Tables **xxiii**

1 Motivation **1**
1.1 State-of-the-Art 1
1.2 Questions and Goals 4
1.3 Thesis Structure 6

2 Background **9**
2.1 Electrophysiology Principles 9
2.1.1 Resting potential 9
2.1.2 Action potential 10
2.1.3 The nerve cell as a conductor 11
2.2 Electrical Stimulation Principles 12
2.2.1 Historical context 14
2.2.2 Excitability 15
2.2.3 Stimulation parameters and physiological impact 16
2.3 Application of current 21
2.3.1 Current Types 21
2.3.2 Transcutaneous stimulation electrodes 22
2.3.3 Electrode Placement 22
2.4 Electrical Stimulation Circuits 23
2.4.1 Micro-controller 24
2.4.2 High Voltage 24
2.4.3 Regulation Mode 25
2.4.4 Stimulation Steering 26

3 Proposed Solution **29**
3.1 Requirements 29
3.1.1 Functional and Technical Requirements 29
3.1.2 Usability Requirements 32

3.1.3 Safety Requirements . . . 32
3.1.4 Software Requirements . . . 32
3.2 Hardware . . . 33
3.2.1 Microcontroller . . . 34
3.2.2 Power . . . 41
3.2.3 High Voltage . . . 43
3.2.4 User interface . . . 44
3.2.5 Current drive . . . 44
3.2.6 Digital port . . . 46
3.2.7 Application interface . . . 47
3.3 Electrical stimulator device . . . 48
3.3.1 Printed Circuit Board . . . 49
3.3.2 Box Enclosure . . . 49
3.3.3 The Product . . . 50
3.4 Software . . . 51
3.4.1 API . . . 52
3.4.2 Interfaces . . . 54

4 Validation **57**
4.1 Device Tests . . . 57
4.1.1 Characterization Tests . . . 57
4.1.2 Production Tests . . . 60
4.2 Scientific Validation . . . 61
4.2.1 Nerve Regeneration on Rat . . . 61
4.2.2 Instrumentation . . . 62
4.2.3 Control Interface . . . 63
4.2.4 Protocol . . . 63
4.2.5 Outcomes . . . 65
4.2.6 Real-time stimulation impact on the ANS . . . 66

5 Application to Neuroplasticity of Tetraplegic Subjects **73**
5.1 Introduction . . . 73
5.2 Methods . . . 74
5.2.1 Subjects . . . 74
5.2.2 Procedure . . . 75
5.2.3 Data analysis . . . 76
5.3 Results . . . 77
5.4 Discussion . . . 81

6 Application to the Waveform Control on CMAP Scan **85**
6.1 Introduction . . . 85
6.2 Methods . . . 87

6.2.1 Subjects . . . 87
6.2.2 Instrumentation . . . 87
6.2.3 Stimulation and acquisition . . . 87
6.2.4 Processing . . . 89
6.3 Results and Discussion . . . 89

7 Application to the Waveform Effect on Fatigue and Comfort 95
7.1 Introduction . . . 95
7.2 Methods . . . 96
7.2.1 Subjects . . . 96
7.2.2 Instrumentation . . . 96
7.2.3 Protocol . . . 98
7.2.4 Data analysis . . . 101
7.3 Results . . . 102
7.4 Discussion . . . 103

8 Conclusions 105
8.1 Overall Results . . . 105
8.2 Contributions . . . 108
8.3 Future Work . . . 111

A List of Publications 113
A.1 Book Chapters . . . 113
A.2 Journal Papers . . . 113
A.3 Conference Proceedings . . . 114
A.4 Oral Communications . . . 115

B Tools 117
B.1 Stimulator Development . . . 117
B.2 Scientific Computation . . . 117
B.3 Thesis Document . . . 118

C Brochure 119

D Test Protocol 121

E Classification of Spinal Cord Injury 127

Bibliography 131

List of Figures

1.1 Illustration of the rehabilitation process through the reeducation of nerve fibers. 2
1.2 Illustration of the scientific and methodological alignment of this work. The scientific questions, the methodological solution and the studies implemented envisioning the answer of those questions. 5
1.3 Thesis structure. 6

2.1 Membrane potential and respective polarity. 10
2.2 Representation of an action potential and excitability threshold. 11
2.3 Diffusion of sodium and potassium 11
2.4 Propagation of the potential and conditioning factors at a fixed time instant. . 13
2.5 Electric model of the cellular membrane by Hodgkin and Huxley. 14
2.6 The strength-duration curve for current, energy and charge of an excitable tissue. 16
2.7 Amplitude and period of a wave. 17
2.8 Strength-Duration curves: Relation between amplitude and pulse-width when relating with the influence on excitability thresholds. 18
2.9 Relation between the pulse-width applied and the accommodation of the nervous fiber. 18
2.10 Muscular strength variation with the stimulus frequency, for stimulation intensities above the motor limit. 19
2.11 Examples of electric pulses with different polarities and waveforms. 20
2.12 Comparison of stimulation waveforms for their ability to generate low threshold stimulation, low corrosion, and low tissue damage. 20
2.13 Electrodes configuration. 23
2.14 Generic configuration of the state of the art stimulators. The Regulation Mode and Stimulation Steering blocks define the Output Stage of the electrical stimulator. 24
2.15 Step-up converter or Boost converter. 25
2.16 Output stage for a constant current stimulator with a voltage controllable current source. 26
2.17 Output stage for constant current stimulator with two high voltages sources and two Wilson current mirrors. 27

2.18 Representation of a typical current steering output stage. 28

3.1 Overview of the hardware architecture. 33
3.2 Overview of the modules for the whole system and correspondent data flow inputs/outputs for the microcontroller. 34
3.3 The three main memory types and its structure on the device. 35
3.4 Structure of the application code. 37
3.5 Illustration of the UART interrupts divided into received or sent commands. . 39
3.6 Illustration of the power module architecture. 42
3.7 Illustration of the high voltage module architecture. 43
3.8 Device button turned off and with green and red LED turned on. 44
3.9 Illustration of the current drive module architecture. 45
3.10 Representation scheme of the acquisition and stimulation system, with synchronization cable. 47
3.11 Illustration of the development cycle of the final solution, composed by three main development classes: hardware design, implementation and miniaturization on PCB and final box enclosure. 48
3.12 Illustration of the PCB version v1.1. 49
3.13 Box assembly illustration of the stimulator 50
3.14 Accessories for a) nerve stimulation; b) muscle stimulation. 50
3.15 Photograph of the final electrical stimulation device and summary of specifications. 51
3.16 Integrated API for biosignals acquisition and control of the stimulator. 52
3.17 Illustration of the system communication and control flexibility. 54
3.18 Diagram representing the standard communication flow (from configure to control) 55
3.19 Examples of waves that can be drawn and stored in the device. 56

4.1 Example of a test point in the device's PCB. The TP circles represent the Test Points of the circuit. 61
4.2 Illustration of the system used to induce muscle contraction and respective force assessment. 62
4.3 Apparatus for force assessment: a) servomotor; b) pedal; c) load cell; d) rotation axis; e) optical encoder; f) rat paw attached to pedal; g) invasive electrical stimulation electrode; h) thermal pad. 63
4.4 First layout interface used for real time calibrations and thresholds definition, before application of protocol: a) Computer based layout; b) Android based layout. 64
4.5 Variation of force with stimulation frequency. 65
4.6 Variation of force with ankle angle. 66
4.7 Illustration of the steps followed in the acquisition protocol. 68

4.8 Example of an EDA event and possible extracted parameters. 68
4.9 EDA signals obtained for all subjects. 69
4.10 Example of the BVP signal from one subject during the segment 2 of the acquisition protocol 70

5.1 Illustration of Test 1 and Test 2 stimulation electrodes positioning and respective evaluated muscles through EMG acquisition 75
5.2 Illustrative schematics for the stimulation and acquisition protocol. 76
5.3 Reflexes mean peak-to-peak amplitude in μV (with SD error bars) related to the stimulation intensity for Test 1 and three groups. 78
5.4 Results of ILR elicited with different stimulation intensities for Test 1 in: a) healthy subjects (example from one subject of Control Group); b) SCI subjects (representative example from one subject of Group 1). 79
5.5 Mean values (and SD error bars) for the reflexes latency related to the stimulation charge for: a) Test 1 and b) Test 2. The stimulation charge is complemented by the indication of the mode and intensity of the original electrical pulse. . . 80
5.6 Results of EMG response with different stimulation intensities of the Test 2 from the unique patient that exposed a different rise pattern of ILR latency related to the stimulation charge. 83

6.1 Representations of CMAP scans. A) From an healthy individual. B) From an ALS patient. 86
6.2 Illustration of the equipment used and electrodes placement 87
6.3 Illustrative schematics for the stimulation and acquisition protocol. 88
6.4 Example of the charge equalization of the four different pulse waveforms. Maintaining the amplitude and the area of the pulse, the only variable parameter is the pulse-width, to equalize the charge. 89
6.5 CMAPs acquired in a fixed intensity step for each waveform: 10.5mA. Differences in the waves' amplitude, with the same intensity stimulation, can be observed. 91
6.6 Four CMAP scans generated with four waveforms, for one example subject. . 91

7.1 Subject prepared to be evaluated by the Biodex system and electrical stimulator. Two electrodes are positioned over vastus medialis and on the lateral border of the femoral rectus. The stimulated limb is maintained in isometric conditions. 97
7.2 Illustrative schematics for the MVIC test acquisition protocol. 99
7.3 Illustrative schematics of the acquisition and stimulation protocol defined to determine the amplitude required to elicit 50% of MVIC. 99
7.4 Illustrative schematics of the acquisition and stimulation fatigue protocol. . . 100
7.5 Example of the declining torque of a subject during fatigue test with SQ shape waveform. Vertical lines mark the portion where force was evaluated. The red dot marks the force value extracted on each contraction. 101

7.6 Decline in percentage of the MVIC over repeated contractions for QU, SQ and TR (mean (SD)). No significant differences between QU, SQ and TR ($P > 0.05$). 103

8.1 Illustration of the final scientific and methodological conclusions of this work. The studies implemented, the scientific questions and the answer for those questions. 107

List of Tables

3.1 Functional requirements and the correspondent technical requirements. . . . 31
3.2 The LEDs indication and correspondent device state. 41

4.1 Description, initial condition and expected results of the communication tests. 58
4.2 Description, initial condition and expected results of the battery and charge management tests. 59
4.3 Description, initial condition and expected results of the current parametrization tests. 60
4.4 Mean values and respective standard deviation error for the heart rate (in beats per minute) obtained during segments 1, 2 and 3. 71

5.1 Number of subjects per group that elicited significant reflexes in the three stimulation modes versus the total number of subjects analyzed. 77
5.2 Linear tendency equations and correspondent R^2 of latency vs charge for all groups and tests. 78

6.1 S95 response amplitudes. SQ corresponds to the monophasic square pulse, TR to monophasic triangular pulse, QU to monophasic quadratic pulse and BSQ to the biphasic square pulse. 90
6.2 Mean CMAP scan slope differences between the different types of waveforms. SQ corresponds to the monophasic square pulse, TR to monophasic triangular pulse, QU to monophasic quadratic pulse and BSQ to the biphasic square pulse. 92
6.3 S5 current intensities. SQ corresponds to the monophasic square pulse, TR to monophasic triangular pulse, QU to monophasic quadratic pulse and BSQ to the biphasic square pulse. 92
6.4 Current intensity differences for each waveform relative to the square wave. SQ corresponds to the monophasic square pulse, TR to monophasic triangular pulse, QU to monophasic quadratic pulse and BSQ to the biphasic square pulse. 93

7.1 Summary of stimulation characteristics for 3 waveforms. SQ - Square waveform; TR - Triangular waveform; QU - Quadratic waveform. 97
7.2 Demographic variables (Sex, Age, Body Mass Index (BMI), Dominant leg, Exercise practice) for 3 groups. Group 1: SQ, TR and QU; Group 2: QU, SQ and TR; Group 3: TR, QU and SQ. *Data presented in form of mean (SD). 98

7.3 Mean (SD) amplitude and charge values obtained for all subjects. 102
7.4 Pairwise comparisons amongst waveforms, relative comfort scores. F: Value of ANOVA Friedman test. *Significantly different $p < 0.05$ 103

8.1 Summary of the stimulator features that were a differentiating factor in each scientific study. 109

GLOSSARY

AC Alternating Current.

ACK Acknowledge.

ADC Analog-to-Digital Converter.

AES Advanced Encryption Standard.

ALS Amyotrophic Lateral Sclerosis.

ANS Autonomic Nervous System.

AP Action Potential.

API Application Programming Interface.

ASIA American Spinal Injury Association.

BMI Body Mass Index.

BVP Blood Volume Pulse.

CMAP Compound Muscle Action Potential.

CPU Central Processing Unit.

CRC Cyclic Redundancy Check.

CRNN Continuous Running if No Network.

DAC Digital-to-Analog Converter.

DC Direct Current.

ECG Electrocardiography.

EDA Electrodermal Activity.

EDR Enhanced Data Rate.

EEG Electroencephalography.

EEPROM Electrically-Erasable Programmable Read-Only Memory.

EMG Electromyography.

FES Functional Electrical Stimulation.

GPIO General Purpose Input Output.

GUI Graphical User Interface.

HCI Human Computer Interface.

HR Heart Rate.

HRV Heart Rate Variability.

HV High Voltage.

I2C Inter-Integrated Circuit.

IDE Integrated Development Environment.

ILR Interlimb Reflexes.

JSON JavaScript Object Notation.

LDO Low-dropout Regulator.

LED Light Emitting Diode.

MAC Media Access Control.

MU Motor Unit.

MUAP Motor Unit Action Potential.

MVIC Maximum Voluntary Isometric Contraction.

NMES Neuromuscular Electrical Stimulation.

NOK Not Ok.

NS Next State.

op-amp operational amplifier.

PCB Printed Circuit Board.

PLF Phase Locking Factor.

PMA Progressive Muscular Atrophy.

PWM Pulse Width Modulation.

SCI Spinal Cord Injury.

SDK Software Development Kit.

TTL Transistor-Transistor Logic.

UART Universal Asynchronous Receiver/Transmitter.

VAS Visual Analogue Scale.

CHAPTER 1

MOTIVATION

The human organism can be defined as a system composed by several subsystems: for example the digestive, circulatory, sensory-motor and respiratory systems. Its operation occurs through complex compensation mechanisms managed by the nervous and endocrine system. The actions, transmissions and management of the nervous system pass through, amongst other mechanisms, a communication protocol based on electrical signals. Biosignals such as Electrocardiography (ECG), Electromyography (EMG), Electroencephalography (EEG) and Electrodermal Activity (EDA) represent functional examples of that inter-systematic communication and management. The application of electric currents to the human body as a tool to interfere with this managing system is currently a field of interest and motivation to worldwide investigators.

1.1 State-of-the-Art

Lack of neural innervation due to neurological damage leads to muscles unable to produce force. Investigators have tried to find a way to restore movement and the ability to perform everyday activities using electrical stimulation.

Whether used alone to improve motor impairment or embedded within complex systems to create functional multi-joint movement, electrical stimulation holds great potential in rehabilitation. Figure 1.1 presents an example of an illustrative rehabilitation process with electrical stimulation through the reeducation of nerve fibers.

Surface electrical stimulation is used in many forms to induce and control muscle action and increase performance [147][166]. Currently, the study and application of electrical currents in the human body is of relevance in healthcare, research, fitness and sports.

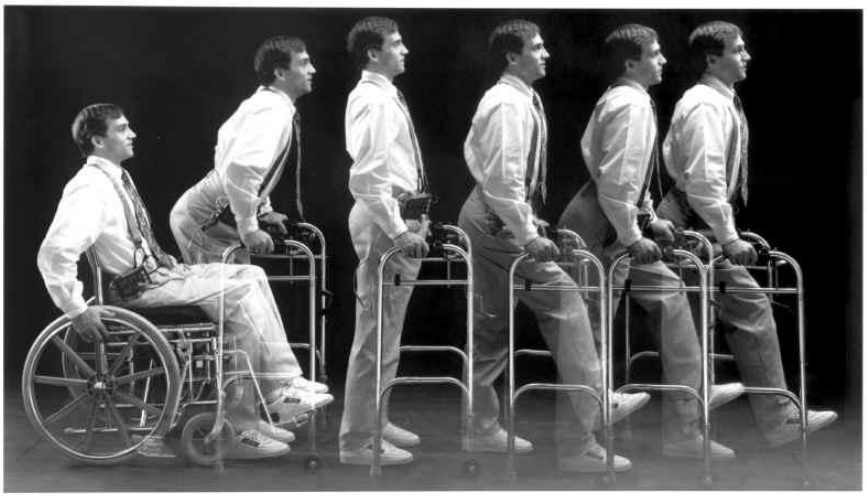

Figure 1.1: Illustration of the rehabilitation process through the reeducation of nerve fibers. Courtesy of Parastep [138].

- *Healthcare*
  In the healthcare context, electrical stimulation is usually associated with: the diagnosis of neuromuscular pathologies (ex: Amyotrophic Lateral Sclerosis (ALS), Progressive Muscular Atrophy (PMA)) [183]; in therapy for wound healing and localized inflammation; treatment of localized neuropathic pain, such as rheumatoid arthritis and lower back pain; to delay the process of inflammation such as tendinitis; and treatment of urinary incontinence and diaphragmatic dysfunction [196]. It can also be used to improve circulation, to increase range of motion and to treat several conditions from sprains, back pain, arthritis, sciatica and scoliosis. Still on the clinical context, it has an important role on the rehabilitation and evaluation of Spinal Cord Injury (SCI) patients. In this field, electric currents are used not only to re-establish functionality or as an assistive method (neuroprotheses), but also as a methodology for muscle spasm relief or clinical condition evaluation [70]. Imaging studies, such as computerized tomography and nuclear magnetic resonance imaging, do not correlate directly to the clinical status of subjects and lack functional information regarding the sometimes subtle recovery of the patients. On the other hand, methodologies that involve somehow the applications of currents in the human tissue and access directly the subject's electrophysiology (Compound Muscle Action Potential (CMAP) scan, Interlimb Reflexes (ILR), EMG), can give detailed information about the clinical condition of the patient [2].

- *Research*:
  Electrical stimulation techniques are a source of motivation for researchers world wide [87][49] and enable several distinct research areas such as bioelectrical impedance [26], neuroscience [123], human electrical physiology studies, the central nervous system, amongst others.

- *Fitness and sports*:
  In this field, the capabilities of strengthening and toning muscles are explored in the context of passive gymnastics [104] [17]. The market offers a wide range of stimulation devices to increase muscle strength, decrease body weight and body fat and to improve muscle firmness and tone [148]. From the literature evaluated, this field has the higher coverage in terms of population but commonly unsupervised by qualified personnel.

In all contexts, electrical currents are applied to the excitable tissue with different stimulus parametrizations. The parametrization traditionally concerns the pulse frequency, amplitude and duration, however, there are also a set of parameters not frequently addressed, such as pulse charge, waveform and polarity.

There are also some known drawbacks to the use of electric currents in the human body. During electrical stimulation, skeletal muscles fatigue more rapidly using repetitive stimulation than with voluntary contractions [153][187]. Muscle fatigue is defined as a reduction in the peak force, with continuous and repeated activation [130]. Rapid fatigue during Neuromuscular Electrical Stimulation (NMES) is thought to result from the differences in motor unit recruitment order, higher activation frequencies and imprecise control of muscle force compared to voluntary contractions [140]. The problem of muscle fatigue is aggravated by the fact that paralyzed muscle shows greater propensity to fatigue than healthy muscle. Consequently, muscle fatigue is an important factor limiting the clinical use of NMES [25].

Another drawback of this technique is related with the user's comfort. Pulsed currents become rapidly uncomfortable to the patient [177] [163]. This discomfort is provoked primarily by the activation of the nervous fibers $A-\delta$[1], given that artificial electric pulses have low fiber selectivity.

Electrical stimulation may induce a perturbation on the natural human physiology. In terms of the skin, it can easily lead to irritation or burns [177]. High levels of total electric charge can be neurotoxic [122][194][27] and cause nerve damage [126]. This assumes higher proportions given that, with the massification of the methodology, unqualified individuals can themselves easily apply voltages up to 120V. Regarding other physiological changes, very few studies address the impact of electrical stimulation on the Autonomic Nervous System (ANS) [90].

Some authors already tried to address and overcome these stimulation drawbacks. Studies in theoretical models reached to promising conclusions about the decrease of the electrical impulse total charge, optimizing the pulse waveform, as a measure to reduce the fatigue induction [84][85][86], to reduce the risk of burns and skin irritation [19] and to increase the comfort for the patient through nervous fibers selectivity [189][158]. However, practical implementations of those theoretical studies find some methodological barriers,

[1] $A-\delta$ fibers, are a type of sensory fibers. They respond to stimuli such as cold and pressure and, the stimulation of them is interpreted as fast/first pain information.

when manipulating unusual parameters such as the pulse waveform, polarity and charge. Bennie et al. [19] was forced to use two different stimulators to apply different pulse waveforms and a complex set of instruments to acquire several physiological aspects. The authors addressed the problem of stimulus comfort, unfortunately, without any guarantee of time synchronization between the biosignals and the electrical impulses, which compromises the cause-effect analysis.

Even when studying the correlation of the standard parameters, pulse-width [99][67], frequency [57][92][179][96] and amplitude [182][93][83] with its implication on fatigue, complex apparatus need to be implemented at hardware and software level, negatively impacting upon the costs, the development time and the reliability of the results.

When addressing the recent electrical stimulation technology, it is imperative to clarify an important aspect: The market offers a wide variety of solutions with characteristics such as reduced size, portability, high usability and commercial appeal. Mostly, those solutions are completely focused on a solo objective and therefore, the parametrizations of the devices are pre-programmed. As an example we have the vast range of electrical stimulation devices used only for NMES. Details of the current systems and discussion about the main circuit topologies will be given in the next chapter.

However, electrical stimulation has a much wider scope and, mainly in the research context, the degrees of freedom that the current electrical stimulation devices allow are still very insufficient. Even the more robust stimulation systems that allow greater control of the parametrization are limited to the standard parameters such as frequency, amplitude and pulse width, and most of them have limitations on usability, dimensions, complexity, setup time and creation of control routines.

In practice, the main drawbacks of the methodology are still the same as before, and few people investigate, implement or develop turn-key solutions. This fact motivates the development of new hardware configurations, enabling custom parametrizations in the control of current or voltage output.

1.2 Questions and Goals

Concerning the state-of-the-art and the problems previously raised, the following questions become of significant scientific relevance:

- What is the physiological effect of the electric pulse parametrization concerning charge, waveform and polarity? Does the effect change with the clinical condition of the subject?
- Can parametrization enable fiber selectivity, optimizing the motor fibers recruitment rather than the nervous fibers, reducing contraction discomfort?
- The parametrization influence on muscle recruitment can retard fatigue onset?

To address these questions, the following methodological developments are required:

1. Develop a new solution for electrical stimulation, that allows:

    - **Parametrization:** Freedom in the electrical pulse control, specifically for standard parameters such as amplitude, frequency and pulse-width, but also waveform, charge and polarity;
    - **Synchronization:** A cause-effect stimulus *versus* physiological response reliable analysis, concerning temporal synchronization and improved signal quality;
    - **Usability:** The solution should have high usability, reflected in a low intrusiveness in clinical and laboratory contexts;
    - **Configurability:** The system should have implementation flexibility for prototyping, configuration and storage of electrical stimulation protocols.

2. With the solution developed, the following studies addressing human electrophysiology are proposed:

    - Compare the electrophysiological response of healthy individuals and spinal cord injury patients, controlling pulse waveform and charge parametrization;
    - Study the effects of pulse parametrization in current diagnosis mechanisms of neurodegenerative pathologies;
    - Evaluate the induction of fatigue and comfort using different pulse waveforms in the context of NMES;

By fulfilling these goals, a solution is developed to mitigate the current drawbacks of electrical stimulation, furthermore enabling new approaches to address fundamental human electrophysiology, as expressed on Figure 1.2.

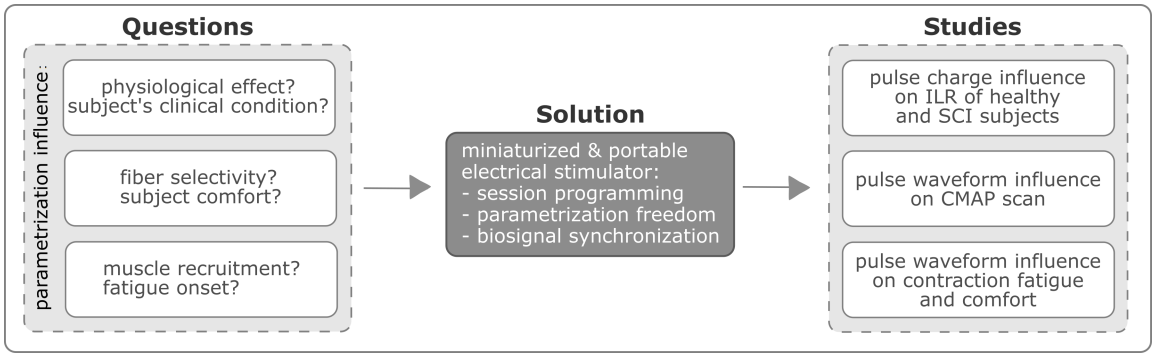

Figure 1.2: Illustration of the scientific and methodological alignment of this work. The scientific questions, the methodological solution and the studies implemented envisioning the answer of those questions.

1.3 Thesis Structure

This thesis summarizes the work developed during the PhD period and divides it into eight chapters and five appendixes. A brief description of the contents of each chapter is described next and Figure 1.3 schematizes its organization.

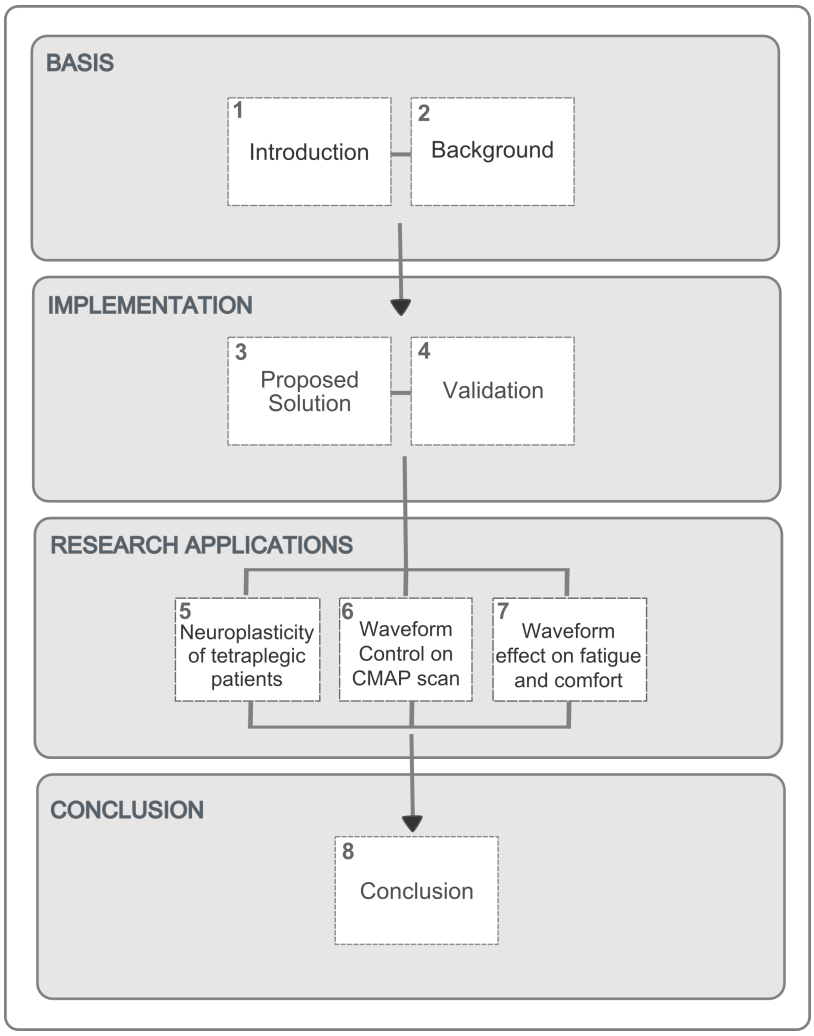

Figure 1.3: Thesis structure.

- Chapter 1 - **Introduction** - The present chapter introduces the relevant questions to be answered in this thesis, providing some insight on the motivation and outlining the main goals of this work. This chapter also describes the thesis structure.

- Chapter 2 - **Background** - Introduces the theoretical concepts which are important for the comprehension of the following chapters. Provides a solid background on the fundamental concepts of electrophysiology and discusses electrical stimulation, from historical context to state-of-the-art applications. This chapter also comprises a technical review of contemporary electrical stimulation circuit topologies.

- Chapter 3 - **Proposed Solution** - Focuses on the development of the electrical stimulator designed to solve the problem foreseen before. This chapter presents the core of the thesis and covers hardware design, firmware development and software implementation. This chapter also introduces the methodologies applied in the context of this thesis.

- Chapter 4 - **Validation** - This chapter presents the characterization and production tests performed with the device to guarantee that the predefined requirements were fulfilled. Two examples of scientific validation studies performed to enrich the development stage are also described in this chapter.

- Chapter 5 - **Application to Neuroplasticity of Tetraplegic Subjects** - The scientific questions raised are addressed in three scientific studies (Chapter 5, 6 and 7). In this Chapter, a study comparing the interlimb reflexes of tetraplegic patients and healthy subjects is presented. A correlation between electrical current parametrization and reflexes parameters is addressed.

- Chapter 6 - **Application to the Waveform Control on CMAP Scan** - The second study analyzes the effect of electrical pulse parametrization in a current diagnose mechanism of neurodegenerative pathologies, the compound muscle action potential scan. This study analyzes how electrical pulses with different waveforms influence the stimulus-response curve given by the CMAP scan.

- Chapter 7 - **Application to the Waveform Effect on Fatigue and Comfort** - Finally, this Chapter presents the last study which evaluates the impact of electrical pulse parametrization in a neuromuscular electrostimulation protocol. A protocol specifically created to induce fatigue was applied with different electrical pulse waveforms and differences in comfort and fatigue rate were assessed.

- Chapter 8 - **Conclusions** - This last chapter presents the conclusions of the work, with a critical discussion of the addressed problems, its contributions and extended implications.

- **Appendix A** - The first appendix provides a list of the author's publications, book chapters, papers in journals accepted and in review, conference proceedings and oral communications.

- **Appendix B** - Provides an overview of the tools used for the conducted research.

- **Appendix C** - A brochure presenting the technical summary of the final stimulator device.

- **Appendix D** - Presents the test protocol template defined during validation phase (Chapter 4).

- **Appendix E** - Presents the American Spinal Injury Association (ASIA) international standards for neurological classification of spinal cord injury used on the study described in Chapter 5.

CHAPTER 2

BACKGROUND

The objective of this chapter is to cover the elementary concepts needed for the theoretical support of this thesis. The electrical properties of the cell are explored in Electrophysiology Principles section. Then, the theoretical concepts on electrical stimulation used for rehabilitation and functional purposes are depicted. Electrical stimulators are analyzed from the historical point-of-view to the current context and the various parameters of electrical stimulation are discussed, including frequency, pulse width, waveform and how they affect human physiology. This chapter goes further within the technical concepts of the electrical stimulators, covering the contemporary circuit topologies in use.

2.1 Electrophysiology Principles

The application of electrical currents in biological tissues is based on deep knowledge of the electrophysiology properties of those tissues. In this section the fundamental concepts on electrical properties of the cell are reviewed.

2.1.1 Resting potential

When the cell is at rest it has a relatively static membrane potential, maintained as long as nothing disturbs it. The resting potential characterizes the difference between the interior (cytoplasm) and the exterior of the cell when it is at rest (Figure 2.1). This electrical potential difference depends on the ionic concentration gradients, which can be altered through the membrane permeability to each ionic species.

The cytoplasm fluid has a high potassium (K+) ionic concentration and a low sodium (Na+) ionic concentration. The cell membrane has higher permeability to potassium than to sodium, so there is a tendency for the potassium ions to move to the exterior of the cell, favoring their concentration gradient and causing a negative electrical potential in the

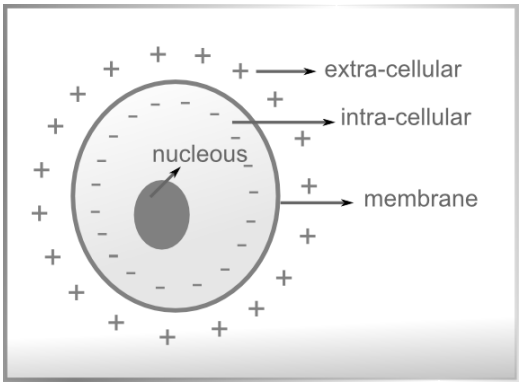

Figure 2.1: Membrane potential and respective polarity.

interior of the cell. The equilibrium potential for each ionic species can be mathematically represented by the Nernst equation [1]. The resting potential varies between -60 and -90 millivolts (mV) depending on the cell type - for instance, in nerves and smooth muscle fibers the resting potential is -70 mV [30]. Any change in the membrane permeability in one of these ionic species will displace the resting potential and may generate an electrical signal, called action potential.

2.1.2 Action potential

In the human body, the basic cell-to-cell communication mechanism over the nervous structures occurs through the Action Potential (AP). The action potential is a wave of electrochemical potential that moves through the membrane. It reverts the membrane potential from -70 mV to +30 mV in less than 1 millisecond (ms). In muscle cells, for example, an action potential is the first step in the chain of events leading to contraction. The electrical impulse is initiated by the membrane's depolarization due to the chemical disturbance of a synapse, a receptor, or another disturbance like an external electrical impulse. The action potential only starts if the membrane is depolarized in approximately 10 or 15 mV, so around -55 mV as it is observed on Figure 2.2.

The potential value that needs to be surpassed to trigger the action potential is called excitability threshold. When an action potential is triggered physiologically, it will only follow one direction (distal if the nerve is efferent and proximal if afferent). If, however, the action potential is triggered by an artificial electrical impulse in the middle of a nervous fiber, two impulses are generated that will move in opposite directions from the stimulus point.

The depolarization above the excitability threshold induces the opening (activation) of the sodium channels, as shown in Figure 2.3 a). When these channels open, there is a current of sodium favoring its concentration gradient and causing a rapid reversion in the

[1] Nernst equation: $V = \frac{RT}{zF} \times \ln \frac{Ko}{Ki}$, in which R is the ideal gas constant, T is the temperature in Kelvin, z is the charge of the ion, F is the Faraday constant, Ko the ions concentration outside the cell and Ki the concentration of the ion inside the cell.

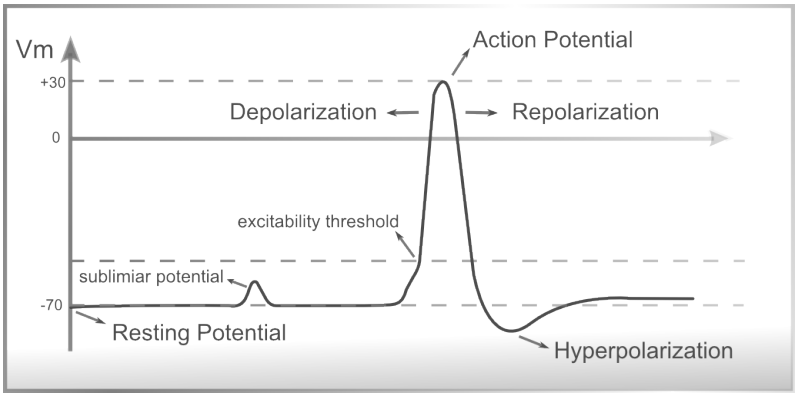

Figure 2.2: Representation of an action potential and excitability threshold.

membrane's polarity, from -70mV to 30mV. This depolarization causes an alteration in the electrochemical gradient of the potassium ions, relative to the resting point, therefore activating the potassium channels and generating a potassium current opposite to the sodium current (Figure 2.3 b)) [78]. Simultaneously to this increase of potassium diffusion, occurs the inactivation of sodium channels - this phase is called repolarization. Consequently, there is a decrease in the intra-cellular potential compared to the extra-cellular potential. The additional potassium channels stay open even when the membrane potential reaches the resting level. So, the potential becomes even more negative than when at rest - this phase is called hyperpolarization [18]. Eventually, the extra potassium channels close and the membrane potential goes back to its resting, 'polarized' level (Figure 2.2).

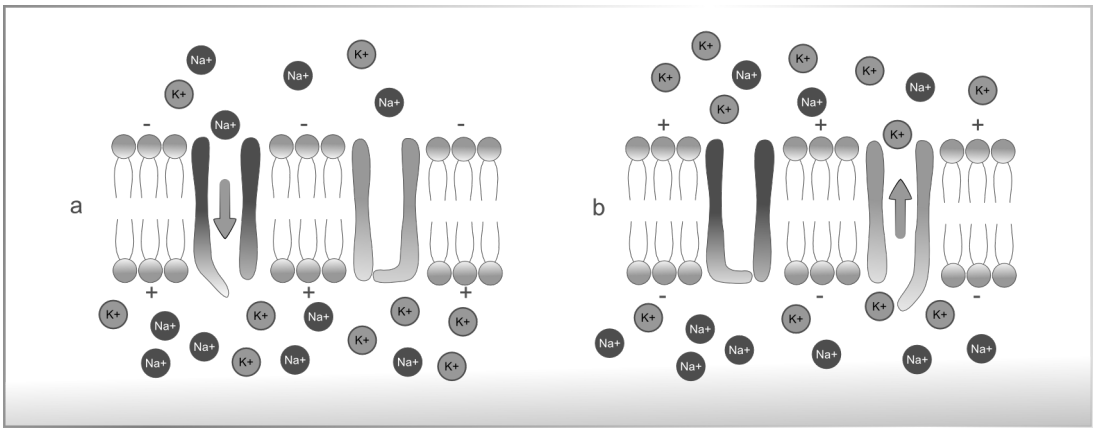

Figure 2.3: Diffusion of sodium and potassium; a) activation of sodium channels, b) potassium reposition.

2.1.3 The nerve cell as a conductor

The transmission of information in the nervous system is a reproduction of the previously described phenomena over the length of the nervous or muscle fiber. When a region of

the membrane generates an action potential it instantly depolarizes adjacent regions and propagates the impulse.

There are three main pathways for the current to flow along the length of the axon: i) An external conductor (extra-cellular fluid) with very low impedance; ii) an internal conductor (axoplasm), with similar impedance from one cell to another due to the uniform ionic composition of the intracellular fluid; and iii) the cell membrane that separates the two conductors. The membrane has an intrinsic capacity and impedance that varies according to each ionic species' permeability, as it is described in the model of Figure 2.5. As current spreads along the nerve fiber pathways, it is attenuated with distance and a spacial decay constant can be defined, like observed in Figure 2.4 a). If that constant is altered by some mechanism, natural or induced, there is a direct change in the propagation speed of the action potential. Figure 2.4 b) exemplifies a constant of lower decay and therefore a higher conduction speed [101].

The propagation speed of the nervous impulse varies with the nervous fiber's dimensions, geometry and membrane characteristics. In normal situations, as larger the fiber diameter is, faster is the conduction. The action potential propagates along the nerve with a velocity of about 30-120m/s, depending on the nerve type, and reaches the axon terminal where the neurotransmitter acetylcholine is released. There are also cases in which the nervous fibers are enveloped by myelin sheaths (electrically insulating), and interrupted with Ranvier nodules (areas without myelin). The electric potential of the nervous impulse travels along the fiber, but the depolarization occurs only in the Ranvier nodules. When a nodule is depolarized, it triggers the depolarization of the next nodule without generating action potentials in the myelin zones. When this happens, the membrane potential changes in about 100mV, which is sufficient to trigger the action potential in the adjacent nodule. So, the nervous impulse can be described as jumping from nodule to nodule (Figure 2.4 c)), using less energy but with higher conduction speed. This speedy conduction is called saltatory conduction. The higher is the conduction speed, larger is the extension of the fiber depolarized in each instant [89].

2.2 Electrical Stimulation Principles

Technological advances have propelled the development of electrical stimulation devices more adapted to current needs. Nowadays, the electrical stimulators are controlled by microprocessors - which means that a single device enables varied types of stimulation, with different parameters and objectives. It is important to understand the evolution of electrical stimulation devices from historical examples to nowadays. It is also fundamental that the operator knows the wave parameters available and their physiological effects. This section addresses basic concepts of electrical stimulation from standard use to the current types and parameters that characterize the electrical impulses.

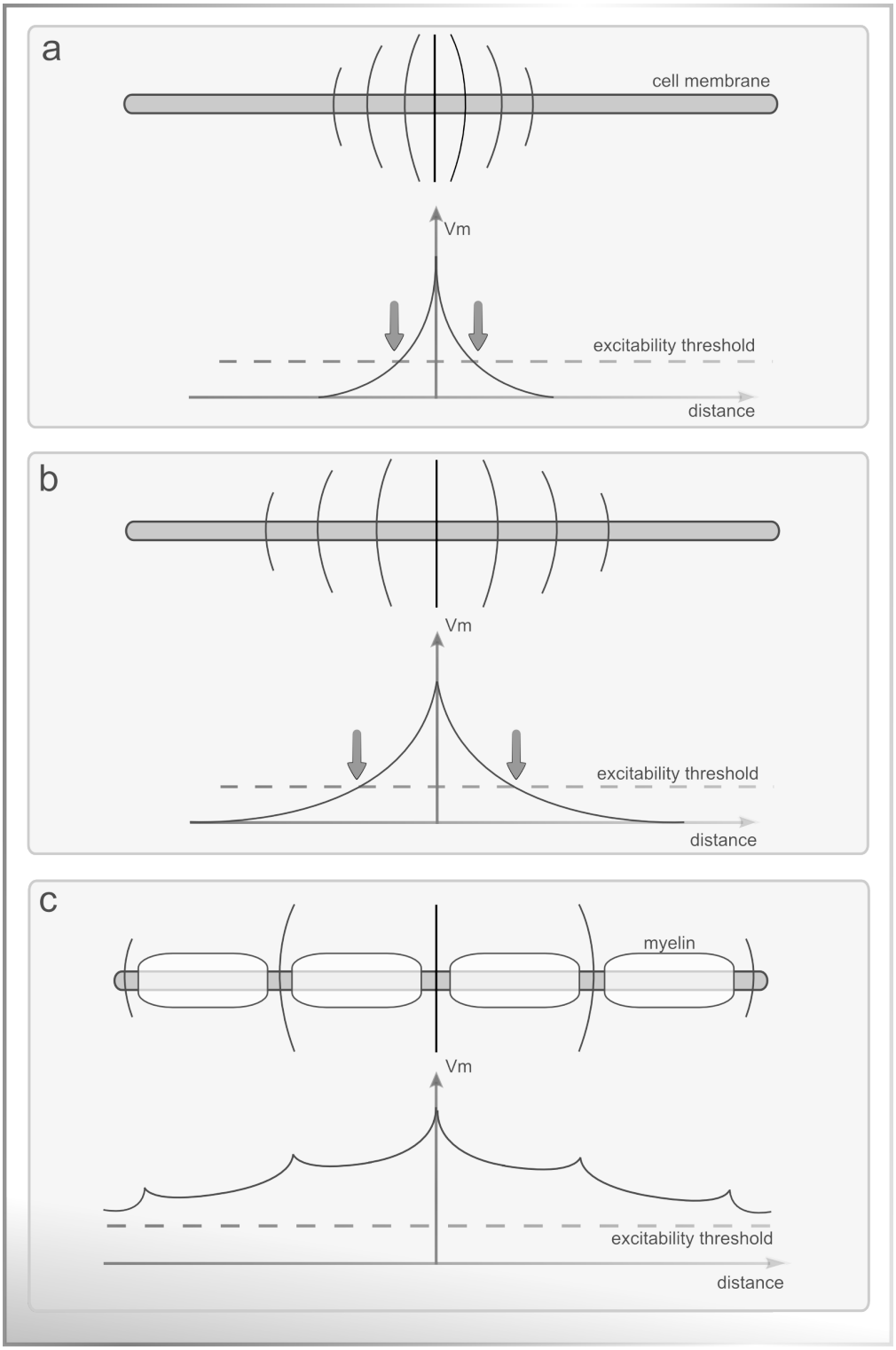

Figure 2.4: Propagation of the potential and conditioning factors at a fixed time instant. a) Exponential fall of the membrane potential (Vm) after the action potential. b) Example of bigger decay than in a). c) 'Saltatory' conduction. The cells that constitute the myelin membrane are insulating, preventing the passage of current in the internodes, increasing the space and the speed of propagation. Adapted from [133].

2.2.1 Historical context

First records of electrical currents application in therapeutic contexts date from the eighteenth century. In 1791 Luigi Galvani initiated the publications of electric current effect in human muscle [142]. In 1831, Michael Faraday showed that electrical currents could stimulate nerves to create active movement [39]. Concerning the therapeutic effects of electrical nerve stimulation, Duchenne de Boulogne, dubbed the 'father of electrotherapy' was a pioneer in the use of surface electrodes, localizing the electrical currents [16].

The theoretical support of cellular excitability comes more than a century later in 1952 with the Hodgkin-Huxley studies [79], where they described the electrical model of the action potential in a giant squid (the model is presented in Figure 2.5).

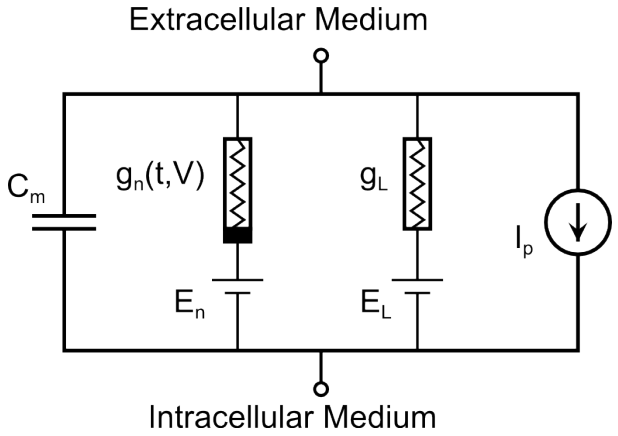

Figure 2.5: Electric model of the cellular membrane by Hodgkin and Huxley [79]. The lipid bilayer is represented as a capacitance (C_m). Linear (g_L) and nonlinear (g_n) conductances represent the voltage-gated and leak ion channels. The electrochemical gradients driving the flow of ions are represented by batteries (E_n and E_L), and ion pumps and exchangers by current sources (I_p).

The electrical model of the cellular membrane is considered as one of the great scientific discoveries of the 20th century. It enabled important and relevant advances on the human physiology field.

This knowledge was the basis for a solid expansion of the electrical currents use in excitable tissue over the years. With this, some concepts emerged, such as Neuromuscular Electrical Stimulation (NMES), associated to the application of current directly on the muscle surface [115], and Transcutaneous Electrical Nerve Stimulation (TENS), associated with the application of currents in the nervous fibers [88].

NMES devices deliver electrical stimulus that depolarize motor neurons, causing an action potential to propagate along its axon, which causes the associated muscle fibers to contract [68][120]. NMES applications can be found in literature in early 1964 [185]. Typically, it uses high frequencies in the range of 20-50 Hz to produce muscle tetanus and contraction. Historically, TENS used high frequencies for pain relief [52] but nowadays, it also applies very low frequencies (sensory level TENS, 2-10 Hz) [168]. TENS propagates

along smaller afferent sensory fibers specifically to override pain impulses. When low frequencies are administered, TENS specifically targets sensory nerve fibers and does not activate motor fibers; therefore, no discernible muscle contraction is produced.

The channeling of electrical stimulation methods with functional purposes led to the appearance of the term Functional Electrical Stimulation (FES), which aims to restore function in people with disabilities [12]. FES was first referred as *Functional Electrotherapy*, by Liberson [107][33]. In 1961, he and his team produced the first electrical stimulation device for the correction of dropped foot due to an upper motor neuron lesion. FES devices treated foot drop by stimulating the peroneal nerve during gait. Only in 1962, the term *Functional Electrical Stimulation* was coined by Moe and Post [129] and used later in a patent by Offner [135]. In 1965, Offner patented the system used to treat foot drop with the title *'Electrical stimulation of muscle deprived of nervous control with a view of providing muscular contraction and producing a functionally useful moment'*. The benefit of FES was demonstrated in several studies which paired the application of electrical stimulation with tasks that demanded the use of intact cognitive and motor skills of the patient [180][43][62][157][71].

Over the years, a great amount of discoveries and technological evolutions were made in the field of electrical stimulation. As it will be discussed further, most of the electrical stimulation devices are controlled by microprocessors. This means that a single device can produce various types of stimulus, with different parameters and objectives in order to obtain a particular physiological response. A full understanding of the current-tissue interaction and the settings that govern the stimulation is vital for the safety of the patient and the success of the intervention.

2.2.2 Excitability

The core concept to control and understand the current-tissue interaction resides in the concept of tissue excitability. In its fundamental sense it can be defined as the quantification of energy necessary to activate certain tissues in reaction to a stimulus, such as triggering an action potential in an axon. Excitability was addressed in 1901 by Weiss through equation 2.1.

$$Q = b(d + c) = Id \tag{2.1}$$

Where Q is the charge and I is the current, multiplied by duration, d. b relates to a physiological value named *rheobase* and c relates to other called *chronaxie*, two fiducial points of tissue excitability. The *rheobase* value is the minimal current amplitude of infinite duration (in a practical sense, around 300ms is enough) that results in the depolarization threshold of the cell membranes being reached, such as an action potential or the contraction of a muscle. The *chronaxie* value is the minimum time required for an electric current to double the strength of the *rheobase* to stimulate a muscle or a neuron [10].

Later in 1907, Lapicque proposed equation 2.2.

$$I = b(1 + \frac{c}{d}) \tag{2.2}$$

Where I is the current, b relates to the *rheobase*, and c to the *chronaxie*, over duration d.

This equation expresses the strength-duration curve (Figure 2.6), which is a plot of the threshold current versus pulse duration required to stimulate excitable tissue. Figure 2.6 also presents the relation of electrical stimulus intensity and duration with stimulation charge and energy.

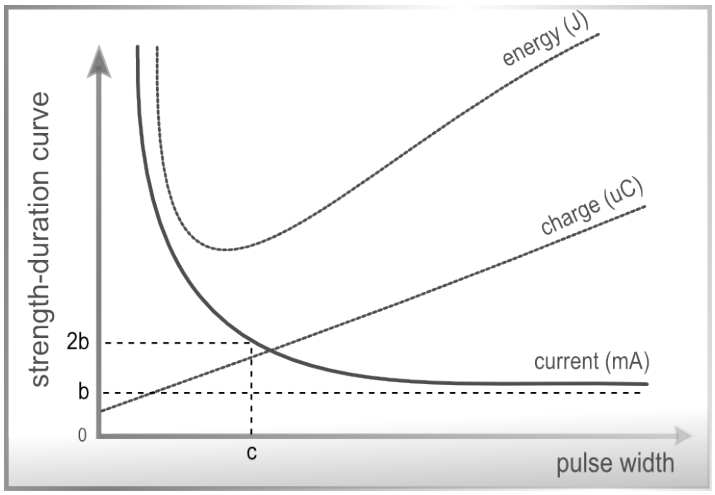

Figure 2.6: The strength-duration curve for current, energy and charge of an excitable tissue.

2.2.3 Stimulation parameters and physiological impact

As mentioned before, the stimulation parameters applied will condition the respective physiological response, so it is necessary to adapt those parameters to the therapeutic objectives. The cause-effect relation of all the parameters and respective physiological consequences should be known for the correct application of the stimulation.

Amplitude: The amplitude of the stimulation pulse (Figure 2.7) can be measured in current or voltage, depending on the modulation type. The amplitude determines the stimulation intensity, which consequently determines the total number of nervous fibers that are recruited and activated. As higher the intensity, stronger the depolarizing effect in the structures underlying the electrodes [127]. Higher intensities enable increases in contraction strength and hypertrophy process [62][118][175][143].

Stimulation amplitude will also influence patient comfort, with higher intensities being typically less tolerated. However, frequency and intensity inevitably will determine the quality of muscle contraction produced [14].

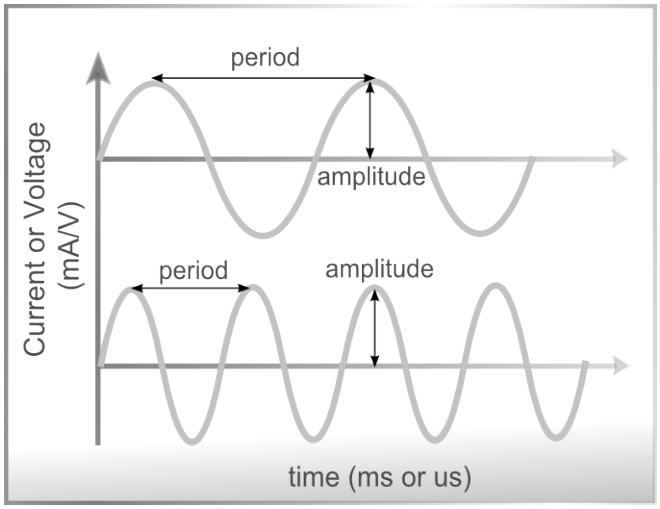

Figure 2.7: Amplitude and period of a wave.

Pulse-Width: The time span of a single pulse is known as the pulse-width or pulse duration. It is defined as the duration of the wave at 50 % of the maximum amplitude, and is expressed usually in microseconds (μs). Research has shown that patients exhibited a strong preference for phase durations of between 200-400 μs which are also capable of producing reliable muscle contractions while minimizing the possibility of skin irritation beneath the electrodes [111]. Recent work comparing 50, 200, 500, and 1000 μs pulse-widths with a stimulation frequency of 20 Hz to the sole muscle, found that wider pulse-widths produced stronger contractions of plantar-flexion and additionally augmented overall contractile properties [103]. In addition, longer pulse durations will typically penetrate more deeply into subcutaneous tissues, so these widths should be used when trying to impact secondary tissue layers [29]. The pulse-width affects the current amplitude which is necessary to trigger the action potential and also determines the sensitivity of sensory, motor or pain stimulation. Pulsed currents with lower pulse-width are less uncomfortable. As illustrated in Figure 2.8, the sensory, motor and pain sensitivity to stimulation amplitudes is maximal when applying pulses with low duration.

However, in this section, it is important to refer an accommodation phenomena [173], which makes the excitability threshold of the nervous tissue adaptive and not absolute. Because of this effect, if the current transfer ratio, which is related to the rise time of the electrical pulse, is longer than several hundreds of μs, the current amplitude required to reach the action potential will be superior (Figure 2.9).

The results of this work enabled a deeply discussion correlating amplitude, pulse-width and an inherent parameter: the charge. This discussion is documented later on Chapter 8.

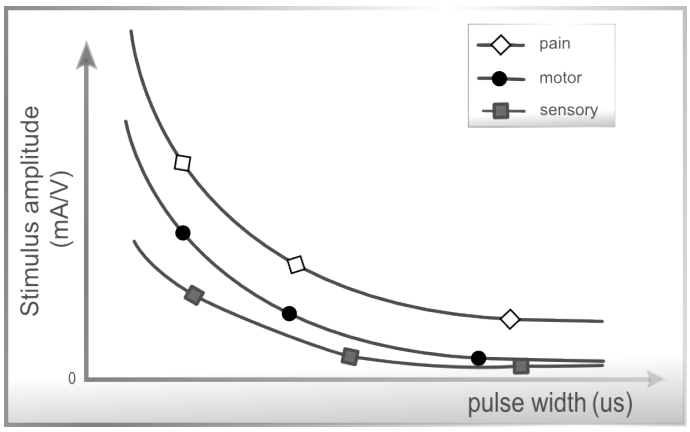

Figure 2.8: Strength-Duration curves: Relation between amplitude and pulse-width when relating with the influence on excitability thresholds: sensorial, motor and pain tolerance. Adapted from Robertson et al. [154].

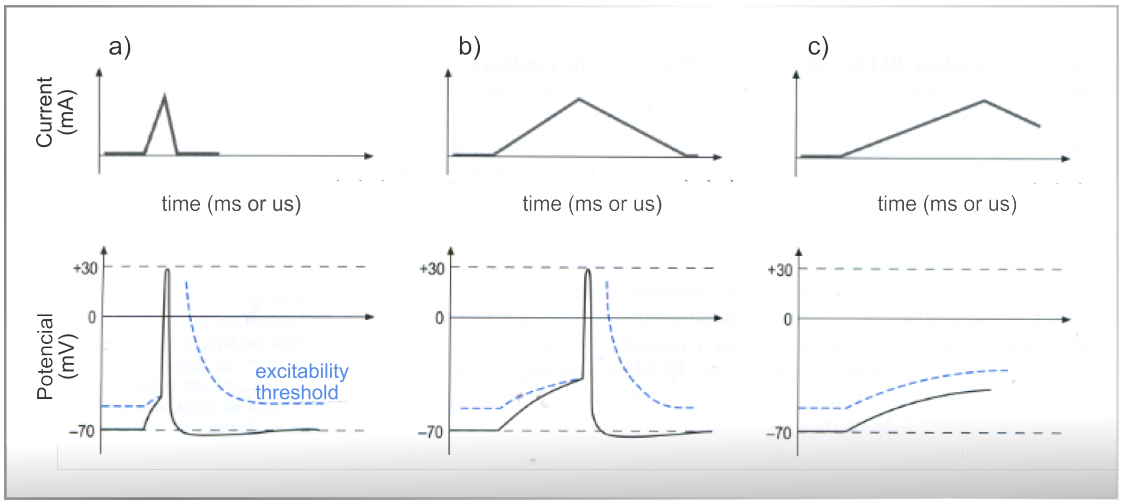

Figure 2.9: Relation between the pulse-width applied and the accommodation of the nervous fiber: a) the small current transfer ratio triggers the action potential; b) a bigger current transfer ratio triggers the action potential but showing threshold accommodation; c) the transfer ratio is very high and never surpasses the excitability threshold.

Frequency: Frequency refers to the pulses produced per second during stimulation. The frequency of a stimulus affects the clinical response as it influences the muscular contraction which can be isolated or tetanic. A tetanic contraction (also called tetanized state or tetanus) occurs when a motor unit has been maximally stimulated by its motor neuron. This occurs when a muscle's motor unit is stimulated by multiple impulses at a sufficiently high frequency. Each stimulus will cause a twitch. If pulses are delivered slowly enough, the tension in the muscle will relax between successive twitches. If pulses are delivered at high frequency, then the twitches will run together, resulting in tetanic contraction. Stimulation frequencies above approximately 30 Hz produce a tetanic contraction [16]. Most clinical applications use 20-50 Hz patterns for optimal results [15][50]. Increasing the

stimulus frequency leads to stronger contractions up to a maximum. However this also increases the rate of muscle fatigue [16][152]. To optimize fatigue, constant low frequency stimulation is used, which produces a smooth contraction at low force levels [21]. However, the muscle fatigue index induced by artificial stimulation is always higher than the voluntary contractions in which the motor neurons activation is triggered asynchronously. The contraction strength is defined by the number of motor units recruited and by the frequency of the action potentials.

In terms of patient comfort, typical NMES stimulator frequencies in the range of 30-60Hz are found to be optimum [111].

Figure 2.10 shows the variation of the fiber strength with the stimulus frequency, for intensities above of the motor limit. A stimulation frequency above 30Hz is indicated for the production of maximum force.

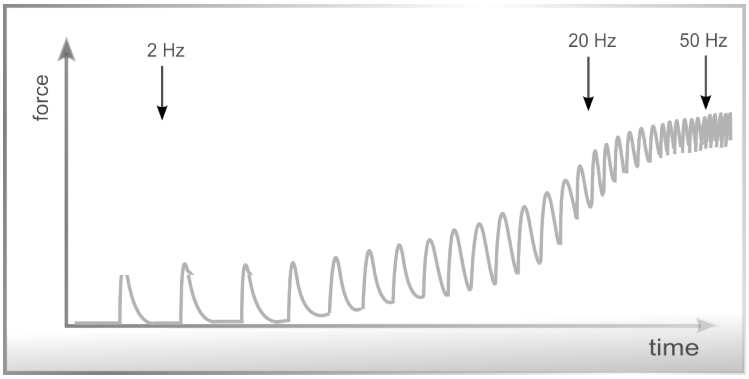

Figure 2.10: Muscular strength variation with the stimulus frequency, for stimulation intensities above the motor limit. Adapted from Kitchen et al. [98].

Waveform: In surface electrical stimulation the waveform is the representation of the variation, over time, of the current or voltage that is injected into the biological tissue. The polarity, in the context of electrical current, refers to the charge way. The pulse may be monophasic (unidirectional / continuous polarity) or biphasic (bidireccional / alternating polarity), as it is represented in Figure 2.11 [66]. The power of the two kinds of current pulses is equal, but if the wave is symmetrical the charge compensation avoids the deposition of ions above the electrodes surface which may cause lesions on the tissue level [140][106].

A typical biphasic stimulus pulse consists of two phases: a stimulating phase and an adjacent phase of opposite polarity. The simple monophasic stimulus is a periodic unidirectional pulse, where current passes in only one direction. This type of stimulus is not used for prolonged periods, as such irreversible faradaic reactions may cause tissue damage. These negative reactions due to prolonged periods of negative (or positive) potentials associated with monophasic stimulation is minimized by the use of a biphasic waveform pulse [20][69][75][82][149][176][128]. Contemporary devices generate pulses of

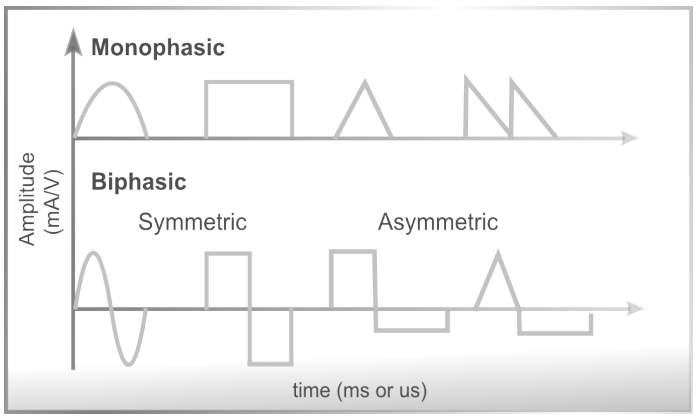

Figure 2.11: Examples of electric pulses with different polarities and waveforms.

voltage/current with predefined geometric shapes, traditionally the square wave. Figure 2.12 shows a comparison of stimulation waveforms regarding their ability to generate low threshold stimulation, low corrosion, and low tissue damage.

There are a very few studies on the practical effect of the waveform on the physiology response. Durand [56], evaluated the standard waveforms and those studies enabled the compilation of the information present in Figure 2.12. However, there are still various waveforms for which the correspondent biological effect is still unknown. The evaluated parameters by Durand - threshold, corrosion and tissue damage - represent only part of the information about the effect of the waveform on the excitable tissue.

	Threshold	Corrosion	Tissue Damage
	+	+	+
	++++++	+++++	++
	+++	+++++	+++++
	+++++	++++	+++
	++	+++	++++++
	++++	++	++++

++++++ Best
\+ Worst
in relation to the patient or the tissue

Figure 2.12: Comparison of stimulation waveforms for their ability to generate low threshold stimulation, low corrosion, and low tissue damage. Adapted from Durand [56].

2.3 Application of current

The current is defined as the quantity of electrical charges that goes through a conductor during a determined time interval, i.e. quantity of single charges moving per time unit. According to Kitchen and Bazin [98] the currents can be direct or alternating and pulsed or constant.

In the electrical stimulation scope, the most common types are the direct or alternating pulsed current and the alternating continuous current.

2.3.1 Current Types

For historical reasons, in the clinical perspective, it is usual to identify the applied current, associating it with a name (example: galvanic current, faradic current) and sometimes with a differentiating characteristic or a set of characteristics (example: interferential currents, russian currents). Below are presented the most common nomenclatures in clinical environments:

- **Faradic current:** A pulsed current with frequencies between 50 and 75 Hz. The pulses are monophasic or biphasic, with duration of less than 1 millisecond (ms), and are traditionally used for motor stimulation;

- **Galvanic Current:** A continuous current, usually used for iontophoresis;

- **TENS Current:** Meaning Transcutaneous electrical nerve stimulation, the TENS current is used to treat pain. The pulse duration is usually a constant value ranging from 50-200 microsecond (μs) and the pulse frequency is usually adjusted between 2 and 120 Hz;

- **Pulsed Current of High Voltage (PCHV):** Has a voltage regulated output which can go up to 500 volts. The stimulus impulse has peaks, has a low duration (approximately 7μs) and the frequency of double pulses combination can vary, usually between 1 and 10Hz.

- **Russian Current:** An alternating current of 2500 Hz, applied in rectangular bursts with a burst frequency of 50 Hz and duty cycle of 50 %. The bursts are applied for 10 seconds on, following 50 seconds off, for a treatment period of 20 minutes. The theory inherent to the Russian Current is based on the application of supramaximal intensities to recruit the maximum number of motor units, favoring the hypertrophy process.

- **Interferential Currents:** Consists in two alternating currents in kHz band frequencies, applied in continuous bursts. The two currents have slightly different frequencies and will interfere in the interior of the tissue, producing higher stimulation

intensity. Interferential current is essentially a deeper form of TENS. The high frequency carrier waveform penetrates the skin more deeply than a regular TENS unit, with less user discomfort for a given level of stimulation.

- **Dynamic Currents:** Consists in sinusoidal currents with rectification of half wave or full wave in the frequency bands of 50 to 60 Hz. As the pulse duration varies between 10 and 8 milliseconds, the stimulation causes high discomfort.

- **Microcurrent:** It is characterized by a very low intensity current, even bellow the sensory threshold. Its usages include treatments for pain,[1] Diabetic neuropathy,[2] age-related macular degeneration, wound healing, tendon repair, Plantar fasciitis[3] and ruptured ligament recovery.

2.3.2 Transcutaneous stimulation electrodes

In surface electrical stimulation, the application of current is made through surface adherent electrodes. For the current to reach underlying tissue, its success highly related to electrode size and placement, as well as the conductivity of the skin-electrode interface [109]. It is important to consider the type and the dimensions of the electrodes.

Self-adhesive electrodes for transcutaneous stimulation use a gel to contact a conductive member with the subject's skin. This sticker, pre-gelled electrodes are currently used for a better convenience, since they are easy to apply and to remove and don't require any extra fixations. They already have adhesive gel, inseparable from the surface, being completely disposable - although suppliers provide some types that can be reused in the same patient. The biggest disadvantage of this approach is its cost. There are other electrodes for surface stimulation: metal plates covered with fabric tissue or carbon electrodes. Those have lower cost but are also less practical since they require water or special electrode gel to equally distribute the current over the electrode surface.

The dimensions of the electrode are also an important factor: Bigger electrodes usually mean a higher comfort in the stimulation [1]. Since the current density per area is lower, the stimulation is more effective for sensory stimulation, like pain control, and for motor control. The reaction is stronger since it recruits a bigger amount of motor units [1]. Smaller electrodes will concentrate current densities, allowing for focal concentration of current with less chance of stimulation crossover into nearby muscles [161].

2.3.3 Electrode Placement

Placement of electrodes will also markedly influence the muscle response and should be carefully considered. The electrodes positioning determines the place of higher current density. The specific positions for the electrodes will depend on the treatment/research/-diagnosis objective. For example, if the objective is to stimulate an innervated muscle, it is important to assure that the nerve which innervates the muscle is in the path of the current [119][169]. Therefore there are usually two options:

- Over the nerve trunk / the muscles motor point;
- In each one of the muscle terminations, so that the nerve is always in the path of the current.

The electrodes positioning is therefore related with its configuration: unipolar or bipolar. The unipolar configuration (Figure 2.13 a)) uses one active electrode which only transmits current to the passive electrode (that only receives current). In this configuration the active electrode has generally an inferior dimension than the passive. Moreover, in the bipolar configuration (Figure 2.13 b)) the current flows bidirectionally between both electrodes which, in this configuration usually have the same dimensions, positioned in each of the terminations of the muscle group to be stimulated.

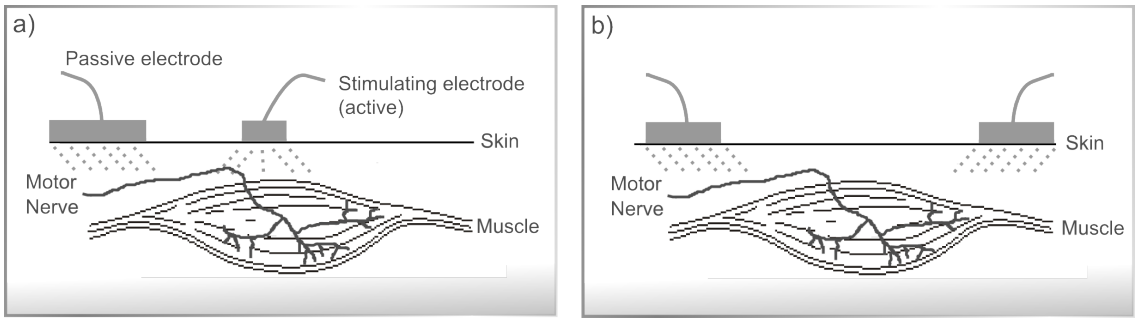

Figure 2.13: Electrodes configuration: a) for unipolar current application; b) for bipolar current application.

The following section describes the most recent circuits used for generic, non-invasive, electrical stimulation purposes.

2.4 Electrical Stimulation Circuits

Independently of the power source, the architecture of current electrical stimulation devices comprise at least an analog module to regulate and drive the current to the tissue, a high voltage module to produce the necessary voltages to overcome the tissue load and a controller unit that can be analog (using for example an oscillator circuit to generate the pulses), or digital (using a microcontroller, offering higher control of the electrical pulse parameters) [44]. Electrical stimulators can be used for specific applications such as the Parastep [146], RGO [171] designed for the lower limbs stimulation; or Freehand [74], Handmaster [131], Bionic Glove [150] for controlling the hand. Another example of specific purpose electrical stimulation devices is the vast list of miniaturized nerve stimulators analyzed in the work of Shariat et al. [162], using low currents, all limited to sensory applications.

There are, however, electrical stimulators for general application, such as Grass Technologies stimulators that provide muscle and nerve stimulation [141][13]. However, due to factors such as cost/benefit ratio, reliability, comfort and functionality of current devices,

there is a limited market access [196][162]. Much of the research in the area of NMES hardware has centered around the use of more sophisticated external sensors, increased number of stimulation channels, flexibility in terms of adjusting the stimulus parameters and new closed loop control techniques to reduce muscle fatigue [16][152].

The state-of-the-art electrical stimulators topologies are described by the scheme of Figure 2.14.

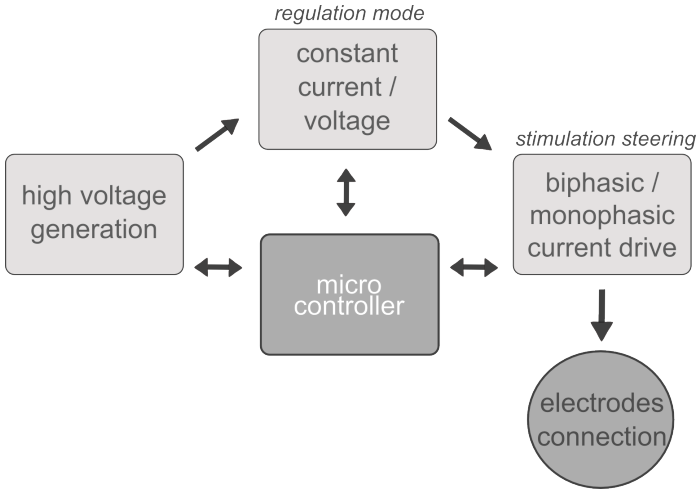

Figure 2.14: Generic configuration of the state of the art stimulators. The Regulation Mode and Stimulation Steering blocks define the Output Stage of the electrical stimulator.

In the following sections the circuit block diagrams, exposed in Figure 2.14, will be individually described.

2.4.1 Micro-controller

Present solutions for electrical stimulation rely on a digital micro-controller device that handles all the peripheral blocks. This module is responsible for managing of the communication with the user, handle the high voltage circuit and apply, parametrize and control the stimuli. If it is a portable device, like the one developed in this thesis scope, the micro-controller module will also handle the battery charge and autonomy.

2.4.2 High Voltage

Typical voltages to induce charge transfer to the biological tissue are in the range of 40-200 V. To achieve this range of voltages, using a battery system, thousands of batteries in series would be required. One way of generating those voltages is through the use of standard transformers. Large secondary side voltages may be generated from low primary side transformer voltages. Transformers also have the advantage of providing *per se* a galvanic isolation between the contact impedance load and the power source. However due to high costs, dimensions, heavy weight and inefficiency, the use of transformers in current

electrical stimulators is out of trend, especially for portable devices [181][44]. A different and recent approach is based on the use of a step-up or boost converter from the class of the switched mode power converters. This circuit is capable of producing an output voltage higher than the input voltage with few components and relative simplicity of design, as shown in Figure 2.15. The efficiency of this circuit will be as higher as the use of the energy generated by the inductor when there are current variations on its terminals.

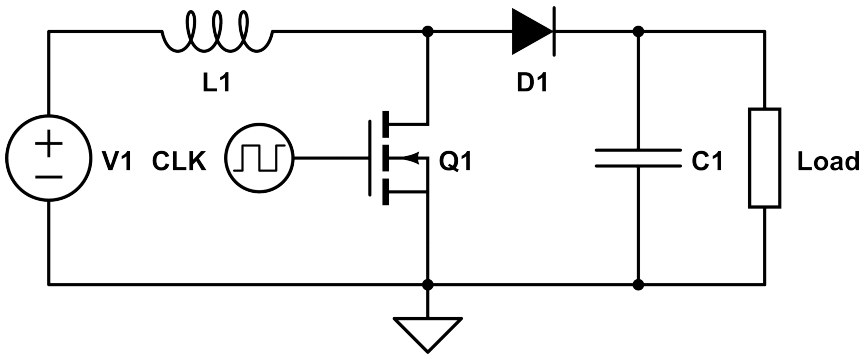

Figure 2.15: Step-up converter or Boost converter.

2.4.3 Regulation Mode

The regulation block makes the control of the electric energy passed to the tissue load. The stimulator must control one of two variables, voltage or current. Therefore, there are two classes of devices:

- *Constant Voltage:* These devices regulate the voltage of the electrical stimuli. In this configuration, the current delivered to the internal tissues is determined by the contact impedance plus the tissue impedance. Any fluctuations that may occur in one of these variables will immediately unbalance the current transferred to the tissue and consequently change the stimulation effect [163][94]. Some implementations of constant voltage stimulators also have a built-in safety system to prevent this effect from causing skin burns due to excessive current density [16][152].

- *Constant Current:* Constant current devices regulate the stimulation current independently of the tissue load and contact load variations. For the majority of the applications this implementation will enable a higher consistency between the stimulus parameter and the respective effect. This position is consensual among the scientific community [193][160][140][184].

A common circuit to generate constant current stimuli is the current source shown in Figure 2.16. In this circuit the output current can be controlled according to Equation 2.3.

$$I_{out} = \frac{V_{in}(inputsignal)}{Rsense} \tag{2.3}$$

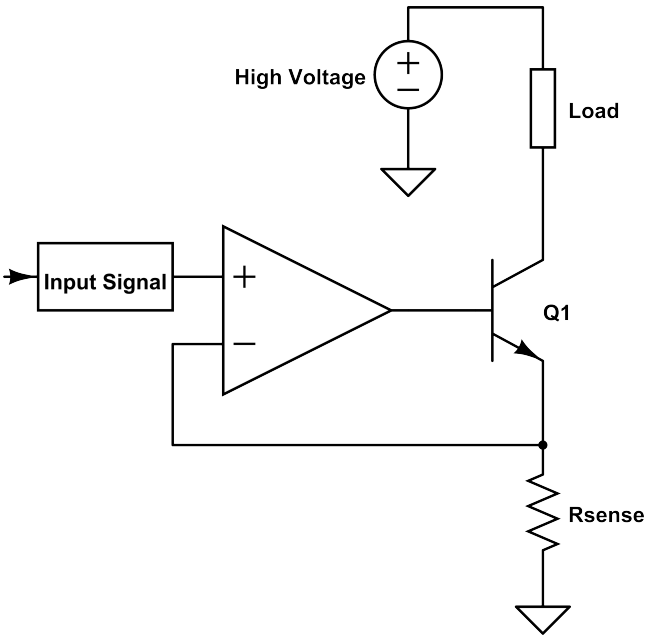

Figure 2.16: Output stage for a constant current stimulator with a voltage controllable current source.

The operational amplifier (op-amp), actuates in an active feedback, managing the base of *Q1* to control the collector and emitter current, equalizing the voltages in the op-amp inputs V_{in+} and V_{in-}. The current that will flow into the tissue, represented by Load, is sensed through a sense resistor, *Rsense*.

An alternative topology for constant current stimulators is presented by Wu et al. [193] and represented on Figure 2.17. In this circuit, two current sources drive the Wilson Current Mirrors. Half circuit is to drive positive stimuli and the other half drives the negative ones. This implementation also needs the use of two High Voltage (HV) power sources, one negative and one positive. The current applied to the skin is given by the nominal value of *R1* and *R2*.

2.4.4 Stimulation Steering

As discussed previously, some applications require the use of biphasic pulses. In this case, the current needs to flow in both directions of the electrodes. The stimulation steering block defines if the hardware only applies monophasic pulses or also biphasic ones. The monophasic approach enables an implementation simplicity that biphasic circuits can not. The circuit in Figure 2.16, previously described, is an example of a monophasic constant current stimulator. Current will only flow from the HV module to the ground connector and never the opposite. An example of a biphasic constant current implementation was also described previously in Figure 2.17. With the usage of two independent HV modules (one for positive stimuli and another for negative ones), the current can flow in both directions on the tissue. Another option for generating biphasic electrical stimuli is through

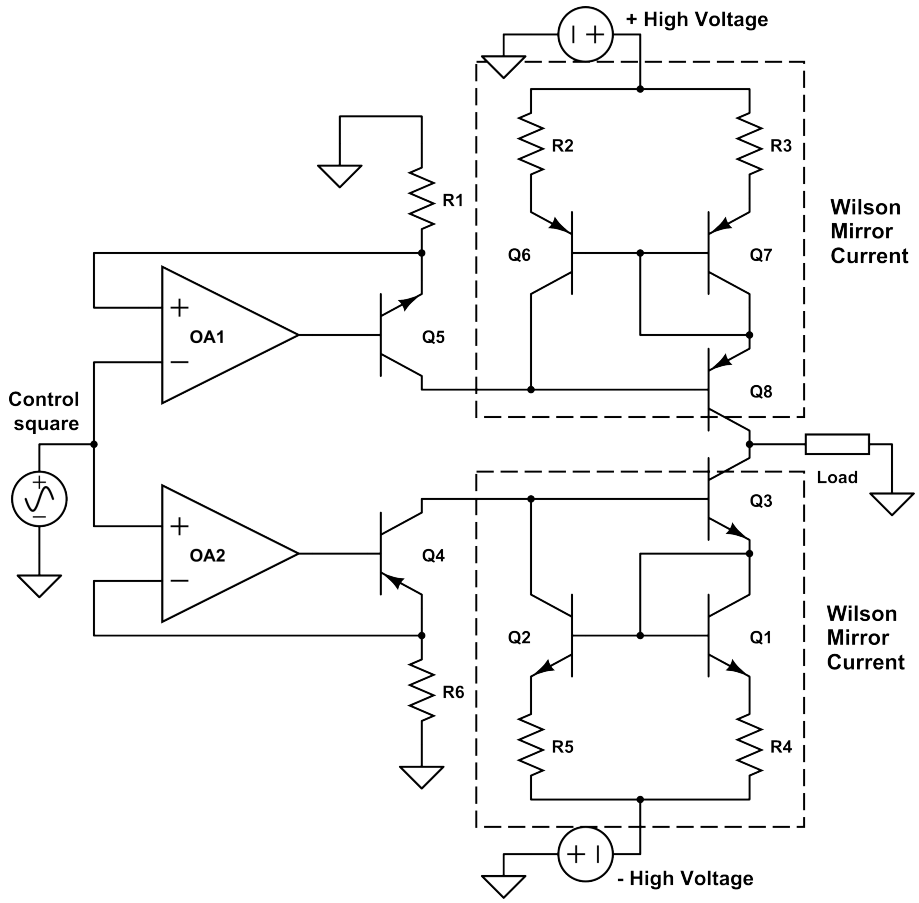

Figure 2.17: Output stage for constant current stimulator with two high voltages sources and two Wilson current mirrors [193].

the use of centered referenced transformers. With two distinct coils on the secondary, it is possible to generate two independent power supplies. This implementation is not very common, for reasons already explained previously, in the generation of high voltages, given the required size and inefficiency.

The most common method currently used for biphasic impulses generation is the polarity commutation, as exemplified in Figure 2.18 [31][100][165]. This is the simplified version of a common circuit for current commutation, and it is known as *H-bridge*. It belongs to the class of constant voltage and enables the application of biphasic pulses with the correct setting of the transistors *Q1*, *Q2*, *Q3* and *Q4* that act like a switch.

As referred previously, electrical stimulation is a fundamental instrument to study a diversity of fields associated with human physiology. When addressing the recent technology used in electrical stimulation, it is imperative to clarify an important aspect: the market offers a set of solutions already validated, with reduced dimensions and characteristics such as portability, high efficiency, high autonomy, among others; these solutions are completely focused in a single objective and therefore, the parametrizations of the devices are pre-programmed. As an example we have the vast range of electrical

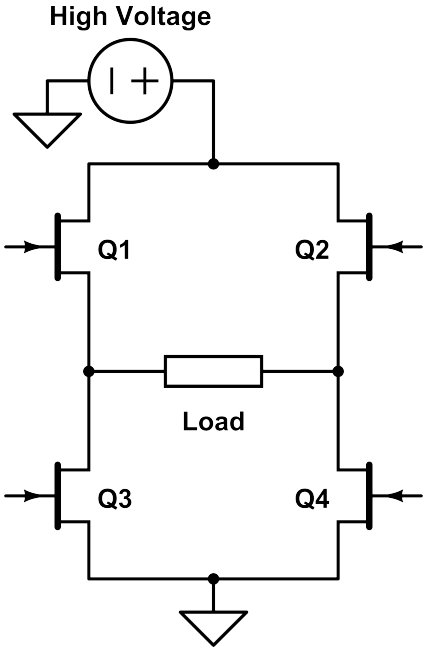

Figure 2.18: Representation of a typical current steering output stage.

stimulation for NMES. However, electrical stimulation has a much larger scope and, mainly in the research context, the degrees of freedom that the current electrical stimulation devices allow are still insufficient. This motivates the development of new hardware configurations, enabling custom parametrizations in the control of output current or voltage.

CHAPTER 3

PROPOSED SOLUTION

The answers to the previously raised questions represent important contributions to achieve new goals and knowledge in the electrophysiological field. The challenges raised by these questions are inaccessible with current market technology. In this regard, it is necessary to develop new methodologies for non-invasive human electrical stimulation. In this chapter, the main steps in the development of an electrical stimulator with reliable temporal synchronization with a biosignal acquisition system are described. All the device's modules and their operation are depicted, as well as the configuration and control software and the device's mechanical components.

3.1 Requirements

The first development stage of any solution is an effective requirement analysis. The requirements for this project were defined as a set of functional, technical, usability and other characteristics that make it possible to answer the scientific questions previously raised.

3.1.1 Functional and Technical Requirements

In order to achieve an efficient operation in the wide contexts of electrical stimulation, during the device design plan, some functional characteristics were defined. Those characteristics are enumerated below.

1. **Parametrization:** The electrical stimulator should allow to completely parametrize the electrical pulses applied. The parametrization of an electrical stimulus has a direct influence on the physiological response of the stimulated tissue. A greater freedom of electrical pulse parametrization allows a broader control of some parameters already

studied (frequency, amplitude, pulse-width) and others in which the physiological response is still unknown (pulse waveform, charge and polarity).

2. **Storage:** The system should be able to store stimulation modes, each one with different waveforms, frequencies, amplitudes and times. It should also store stimulation sessions, which enable changes between modes in pre-programmed times. Data must be retained for the same duration of the hardware's lifetime.

3. **Communication:** In order to maximize usability and autonomy, all the control and device configuration should be done using a generic wireless application.

4. **Synchronization:** The system should be interoperable with a biosignal acquisition system. This key feature is fundamental for the evaluation of stimulus/response studies which are essential for the understanding of the human physiology and in the diagnosis of neurodegenerative pathologies. This feature is also important for the closed loop systems used in Functional Electrical Stimulation (FES). In those cases, the electrical stimuli are optimized according to the biofeedback acquired from the sensors.

5. **Input/Output external trigger:** The possibility of assigning an external pin as an input or output trigger could be an important feature for market systems integration and for external devices control, such as servo motors, among others.

6. **Low Intrusiveness:** The system should contain characteristics which minimize as much as possible the impact of its usage on the test subjects. Constraints such as weight, dimension or wires can cause a psychological impact that may have an effect on the results or on the clinical methodology efficiency.

7. **Enclosure:** The hardware should be completely closed, with a simple On/Off button, a status indicator and the necessary plugs for stimulation, external communication and charging.

8. **Autonomy:** The device should have a high energy efficiency to increase the autonomy of the system and consequently increase the usability.

To fulfill each of the functional requirements here depicted, the device needs to meet one or more technical characteristics, requiring specific technical dimensioning. Table 3.1 gathers the functional requirements and presents the respective technical requirements of the developed system.

Other requirements, non functional or technical, were also taken into account, and are briefly described in the following sections.

Table 3.1: Functional requirements and the correspondent technical requirements.

Functional Requirements	**Technical Requirements**
1. Parametrization	Current modulation; Current range: [-100:100] mA ($\leq$0.1 mA); Frequency: [1:200] Hz ($\leq$1 Hz); Pulse-width: [5:500] us ($\leq$5 μs); Monophasic and Biphasic drive possibility; Waveform Design Possibility;
2. Storage	Possibility to have a storage architecture in the device memory to automate the stimulation protocols (modes and session storing);
3. Communication	The circuit should contain a *Bluetooth* module with protocol v2.0;
4. Synchronization	Development of specific electronics for synchronization cable, connected through digital port;
5. Input/Output external trigger	Digital pin Transistor-Transistor Logic (TTL), Inter-Integrated Circuit (I2C) for other systems interoperability;
6. Low Intrusiveness	Small dimensions and light weight; Portable; Wireless;
7. Enclosure	Closed hardware; On/Off button switch; LED bi-color interface, informing device state using color and frequency; Jack plug for stimulation, digital plug for external communication and jack plug for charging;
8. Autonomy	The circuit should maximize the energy efficiency, supplied by a single Lithium battery of 3.7V.

3.1.2 Usability Requirements

Usability requirements are also very important and need to be considered carefully in the development of the system.

Ease of use affects the users performance, their satisfaction and affects whether the product is used or not [80]. To answer the scientific questions raised before and for reliability purposes, the methodology needs to be applied on subjects with different clinical conditions and pathologies with different severity. Those conditions can drastically compromise the freedom of movement, the comprehension and the cooperation capacity in the clinical application. Characteristics such as portability, wireless communication and simple hardware enclosure, as noted before, already improve usability. It is important that the device itself has an high usability, a steep learning curve and that the user-interface should have a clean and easy to use control.

3.1.3 Safety Requirements

As this device will drive high voltages to the human body (hundreds of Volts), specific safety requirements must also be considered.

For any error that the system may have, the device should automatically stop the current flow that goes to the human body. The high voltage module should be immediately turned off.

The system should detect if the connection between the interface and the device is lost. When that happens, the device should immediately stop the electrical current application and turn off the high voltage module.

An excess of bad usage or skin saturation may cause short-circuits in the stimulation electrodes. The device should detect the short-circuits and immediately limit the output current.

3.1.4 Software Requirements

The hardware architecture enables command input from an external software currently running in Windows or Android Platform.

The software interface should enable the full parametrization and control of the device and can be developed with no language restrictions, as long as it implements the communication layer between software and firmware, called Application Programming Interface (API). The main requirement for the API resides in the fidelity and reliability of communication when sending or receiving commands between device and interface.

Whichever interface that may be implemented needs to fulfill all safety regulations or standards for electrical stimulation devices.

The interface should inform about the device state: turned off, idle mode or stimulating. The interface should also inform the *Bluetooth* connection status: if the connection is being lost or if the device is out of range.

These requirements guided the development of a transcutaneous neuromuscular electrical stimulator. Its design, concerning hardware dimensioning, will be described in the following section.

3.2 Hardware

The hardware for the solution developed can be divided into several modules and sub-modules. The main modules of the electrical stimulator are illustrated in Figure 3.1 and enumerated next.

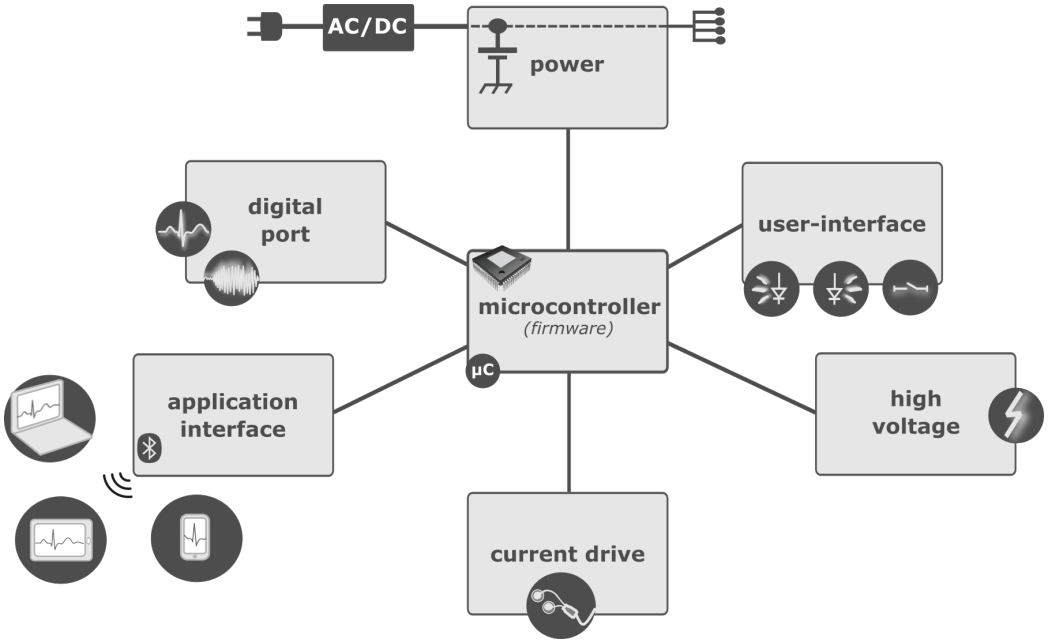

Figure 3.1: Overview of the hardware architecture.

- **Microcontroller, μC**: This is the main module of the device, being the intelligent processing unit which controls the whole system.
- **Power**: Responsible for power supply of all the modules and battery charge management.
- **High Voltage**: Responsible for generating high voltage which is used in non-invasive electrical stimulation.
- **User interface**: To control, secure and inform the basic device functions.
- **Current drive**: Responsible for current control and steering.
- **Digital port**: Used for the synchronization with the biosignals acquisition unit, as an external actuator, or as an input/output trigger.

- **Application interface**: Establishes the communication interface with the control application (software).

In the following sections, each module will be described in detail.

3.2.1 Microcontroller

The microcontroller ensures the management of the whole system. This processing unit is connected to all the submodules, transmitting or receiving control commands. It is configured to make decisions based on the external commands received through the Universal Asynchronous Receiver/Transmitter (UART) from the serial port and the information from the system modules. The microcontroller is also capable of sending information in the opposite direction, to the application.

On the scheme in Figure 3.2, the input/output flow between the microcontroller and the system constituent modules are represented.

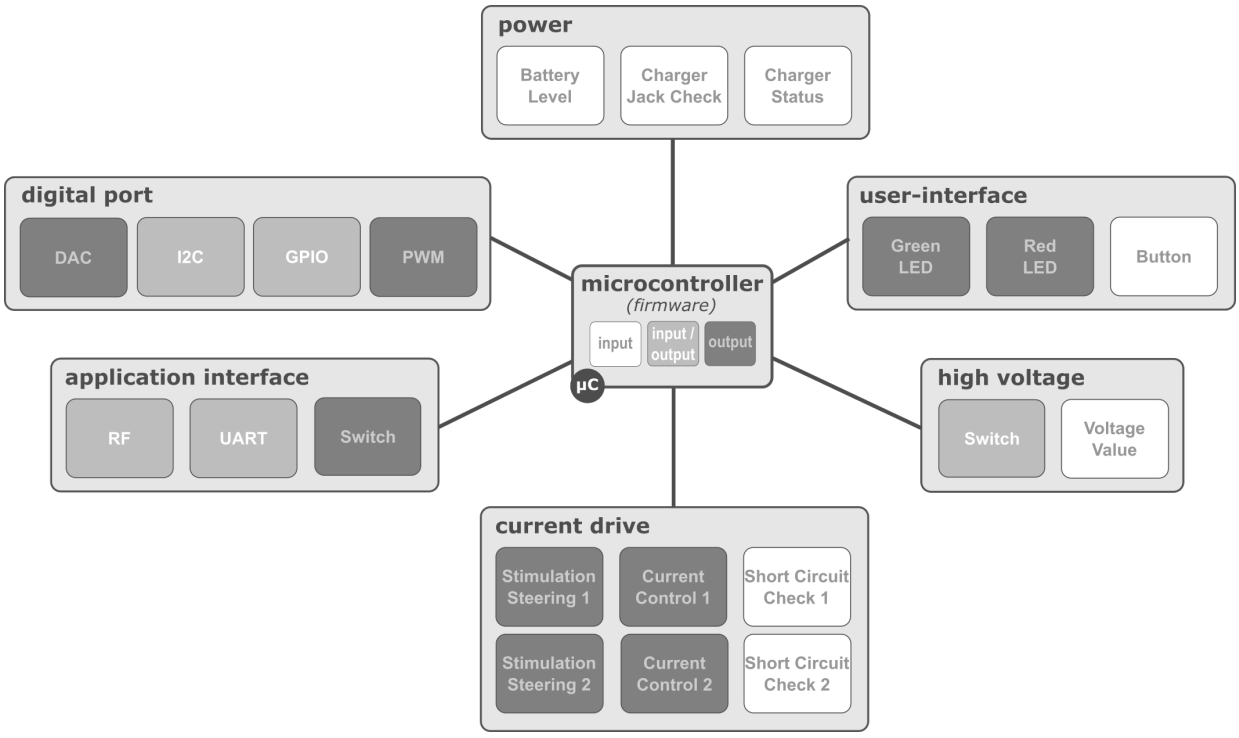

Figure 3.2: Overview of the modules for the whole system and correspondent data flow inputs/outputs for the microcontroller.

The microcontroller acts according to an embedded code, called firmware. The following sections will describe the developed firmware architecture and the microcontroller's memory allocation.

3.2.1.1 Memory

To fully understand the mechanism of the microncontroller, first it is important to clarify its memory structure. The architecture of a microcontroller has two main memory partitions: the program memory and the data memory. The executable code can reside only in the program memory, while data can be stored both in program memory and data memory. The data memory has volatile spaces, which comprises data erased every time the microcontroller reboots, and non-volatile memory spaces, the data that is kept during the lifetime of the microcontroller [11].

Figure 3.3 represents the memory structure of the microcontroller used. In this specific device the memory is allocated in three main types that will be described next

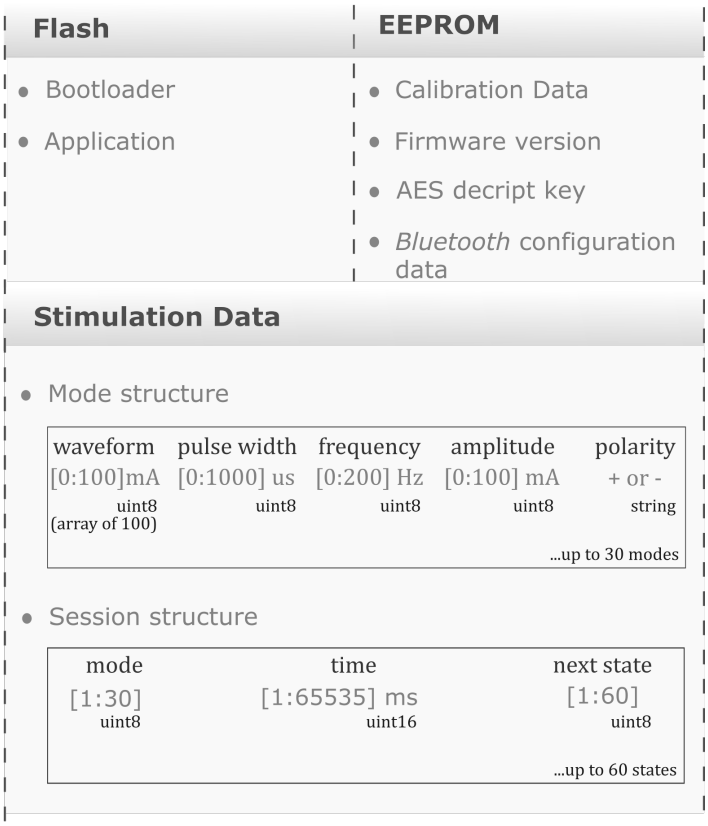

Figure 3.3: The three main memory types and its structure on the device.

The **Flash Memory** stores the application code and the bootloader. It is a non-volatile memory which can be accessed to read and write from an external programmer or from application software. The application code is the set of instructions that define the behavior of the system. A bootloader is a program that runs in the microcontroller and upon receiving new code instructions, writes it into the program memory. Therefore, the bootloader gives the microcontroller the ability to reprogram its own flash. It is mostly used to make firmware application updates [48]. The bootloader code is only executed

when a new firmware version is detected in the first set of instructions of the application.

The **Electrically-Erasable Programmable Read-Only Memory (EEPROM)** is also a non-volatile memory, used to store data. It is possible to read from the EEPROM unlimited times, but the writing is limited (between 100000 and 1 million). Being non-volatile, the EEPROM retains its contents even when the power is turned off. The EEPROM is similar to the Flash Memory, but much slower to access [156]. This memory space was used to store static values such as:

- The calibration data of the Analog-to-Digital Converter (ADC) and the Digital-to-Analog Converter (DAC);
- The firmware version number, for updates control and hardware compatibility management;
- The Advanced Encryption Standard (AES), an encryption key used for the command encryption;
- The data for the *Bluetooth* module name, baud rate and communication configuration.

Finally, the **Stimulation Data**, is stored on a volatile memory space, meaning that the information is erased in every reboot. One of the gaps in current electrostimulator devices is the lack of freedom to schedule a stimulation session, *i.e.*, a set of different stimuli, applied for a specific time and order. To overcome this, a static memory structure was conceived, enabling the storage of one electrostimulation session, with different impulse parametrization, different durations and different ordering. This structure can be divided into modes and sessions.

A mode is a set of impulse parametrizations: pulse-width, frequency, amplitude, polarization and the waveform itself. In Figure 3.3 it is possible to see the type and range of each parameter. For the waveform, the system receives an array (of 100 points) with a temporal representation of the electrical impulse. This array has a resolution of 5 μs in time and 25 μA in amplitude. Each mode stored is associated to a number, and is possible to store up to 30 different modes. A session is a set of scheduled modes and correspondent duration. Each line of the session table is called state and is composed with a mode, a time duration and the indication of the next state. The next state parameter allows the creation of loop sessions. It is possible to store up to 60 states in one session.

The stimulation data stored in the device memory can be read and re-written through the application interface, using a set of instructions defined in the firmware that access and changes this memory space.

3.2.1.2 Firmware

The firmware is the source code with all the instructions that the microcontroller runs. The general operation of the application code is schematized in Figure 3.4.

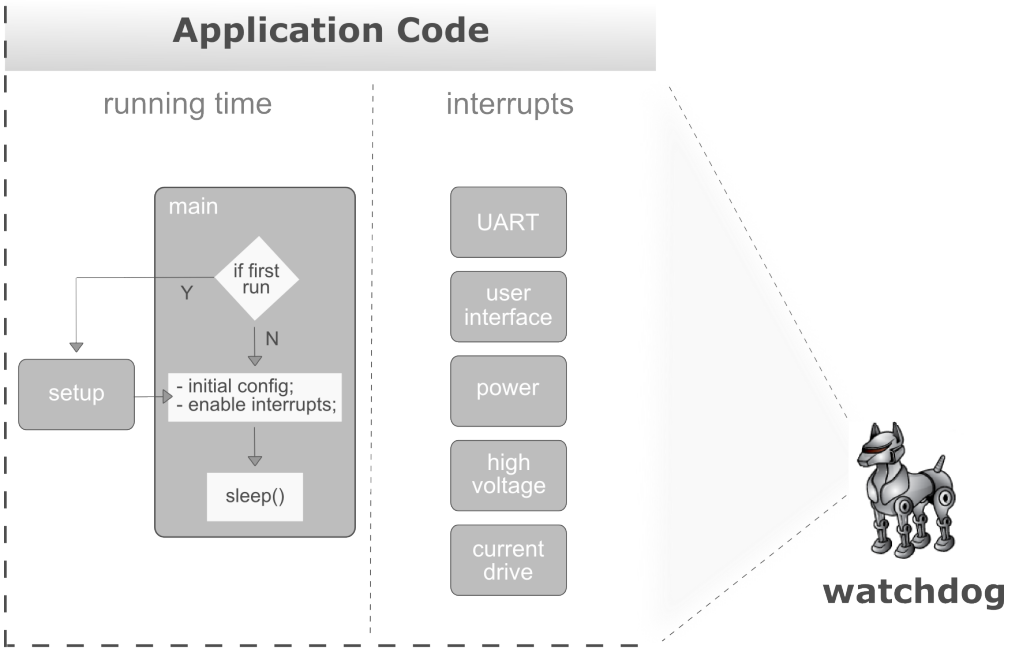

Figure 3.4: Structure of the application code.

To optimize energy consumption and processing capacity, the code structure is based on a workflow which allows the main cycle, the one that is most called, to be just a sleep instruction. That will make the microcontroller spend most of the time on an energy saving mode. To achieve that, all the operation code and system management works with interrupts, minimizing blocking routines. The microcontroller used works at 32 MHz, which allows a very fast execution of the instructions given, and spend the rest of the time on energy saving mode. Five groups of system interrupts were defined:

1. The UART interrupts, which are associated with the communication command exchanging with the control application;
2. The interrupts of the user interface: the Light Emitting Diode (LED) and the button;
3. The interrupts of the power module;
4. The interrupts of the high voltage module;
5. The interrupts of the current drive module.

In the event of an abnormal operation of the microcontroller, there is a protection mechanism, called 'Watchdog', which will reset the program counter, forcing the system to reboot and return to the factory settings.

The main application routines and the interruption groups will be briefly described next.

MAIN():
In many programming languages, the main function is where a program starts its execution. The first instruction of the MAIN routine is to verify if this is the first run of the application or not. If yes, it will call the SETUP routine, otherwise it will perform some extra configurations, like turning on the *Bluetooth* module and other peripherals that need to be initialized, enable the interrupts and turn on the sleep mode waiting for the next interruption.

SETUP():
The SETUP routine is called in the the first run of the system or after an hard reset done by the watchdog. This routine is the responsible for the configuration of the microcontroller and its peripherals.

This routine first evaluates if there are firmware updates available. If so, the stack is passed on to the *bootloader* so that the application code is re-written. However, most of the times there are no updates, and therefore the application code proceeds with the following configuration steps:

1. Peripherals configuration (DAC, ADC, timers, etc);
2. Peripherals calibration (DAC and ADC);
3. Port configuration and assignment;
4. *Bluetooth* programming (name, baud rate, communication set up);
5. Variables and structures memory allocation;
6. Prioritization of interrupts.

The last step of the SETUP configuration process is crucial for the correct functioning of the system. With all the application codes based only on interrupts, there is a possibility of simultaneous occurrences. In these cases, the microcontroller needs to know which interrupt should be handled first, and therefore a prioritization is very important. The microcontroller enables 3 priority levels for the interrupts.

UART INTERRUPTS():
The UART will raise an interrupt any time the system needs to send or receive a command from or to the application control. In the application code, these commands are divided into received or transmitted commands. For the commands being received, the first step is to validate them. Several validation mechanisms were implemented, such as the Cyclic Redundancy Check (CRC) of 8bits [192], which guarantees that the command is not

corrupt and comes from the application control. Then, the command is forwarded to its class. Received commands are described in the API section and concerns mainly the configuration of the device, start or stop stimulation and system test. For each command received, there is always an immediate response to the application control, after the command validation, with an Acknowledge (ACK) or Not Ok (NOK). The integrity command validation process is reversed in terms of command transmission. The data being transmitted can be divided into three classes:

1. **Stimulation Data**: Skin impedance, short circuit check, stimulation trigger when in automatic session mode;
2. **Test data**: Used in the system test;
3. **System data**: Battery value, loss of communication, hardware and firmware version, high voltage module state and value

On Figure 3.5 it is represented the command reception and data transmission.

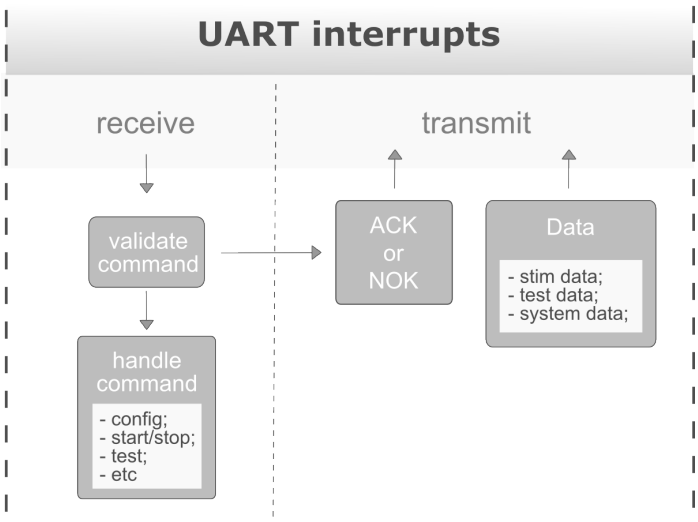

Figure 3.5: Illustration of the UART interrupts divided into received or sent commands.

POWER MODULE INTERRUPTS():

The power module will raise tree types of interrupts.

- **Jack check interrupt**: To notify the system if the jack charger is on. If so, the system will automatically turn off the stimulation.
- **Battery charge state interrupt:** The interrupt will be raised any time that there is a change in the internal battery charging state. The charger states are:
    1. Not charging;

2. Charging;
3. Charge error number 1 (over temperature, which is related to over current on the battery);
4. Charge error number 2 (the jack is on but there is no current on the system to perform the battery charge).

- **Battery level interrupt:** This interrupt warns the user when the device battery is below 30% of its nominal value. When this happens, there is also a change of the LED state (described in the User Interface interrupts class).

`HIGH VOLTAGE INTERRUPTS():`

The high voltage module raises two groups of interrupts: state and value interrupts.

- **State interrupts**: The state interrupts can be '*high voltage is ON*', '*high voltage is OFF*' and '*error on generating high voltage*'.
- **Value interrupts**: This interrupt updates the system with the output high voltage value, programmable between 80V and 120V, and the input voltage of this module, so that the system can handle possible bad behaviors.

`CURRENT DRIVE INTERRUPTS():`

The current drive interrupts are divided into three subclasses, as it can be seen bellow.

- The **Stimulation control:** Contains the current steering interrupts (controlling the polarity of the electric pulse), the current control (controlling the current intensity of the electric pulse) and all the remaining stimulation parameters gathered from the mode structure and session structure. These sets of interrupts are specially optimized as they occur at least at a 200kHz rate.
- **Stimulation data:** These interrupts are responsible for giving information to the system regarding skin impedance, short circuit check and stimulation trigger, when in automatic session mode.
- **Digital port:** Handle all the communications of the digital port. This will be described in more detail in the Digital Port Module section.

`USER INTERFACE INTERRUPTS():`

The physical interface with the user consists in a single button and two LED indicators, one red and one green. Table 3.2 gathers the system states and correspondent LED changes. The system state's changes will automatically trigger an interrupt concerning the LED color and frequency.

The button essentially toggles the system state between ON (idle) and OFF. If the button is pressed on idle mode or stimulating, it will turn off the device and disable all interrupts, except the button and power interrupts. If the button is pressed when the

Table 3.2: The LEDs indication and correspondent device state.

LEDs	**State**
Green: OFF Red: OFF	System sleeping
Green: 1Hz Red: OFF	Idle mode
Green: 2Hz Red: OFF	Stimulating
Green: OFF Red: 1Hz	Idle mode with low battery
Green: OFF Red: 2Hz	Stimulating with low battery
Green: Permanent Red: OFF	Charging
Green: Permanent Red: Blink Once	Charging error 1
Green: Permanent Red: Blink Twice	Charging error 2
Green: 1Hz Red: Blink three times	Device is ON and the High Voltage was turned on

device is turned off, automatically it will run the main code. There is also a security mechanism associated with the button event: if the button is pressed when stimulating, it will automatically turn off the high voltage module and the current drive module.

Through the firmware, the microcontroller communicates with all the peripheral modules. In the following sections, the data flow between the microcontroller and the specific module will be described.

3.2.2 Power

The power module controls the supply maintenance of the system. This module comprises a battery, a battery charge management block, an instantaneous current control and a linear regulation block (Figure 3.6).

For safety reasons, the stimulation device is powered by a 3.7 V Lithium battery pack with a capacity of 800 mAh. This allows for 5 hours of continuous supramaximal

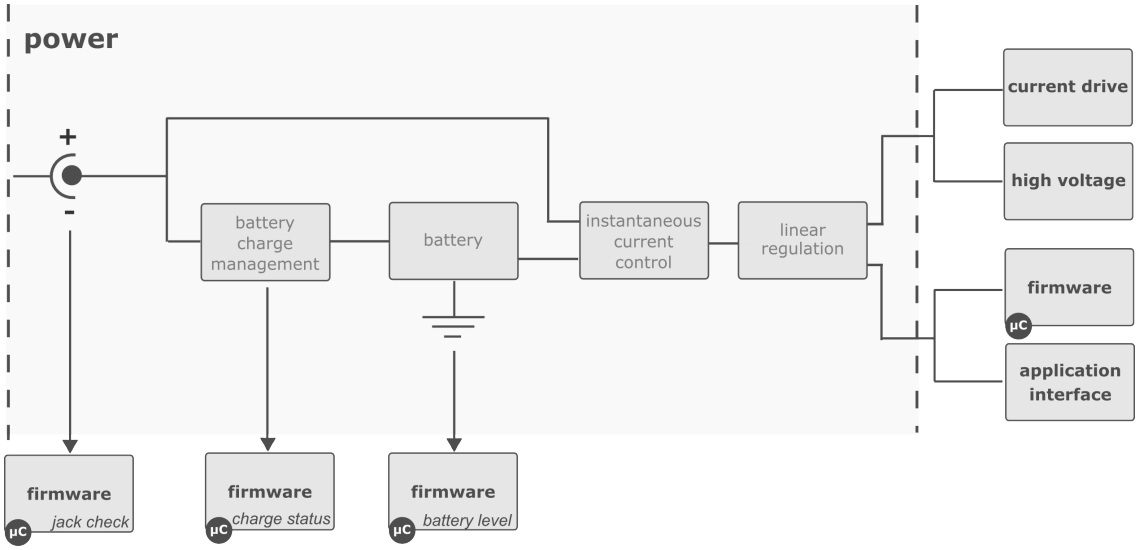

Figure 3.6: Illustration of the power module architecture.

stimulation and up to 24 hours of idle mode. The battery has a control block integrated, that verifies if the battery is working correctly in order to prevent over-heating and over-charging. Whenever one of these situations occurs, the electrical flow is automatically interrupted, and the system is turned-off.

The battery charge management block assures correct battery charging. This block transmits the information regarding the charging status (*'in process'* or *'concluded'*), to the microcontroller, and reports the errors that may occur. This block has also a protection chip which controls the current and charge that are given to the battery. The device has a protection mechanism that interrupts the charging if an excessive current is provided.

The system was dimensioned for exclusive use of a medical grade Alternating Current (AC) Power adapter. The wireless stimulation unit can be used when in charging mode, without any possible harmful effects to the users, since the AC power adapter follows the human electrical safety standards. However, as an additional safety measure, when the device is charging its usage is limited to configuring sessions, modes or the device itself, not allowing electrical stimulation. To prevent incorrect usages, the power module detects if the charger jack was connected and immediately turns off the high voltage module and current drive module.

An instantaneous current control module was implemented, enabling the control of instantaneous current consumption. This also guarantees that the current does not exceed a critical safety value and that, regardless of the current drawn from the other modules during charging, the battery charging time is always standardized, depending only on the battery capacity. To maximize the battery life, its voltage never reaches full discharge. When the battery is at its lowest charge, it takes around 1 hour and a half to totally re-charge.

Finally, the voltage control of the system submodules is done through a Low-dropout Regulator (LDO). An LDO with two independent outputs is used. One of the outputs refers to the supply and stabilization of the high voltage and current drive modules, which are essentially analog. The remainder output supplies the digital modules: the communication and the microcontroller modules. This way, possible interferences between digital and analog modules are mitigated.

3.2.3 High Voltage

Due to rather high electrode-skin impedance (several kΩ), a high Direct Current (DC) voltage is needed for the generation of 50 to 100 mA current pulses that are used for supra maximal stimulation of muscles, for example. The production of constant voltages near 100 V, with currents that can easily reach 100mA in a portable system powered at 3.7 V is an engineering challenge. This circuit is based on the basic principle of the DC-DC step up converter or boost converter, described in the previous chapter (as schematized in 2.15). It is highly optimized to reach the output power needed with the lowest consumption possible.

As seen in Figure 3.7, the module contains a management unit and a step up circuit. The former reports informations to the microcontroller, such as errors in the generation of high voltage or simply the input voltage value. It also physically turns on and off the step up boost module and selects the voltage output value, which can be adjustable between 80 and 120 V. The step up boost module powers the constant current stimulation pulse generator on the current drive module.

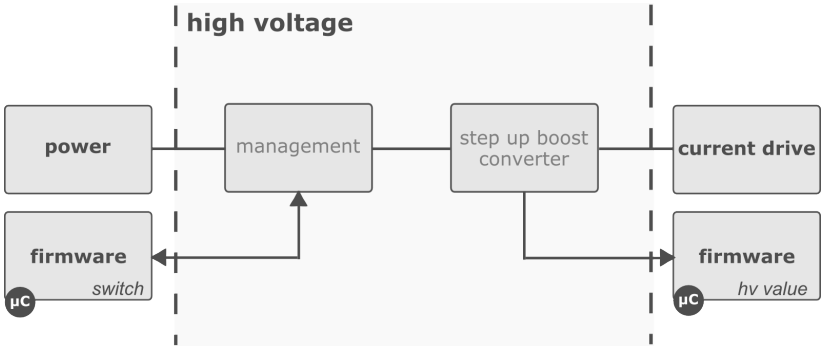

Figure 3.7: Illustration of the high voltage module architecture.

This is a critical module, not only because of the performance required but also because of its impact in the whole circuit. The generation of high voltage in a boost converter topology forces the usage of several frequencies varying between 100 kHz and several MHz. Such frequencies originate current glitches in the maintenance circuit. If not handled adequately, those glitches easily condition the whole system and contaminate all signals of the circuit. For that, it was necessary to efficiently isolate the high voltage circuit, working at the physical layers of a Printed Circuit Board (PCB) and respective signal planes.

3.2.4 User interface

To maintain a high usability, the system only has a physical button and two LED indicators (red and green). The detailed operation modes of the indicator LED and the button were described previously in the firmware section. One of the button's features is the emergency stop of the electrical stimulation. Therefore, the button needs to be very responsive, enabling high precision in the detection of true actions and maximum discrimination of false positives. The design of the button was optimized taken into consideration the reliability and responsiveness of its function. It was printed on a PCB and actuated through a conductor circumference which closes the button's contact in 360°. This conductor surface is coupled to a rubber interface available to the user. The indicators LED are placed in the center of the button and with custom optical guides the light is uniformly transmitted over the rubber interface. This way, the button is more reliable and sensitive, and allow an easy visualization of the device state through the LED. Figure 3.8 presents a photography of the device's button with integrated green and red LED.

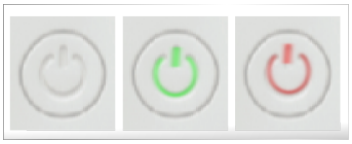

Figure 3.8: Device button turned off and with green and red LED turned on.

3.2.5 Current drive

The current drive module is responsible for providing the final current to the biological tissue. This module needs to control the intensity and polarity of the electrical stimulus. In some contemporary approaches, the control of the intensity and the polarity is done in different modules. However, such approach adds complexity and limitations to the system, regarding the response time and the current dynamic range. The following set up implements in the same module current steering and control, for polarity and intensity control, respectively, using an architecture based in the traditional H-bridge[1]. For that, the microcontroller needs 4 control signals: Steering 1, Steering 2, Control 1 and Control 2. The functioning principle of this module is schematized in Figure 3.9.

The steering signals 1 and 2 serve as ON/OFF switches, controlling the current flow. The control signals 1 and 2 come from two DAC outputs and control the nominal current intensity in the inferior flank of the H-bridge. To allow commutation control and waveform, the control signals are updated every 5 μs.

[1]The H-bridge is highly used for all types of circuits which need current commutation, as the steppers control. In Chapter 2, the use of an H-bridge in electrostimulation is exemplified, however without integrated current control.

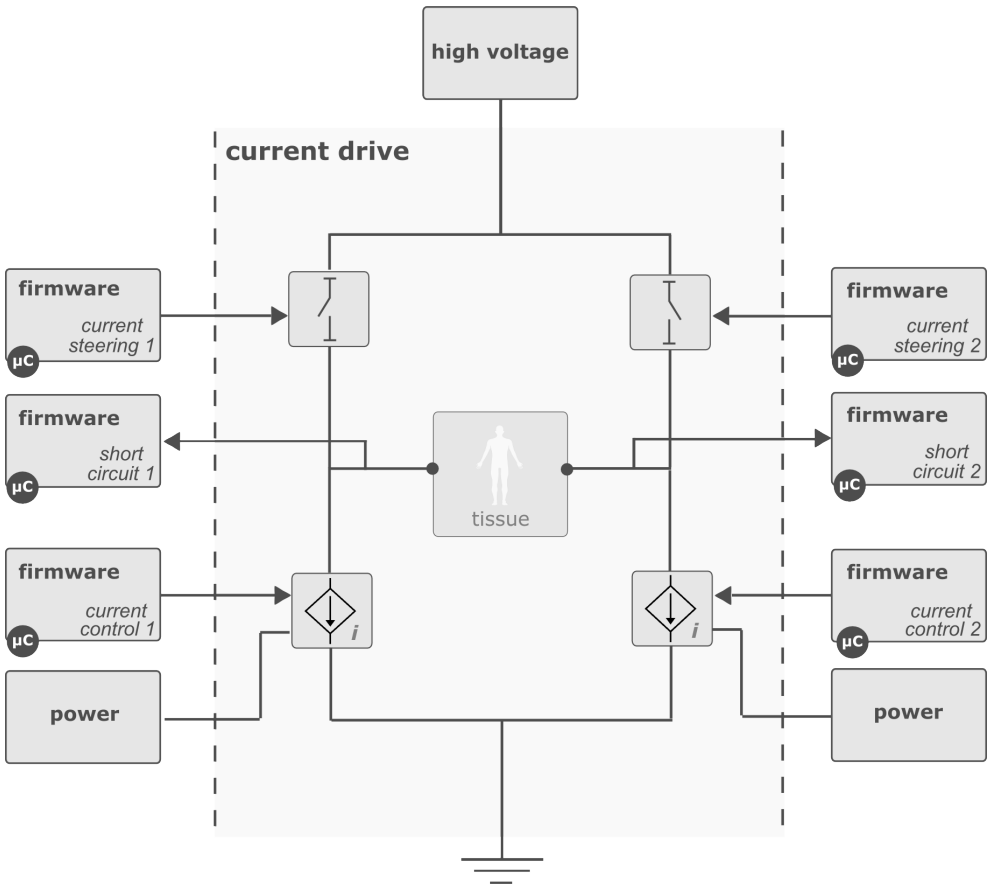

Figure 3.9: Illustration of the current drive module architecture.

To avoid distortions in the waveform of the stimulus, the analog hardware for current control needs to have a response time smaller than the time for digital control. For that, a feedback loop was implemented, with feedback times in the order of nanoseconds. The current control's digital signals are filtered for high frequency noise reduction that may appear in the circuit line that passes from the microcontroller to the current drive module. The system is designed to output a dynamic range of 0-100 mA with a resolution of 0.024 mA.

There are two states for the control signals, which correspond to the two opposite current flows:

- Positive: Steering 1 ON, Steering 2 OFF, Control 1 OFF, Control 2 controlling current;
- Negative: Steering 1 OFF, Steering 2 ON, Control 1 controlling current, Control 2 OFF.

The implementation of this module raises technological challenges worthy of attention. The steering signals actuators, represented in Figure 3.9 as switches, in OFF mode suffer from high reverse voltages that can go from some Volts to near the maximum value of

the High Voltage output. The control loops actuated by the control signals 1 and 2 in OFF mode withstand very high voltages (a value close to the High Voltage's). Given that this circuit requires quick response times, special care in the component dimensioning phase was necessary. Since the control signals can be updated every 5 μs, as mentioned before, transient signals on the analog component may need to be attenuated and handled in order to minimize its impact on the current drive and control.

This module also gives the microcontroller some information regarding the stimulation. The short circuit signal is properly conditioned to be read in ADC ports of the microcontroller. The system gathers information about the electrode impedance, skin load, possible short circuits and electrodes detachments.

3.2.6 Digital port

One of the stimulator's differentiating characteristics and of high scientific relevance is the possibility of synchronization with a biosignal acquisition system. This synchronization is one of the features enabled by the digital port module.

As defined by requirements, the digital port has an I2C communication, General Purpose Input Output (GPIO), which is used to obtain a TTL wave synchronized with the stimulus being applied, or to be an external trigger to a pre-associated stimulus. This port also has a DAC output, which allows it to obtain a low voltage replica of the stimulus being applied. As output, it has also a Pulse Width Modulation (PWM) signal, which can be used to control an external device, like a servomotor.

3.2.6.1 Synchronization with biosignals

The synchronization with the biosignal acquisition system is done through the stimulation replica signal or through the square signal of the GPIO, which can be set to oscillate from 0 to 3 V for each stimulus. The conclusions taken on the stimulus-response physiological effect are only valid if the synchronization has a much higher temporal resolution than the process that is being studied. Generally, the fastest physiological responses of human body are done in the millisecond scale. Therefore, it is reasonable to assume a synchronization definition of nanoseconds. There are no constrains regarding the processor, since it has an execution speed of 32 MHz, which means that each execution takes 31.25 nanoseconds (ns).

It is also required that the signal coming from the stimulator is galvanic isolated from the input signal of the acquisition signal. For that, optical decoupling electronics were developed. Without it, the acquisition system would suffer interferences caused by the stimulation system, affecting the reliability and quality of the signals acquired. Since the microcontroller speed of both the stimulator and the acquisition system is very high (nanoseconds), the bottleneck of this synchronization system would be in the decoupling circuit. To avoid delays in the synchronization signal, the execution speed of the decoupling system needs to be as high as possible. For that, the components

dimensioning was carefully chosen. The temporal resolution of the developed decoupling system is 3μs.

Figure 3.10 presents an illustration of the stimulation system connected with the system for biosignals acquisition through the synchronization cable.

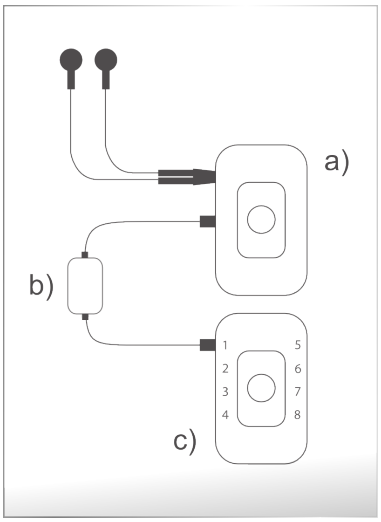

Figure 3.10: Representation scheme of the acquisition and stimulation system, with synchronization cable: a) electrical stimulator; b) synchronization electronics enclosed; c) biosignals acquisition system.

In the following chapters, where the application of the stimulator in objective studies is presented, the importance of the temporal synchronization process will be described.

3.2.6.2 External system drive

As it was described before, an important feature present in the digital port is a PWM signal. This signal, as other communication signals like the I2C protocol, can be very useful in the control of an external actuation system. An example of its usage is presented in the next chapter, where the PWM pulse is used to manage the rotation speed, the angle and direction of an external servo motor.

3.2.7 Application interface

The application interface module establishes the communication channel between the microcontroller and an external control application that integrates the API in a smartphone, a computer or a tablet device.

This module is composed by an integrated *Bluetooth* block[2], which contains a 2.4GHz

[2]Bluetooth protocol v2.0, Enhanced Data Rate (EDR), with CE and FCC certifications:

- Directive EMC 89/336/EEC, from 92/31/EEC and 93/68/EEC (electromagnetic compatibility); Directive 2002/95/EC (restriction of dangerous substances); FCC ID: QOQWT12.

Radio Transceiver, a radio frequency microcontroller and an UART serial port. The maximum range of wireless connectivity is 100 meters. This range is highly dependent on the gain of the *Bluetooth* block in the controlling device (PC, smartphone or tablet).

The wireless communication module guarantees the galvanic isolation between the user or test subject and the control system. However, using a wireless system requires additional safety considerations. The radiations emitted are electromagnetic, non-ionizing, in the radio frequency range and are intended only for air communication between the device and the control application. These radiations may interfere with other devices which use radio communication. The communication block itself may suffer interferences from other devices.

To mitigate this physical risk, it was necessary to:

- Guarantee that this radiation is inside the limits of operation, allowing the normal functioning of the device and not interfering with neighboring devices, according to directive 89/336/EEC;
- Guarantee that the *Bluetooth* technology confirms the reception of data and indicates the user when the environmental noise conditions do not allow for a reliable reception.

This section closes the hardware module description. The following section summarizes the necessary steps for the development of a final product, both to enhance usability of the system and for a quick integration in a product line. Also in the next section there will be a quick presentation of the final device main characteristics.

3.3 Electrical stimulator device

After all hardware modules are dimensioned, the next step is to layout a PCB, which will contain all components and links needed in a miniaturized way. With the PCB completed, the final step is to integrate the system in an appropriate enclosure box (Figure 3.11).

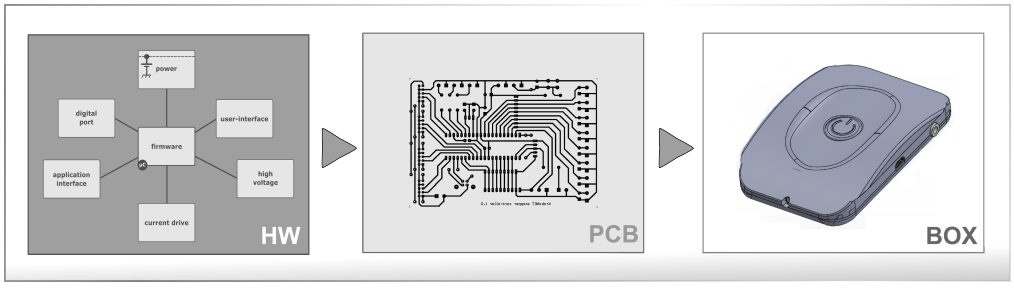

Figure 3.11: Illustration of the development cycle of the final solution, composed by three main development classes: hardware design, implementation and miniaturization on PCB and final box enclosure.

3.3.1 Printed Circuit Board

During the development stages of this device, three different PCB versions were conceived: a beta version (v0.1), still without the power module, the v1.0 version already with that module, and the current version v1.1, an enhancement of v1.0 with the possibility of session scheduling and control of the High Voltage value.

The designed PCB is composed of 4 layers with conductive tracks, drills routes for transmission of signal or power lines. The top and bottom layers host the circuit components, as illustrated in Figure 3.12.

As already referred, the design and implementation of a high performance circuit regarding voltage levels, portability and low consumption, required extra care in the PCB layout. The ground planes of high voltage occupy a dedicated area and the connection with the remainder ground planes of the board is made in a single PCB point with the aid of a filter. This way, the effects of the current peaks and the high voltage generation noise are minimized.

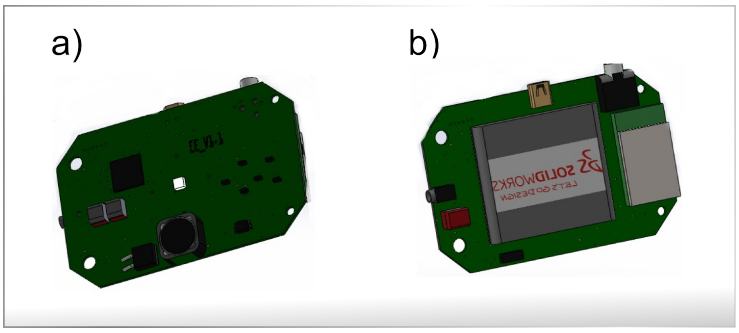

Figure 3.12: PCB version v1.1 illustration: a) top layer, with the microcontroller and indicator LED's components positioning; b) bottom layer, with the battery, the *bluetooth* module, the micro-usb synchronization channel, the stimulation and the charger jack connectors positioning.

3.3.2 Box Enclosure

For an ergonomic usage of the system, the casing enclosure has sideways connections for stimulation jack and digital port and a clip for belt attachment. In the frontal part of the casing, there is an ON/OFF button, limiting the possibility of turning on the device by accident. The casing has reduced dimensions and is light weight (84x53x10mm, 50g), given the decisions of miniaturization taken. It is composed of a top case, a base, a clip and a button, as illustrated in Figure 3.13.

There are no bulges, sharp vertexes or moving parts, minimizing the risk of physical injuries for the user. The wireless communication option also guarantees that the movement constraints during the treatment are minimum or non-existent. The casing box is sealed and does not contain any holes that would allow the non intentional introduction of solid

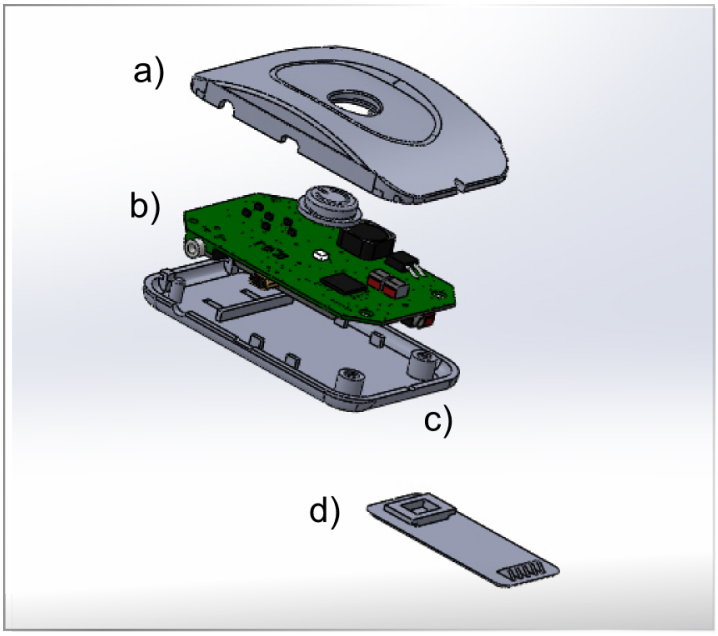

Figure 3.13: System assembly illustration: a) top case; b) PCB; c) bottom case; d) attachment belt.

substances. The system uses a micro USB plug for the digital port, because of its reliable nature, a specific jack for the charging, and a 2.5mm jack for the electrical stimulation.

The usage of the 2.5mm jack for the electrical stimulation allows the adoption of a wide range of electrical stimulation standard accessories, either within nerve stimulation, or muscular stimulation (Figure 3.14). With this standardization, a varied range of electrodes can be used with the system [172].

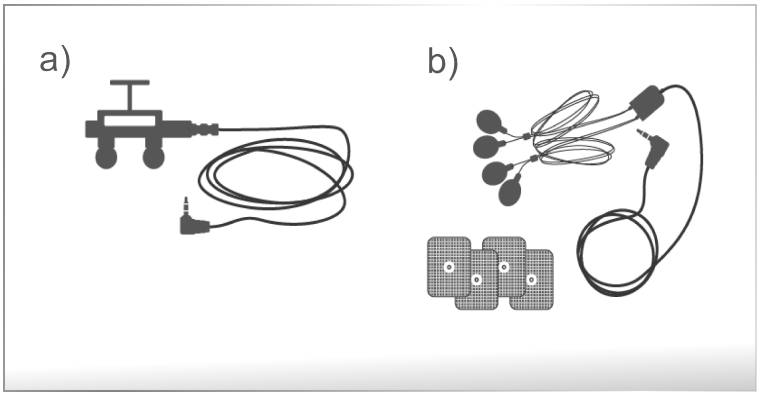

Figure 3.14: Accessories for a) nerve stimulation; b) muscle stimulation.

3.3.3 The Product

Figure 3.15 presents a photograph of the final assembly of the developed electrical stimulator. This figure also gathers the device's technical specifications.

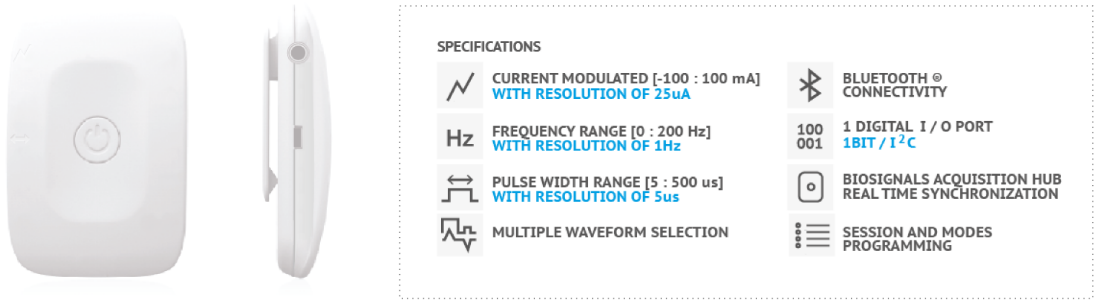

Figure 3.15: Photograph of the final electrical stimulation device and summary of specifications.

The final system that enables the electrophysiological studies performed in this PhD is composed by the electrical stimulator, the synchronization electronics here described, and the biosignalsplux system [144], a signal acquisition device from PLUX, Wireless Biosignals, S.A. [145], where this doctoral study was inserted, together with FCT-UNL. The fatigue evaluation study, that will be described in Chapter 7, is an exception since the force was evaluated through a Biodex system that was synchronized with the electrical stimulator, instead of the biosignalsplux system.

The electrical stimulator and synchronization circuit was not only developed in a purely scientific alignment, but also to fill in the gaps existent in most market devices and to include this device in the company's line of products [145]. This concern is reflected in the high usability of the system and the integration flexibility with other products, such as in the physiotherapy line, in which it is already being integrated for pelvic floor training usage.

This also has repercussions in the deeply characterization and evaluation performed to the system final specifications, executed through extensive test protocols. In the following chapter, a summary of the main procedures from the test characterization and security protocol will be described.

Attached in appendix - Appendix C - is a brochure for the electrical stimulation device developed, in which all technical features are summarized.

To fully complete the final package, software solutions were also considered and will be described next.

3.4 Software

To control the electrical stimulator device, the implementation of a software architecture was required. The hardware was designed and developed to allow greater flexibility in the stimulation control parameters. The hardware implementation delegates the real-time control in an external application where it is possible to manipulate the entire stimulation protocol. To consider a vast set of applications, from the generic to user-specific and also

to enable the control software to be platform independent, an Application Programming Interface (API) was designed.

3.4.1 API

The API is composed by a series of methods created to control and directly communicate with the device. Also, it makes the bridge between the Human Computer Interface (HCI) software and the actuation hardware. Through this API, the hardware is configured with the necessary information for the stimulation protocol and the start/stop of the session.

The API for the actuation and control of the electrical stimulator is integrated in the same architecture as the one previously developed for biosignal acquisition. The intention was to make a fully integrated acquisition and stimulation system, enabling the user the possibility of controlling both the stimulation and the acquisition in an easy and complete way. The integrated API was implemented in C++ with wrappers already developed for Python, Java and Android (Figure 3.16).

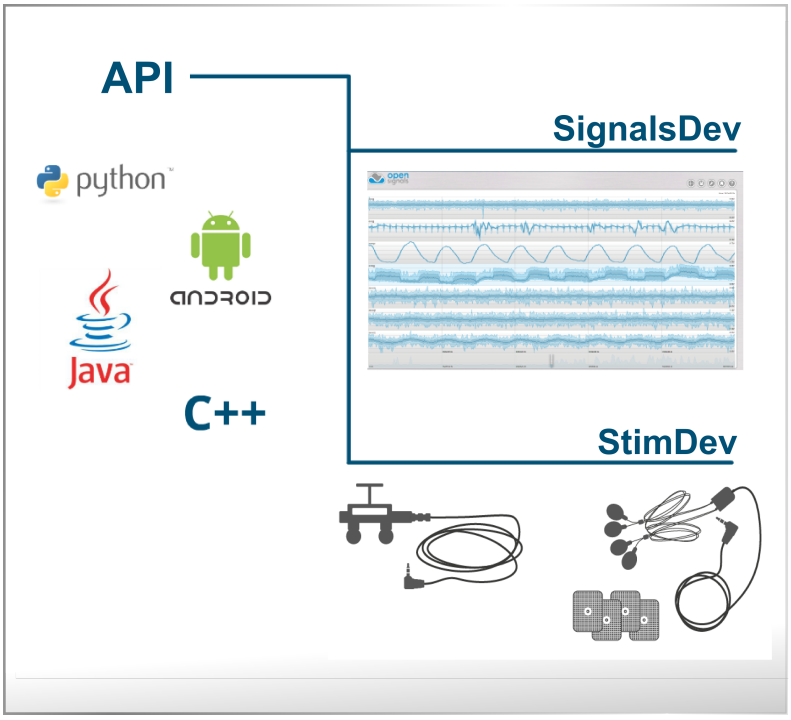

Figure 3.16: Integrated API for biosignals acquisition and control of the stimulator.

The methods comprised in the *StimDev* class of the API, are divided into five subclasses: **Device**, when referring to configurations in the stimulation device; **Stim**, with methods for the device actuation; **Mode**, for the modes configuration; **Session**, for the configuration of the sessions; **Digital Port**, for the digital port configuration. Below are small descriptions of each method in those subclasses.

- **Device**
  findDevices(): Finds a list of devices in range and return their Media Access Control (MAC) Address and description in a list. *getBattery()*: Returns the percentage of the remaining battery charge.
  setCalib(): Sets the DAC Calibration.
  setHVoltageState(bool): Sets high voltage state.

- **Stim**
  outputUnitPulse(mode): Applies an output unitary pulse of the given mode.
  startMode(mode, time): Starts a stimulation mode with the time duration given.
  readImpedance(): Returns electrodes and body tissue impedance.
  continuousRunningIfNoNet(bool): Sets if the system should continue the session or not, in case the communication is compromised.
  startSession(stateChanges): Starts a stimulation session.
  stop(): Stops any stimulation.

- **Mode**
  setWaveOnMode(wave, mode): Sets a stimulation waveform, received in an array [0-100]mA on a mode.
  setFreqOnMode(freq, mode): Associates a stimulation frequency to a mode.
  assignTriggerToMode(pin, mode): Assigns an external trigger pin to the onset of a defined mode.

- **Session**
  setTimeOnState(time, state): Sets the duration of a state, in seconds.
  setModeOnState(mode, state): Associates a stimulation mode to a state.
  setMaxStateChanges(maxChanges): Defines the maximum number of iterations of the session, in case of a closed loop.
  setTimeout(time): Sets the received timeout, in milliseconds.
  setNextStateOnState(state, nextState): Sets next state on a state.

- **Digital Port**
  setIO(bool): Sets the IO pin High or Low.
  readIO(void): Returns the value of the IO pin.
  setPWM(freq, duty): Controls the frequency and dutycycle of the PWM pin.
  I2C Command Class: This is a class for the I2C communication protocol.

This API enables the design of a closed system with pre-defined configurations, actuating the stimulator for a user's specific need, or the design of a generic interface capable

of easily change the configurations of the stimulator in each usage. Neurophysiology research, and research in general, requires differentiated applications dedicated to a specific goal. Because of this, a high percentage of the researchers usually writes custom software routines. These custom solutions rarely offer the flexibility and extensibility needed for them to be transferable across platforms, hardware configurations, and experimental set ups without significant modifications. Therefore, software/hardware solutions intended to create multi-purpose platforms (for sports, therapy or investigation) need a strong, generic and dynamic interface, which enables the user to create its own protocols [178][150].

3.4.2 Interfaces

For the intended use of a generic user interface, the core features considered were:

- Parametrize the electrostimulator with the specific needs for each protocol;
- Operation of the electrostimulator with start/stop of a session, a mode or a unit pulse;
- Real time synchronization with biosignals acquisition;
- Possibility to apply algorithms in the acquired signal and transmit feedback to the electrostimulator.

The flexibility of the developed API enables the hardware architecture to accept input commands from an interface hosted on a computer or an Android based system, via *bluetooth*. This raises new possibilities of portability and processing performance in the electrical stimulation field, as illustrated on Figure 3.17.

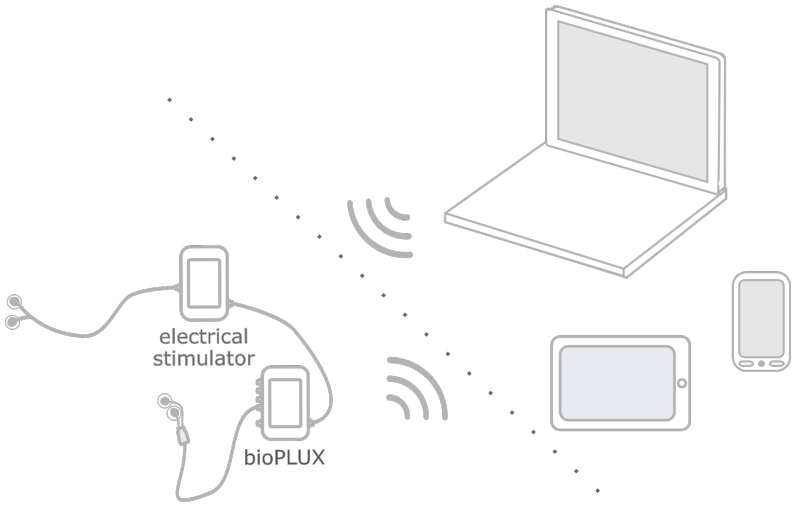

Figure 3.17: Illustration of the system communication and control flexibility.

For the integration of the stimulator with a biosignal acquisition software, a novel HCI framework was developed, enabling the final user to configure and control a variety of

electrical devices [46][47]. With the data structured by a JavaScript Object Notation (JSON) Schema [197], the software becomes robust, error free and human readable. Since the API is transversal to both devices, the HCI was also integrated in a web based software for biosignals acquisition and processing from PLUX - Wireless Biosignals, S.A. [145]. In this way, actuation, acquisition and processing is possible in a closed-loop cycle [32].

The main purpose of this software is to provide the final user the freedom to create and sequentially compile electrical impulses. This allows the user to create actuation sessions for electrical devices. Following this idea, the software was divided into configuration, where clinical professionals can configure an electrical stimulation with modes and sessions, and control, where the user just needs to choose the device and session previously configured, then start the session (Figure 3.18).

The configuration is divided into device, mode and session. In the software the modes are designed and sessions created and sent to the electrostimulator. Then, for the control phase, it is only necessary to choose the device and apply the pre-configured session, or individual mode.

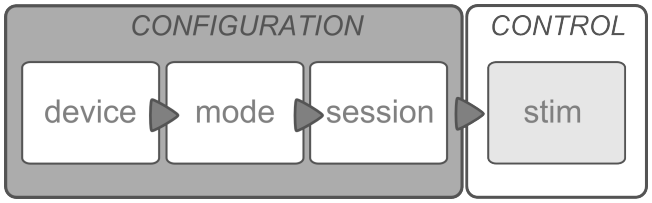

Figure 3.18: Diagram representing the standard communication flow (from configure to control). First, the device itself is configured, then the modes for the electric pulse waves and finally the sessions, using the modes created. Following the configuration it is possible to control the device and apply stimuli.

An interesting concept was developed for the creation of modes in the software. Since the hardware allows for the storage of a waveform composed of 100 points, in the interface there is a possibility for choosing pre-defined waveforms (such as square or triangular) or draw a custom waveform. Figure 3.19 shows an example of the drawing mode, in which the user can move specific dots in the interface to create the wave.

In the course of the actuation it is possible to real time monitor multiple biosignals (e.g. EMG, ECG, EEG, EDA) and synchronize them with the electrical pulse applied by the device. With this integrated tool, a user-friendly software solution is provided, using a multi-purpose platform for sports, therapy and research [46][47].

This tool allows flexibility to create electrical stimulation protocols from the fast prototyping of a pilot study to the final application on human electrophysiology. It enables the quick and easy establishment of a protocol, obtaining an overview of the previous results. However, in the in-depth studies performed, there was a necessity to manually implement dedicated protocols, using directly the API for signal acquisition and stimulation. The following chapters will present the in-depth studies performed in which the methodologies developed had a *sine qua non* role for understanding human electrophysiology.

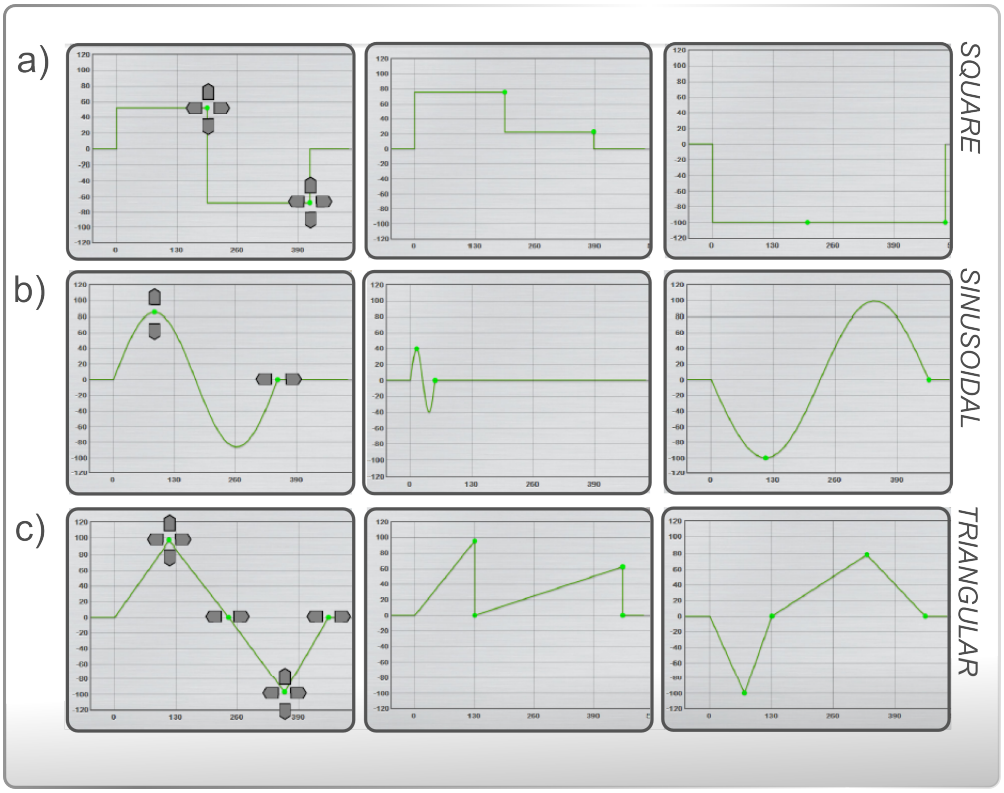

Figure 3.19: Examples of waves that can be drawn and stored in the device: a) square; b) sine; c) triangle. The arrows mark the direction in which the interactive points can be moved.

CHAPTER 4

VALIDATION

To ensure that system specifications fulfilled initial requirements, characterization and production tests were defined and performed. This chapter begins describing the implementation of those tests and expected results. During the development stage, the device profited with feedback derived from its application in the scientific context. Later in this chapter two examples of preliminary scientific validation studies will be also described.

4.1 Device Tests

Conformance testing is usually made after the development stage to determine whether a product or system complies with the requirements of a specification, contract or regulation. The tests performed to the device can be divided into characterization tests and production tests. The characterization tests were performed extensively only once, after each PCB version release to guarantee the integrity of the device. The production tests are performed for each unit that is manufactured to ensure the proper device operation.

4.1.1 Characterization Tests

The characterization tests are applied to verify all device features, technically characterize those features and ensure its integrity. The characterization tests were performed in a sampling of 5 devices by 3 different test engineers for each PCB release. The characterization tests are divided in: communication tests, battery and charge management tests and current parametrization tests.

4.1.1.1 Communication tests

The communication tests validate the *bluetooth* connection and the impact of possible signal failures in the device operation.

Table 4.1 summarizes the communication tests performed, the initial conditions required for the device and expected results. The tests evaluate how the system handles the continuous communication in standard and Central Processing Unit (CPU) overload scenarios. The system detects loss of connection and the user can predefine, through the variable Continuous Running if No Network (CRNN), if the system will continue or stop the stimulation session in eventual connection failures.

Table 4.1: Description, initial condition and expected results of the communication tests.

Description	**Initial Condition**	**Expected Results**
Keep *bluetooth* communication for an extended time period.	Device stimulating in a continuous start/stop cycle, for a minimum of 4 hours. The device should be within the *bluetooth* range limits.	Device remains in communication throughout the time of stimulation without unexpected breaks.
Communication stress.	Device stimulating in a continuous start/stop cycle, for a minimum of 4 hours. Run HeavyLoad software to overload the CPU performance.	Device remains in communication throughout the time of stimulation without unexpected breaks.
Losing range with CRNN on.	Device stimulating in a continuous start/stop cycle. CRNN true.	The device should remain in stimulation throughout the preprogramed session or mode.
Losing range with CRNN off.	Device stimulating in a continuous start/stop cycle. CRNN false.	The device should stop the stimulation and pass to the idle mode.

4.1.1.2 Battery and charge management tests

The battery characterization tests are executed by running a predefined autonomy test session that stresses at the maximum level the current output stage. The result of this test is the minimum value of autonomy that the system ensures. The tests to the charge modules confirm the correct operation of the charge management and also assess the impact of possible failures.

Table 4.2 summarizes the battery and charge management tests performed, the initial conditions required for the device and expected results.

Table 4.2: Description, initial condition and expected results of the battery and charge management tests.

Description	**Initial Condition**	**Expected Results**
Autonomy with standard battery (3.7V, 700mAh).	Device with full battery. Setup and start the predefined autonomy test session.	**Time to discharge:** minimum of 5 hours.
Power supply.	Medical class power supply.	The medical grade charger meets all required specifications or safety standards of medical device (ISO 13485).
Battery charge and time to charge.	Device with discharged battery. Medical class power supply.	The device charges without any problem or thermal overload. **Time to charge:** maximum of 1.2 hours.
Device states on charge modes.	Device charging. Medical class power supply.	The device enable idle and standby mode.
Low battery state when the device is in stimulation mode.	Device with low battery and in stimulation mode.	LED green off. LED red blink twice per second.
Low battery state when the device is in idle mode.	Device with low battery and in idle state.	LED green off. LED red blink once per second.
Discharged battery state.	Device with completely discharged battery.	The device shuts down independently of the state before discharge. LED green and red off.
Connect the charger during stimulation mode.	Device in stimulation mode. Medical class power supply.	The device stops stimulation.

4.1.1.3 Current parametrization tests

The current parametrization tests ascertain and validate the control of electrical current parametrization. Table 4.3 summarizes the current parametrization tests performed, the initial conditions required for the device and expected results.

Attached in appendix is the template grid defined to generate a test record, performed by the test engineers - Appendix D.

Table 4.3: Description, initial condition and expected results of the current parametrization tests.

Description	**Initial Condition**	**Expected Results**
Zero wave.	Device in idle mode. Set and start the zero wave on mode 1 with 0Hz.	The device do not drive current.
Stimulation modes.	Device in idle mode. Set and start the 30mA quadratic (monophasic) wave on mode 1 with 120Hz and 500 μs of pulse-width.	The device drives the quadratic wave. With the oscilloscope in run mode visualize the wave on a 400 Ohm resistor.
Drive a stimulation session.	Device in idle mode.**1-** Set 3s to state 0, 5s to state 1, 3s to state 2 and 5s to state 3. **2-** Configure mode 0 with zero wave, configure mode 1 with the quadratic monophasic wave 30mA, configure mode 2 with square wave biphasic with 60mA. Set mode 0 to state 0, mode 1 to state 1, mode 0 to state 2 and mode 2 to state 3. **3-** set Next State (NS) 1 to state 0, NS 2 to state 1, NS 3 to state 2 and NS 0 to state 3. **4-** set maximum state changes equal to 8; **5-** start the session.	With the oscilloscope in run mode visualize the wave on a 400 Ohm resistor. Evaluate if the session corresponds with the configuration done. When the session starts, the device ends the idle mode and starts the stimulation mode (green LED blinking twice per second). The stimulation session will repeat once and then will end (maximum state changes equal to 8).
Unitary stimuli drive.	Device in idle mode; Drive a unit pulse of mode 2.	With the oscilloscope in single mode visualize the wave on a 400 Ohm resistor.
Stimulation stop.	Device stimulating in a continuous start/stop session. A stop command is sent through the control application.	The device ends the stimulation mode and starts the idle mode (LED green blinks once per second).
Button pressed.	Device stimulating in a continuous start/stop cycle and on/off button is pressed.	The device will pass from stimulation mode to standby mode and immediately stops the current output.

4.1.2 Production Tests

To assure that any device manufactured operate in accordance with the guaranteed specifications, the last phase of the conception process is the execution of production tests. The production tests consist in an optimized, less exhaustive version of the characterization tests. The production tests are executed to all devices manufactured and therefore

are included in the production process. To ensure an optimized production, these tests should be executed as independent and as fast as possible. Production tests are performed evaluating specific circuit test points, while the device is in different operation modes. To verify the voltage value in the specified test points, a calibrated multimeter is used. Figure 4.1 presents an example of a circuit test point.

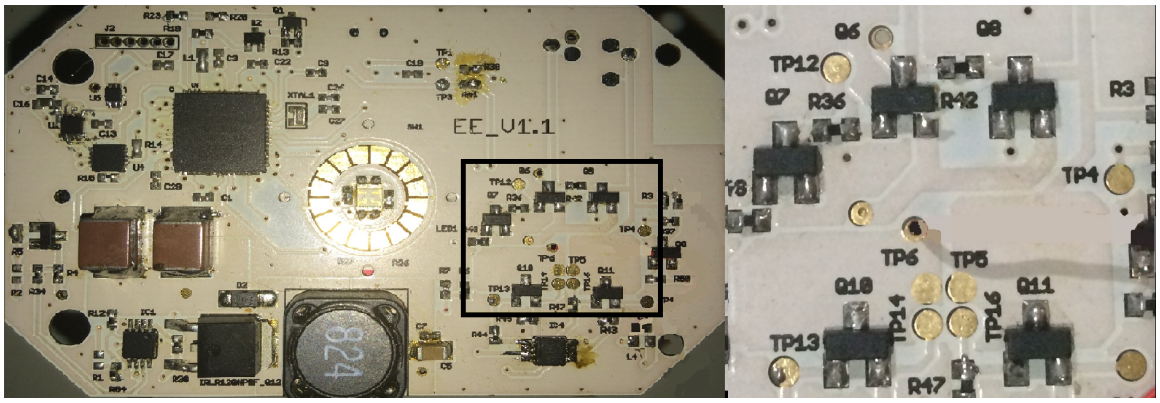

Figure 4.1: Example of a test point in the device's PCB. The TP circles represent the Test Points of the circuit.

4.2 Scientific Validation

As previously stated, the development phase of this PhD was done in an business environment with close proximity to the research context. During the development, the device was iteratively recruited as a methodological base for two studies: i) Nerve regeneration on rats[1] and ii) Real-time stimulation impact on the ANS[2].

These studies, although performed still during the development phase of this PhD, were important contributes to assess and validate the device specifications, as well as its scientific applicability. The following sections briefly present the methodologies' role in these studies.

4.2.1 Nerve Regeneration on Rat

The main goal of this study was to evaluate nerve regeneration and psycho-motor strategies recovery on twelve rats after induced injury.

The rats' peroneal nerve were surgically incised and the rats were subsequently divided into three different groups regarding the posterior training methodologies: Control Group, Group 1 and Group 2. Control group was not submitted to any form of training. Group 1 and 2 were submitted to a specific continuous training session during six months after surgery but with different protocols. After six months the rat were evaluated concerning

[1]Study performed in partnership with Faculdade de Motricidade Humana and Faculdade de Medicina Veterinária, Universidade de Lisboa

[2]Study performed in partnership with Faculdade de Medicina, Universidade de Lisboa

which training protocol empowered the nerve regeneration and psycho-motor recovery. For that the study is divided in three analysis groups: i) Analysis of the absolute plantar flexion force; ii) Histological analysis of muscle and nerve tissue. iii) Motion strategy assessment through video analysis. The methodologies developed in this PhD were applied only in the context of force evaluation.

4.2.2 Instrumentation

To guarantee complete control of muscle recruitment, invasive electrical stimulation need to be applied directly on the rat peroneal nerve. Figure 4.2 illustrates the system used to induce muscle control and evaluate the force executed by the rat during stimulation.

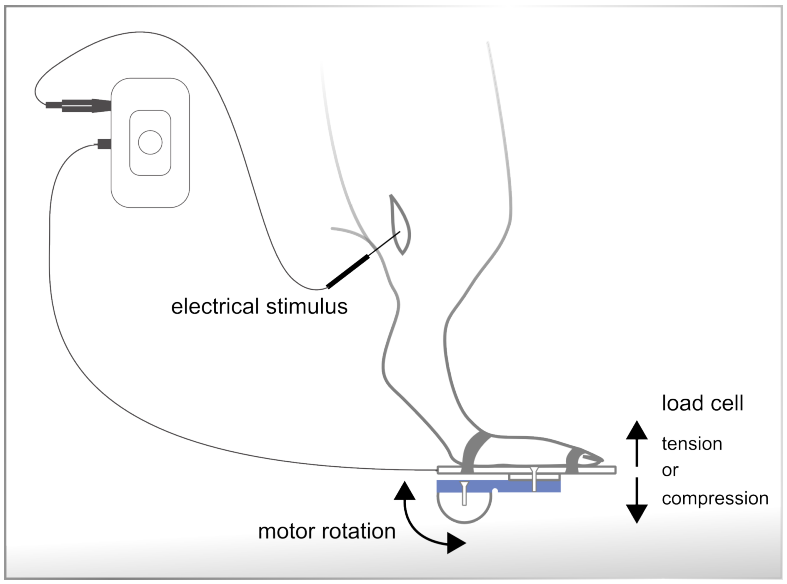

Figure 4.2: Illustration of the system used to induce muscle contraction and respective force assessment.

To properly evaluate contraction force, control and synchronization between the following events were required:

1. Invasive nerve stimulation: To induce and control the rat muscle contraction;
2. Control of a servomotor: To control the angular speed and displacement of the rat's paw;
3. Force signal acquisition: Through a load cell adapted to the pedal;
4. Angular speed and displacement acquisition: Acquire the signal coming from an optical encoder attached to the rotation axis.

This study led to the device's first PCB release (v0.1) [4]. The digital port PWM signal of the stimulator was used to control the external servomotor. The electrical stimulation and servo control needed to be automated in a customized script session. In the photography

of Figure 4.3 the overall apparatus developed to assess the force component of the study is presented.

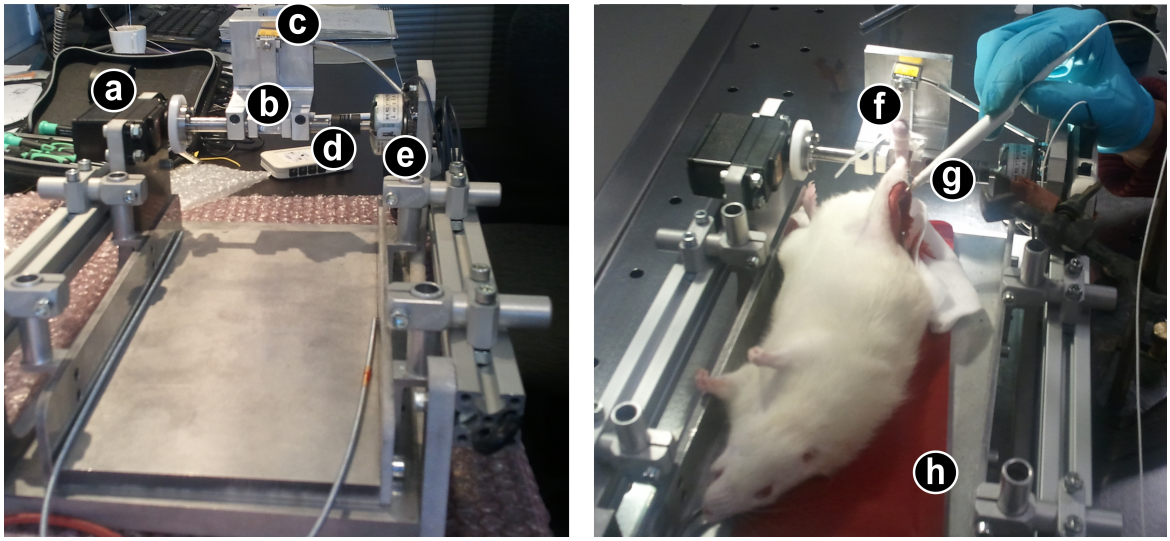

Figure 4.3: Apparatus for force assessment: a) servomotor; b) pedal; c) load cell; d) rotation axis; e) optical encoder; f) rat paw attached to pedal; g) invasive electrical stimulation electrode; h) thermal pad.

4.2.3 Control Interface

Despite the evaluation protocols are usually automated and implemented in customized dedicated plugins, in this study, an animal experiment specialist needed to evaluate and control some initial conditions like the evaluation of the nerve excitability threshold, electrode positioning accuracy, joint angle, among others. In order to ease that process, a user friendly Graphical User Interface (GUI) was developed to enable a faster calibration of the device. Figure 4.4 shows two illustrations of the developed GUI for a Windows computer and for an Android device. Both designed interfaces allowed the user to choose the frequency, duty cycle and stimuli amplitude. This layout interface is used for previous real-time calibrations and thresholds definition, before the application of the evaluation protocol. A start and stop command can also be sent through this interface and eventual communication failures are detected.

4.2.4 Protocol

For this protocol the rats were anesthetized, placed on a thermal pad and their paw firmly fixated to the platform pedal. The pedal was rotated to 90° and the rotation axis was in isometric mode to immobilize the pedal. The isometric mode forces a type of contraction in which the muscle length does not change, since the force generated is not sufficient to move the load holding the limb. Electrical pulses with increasing amplitudes were applied

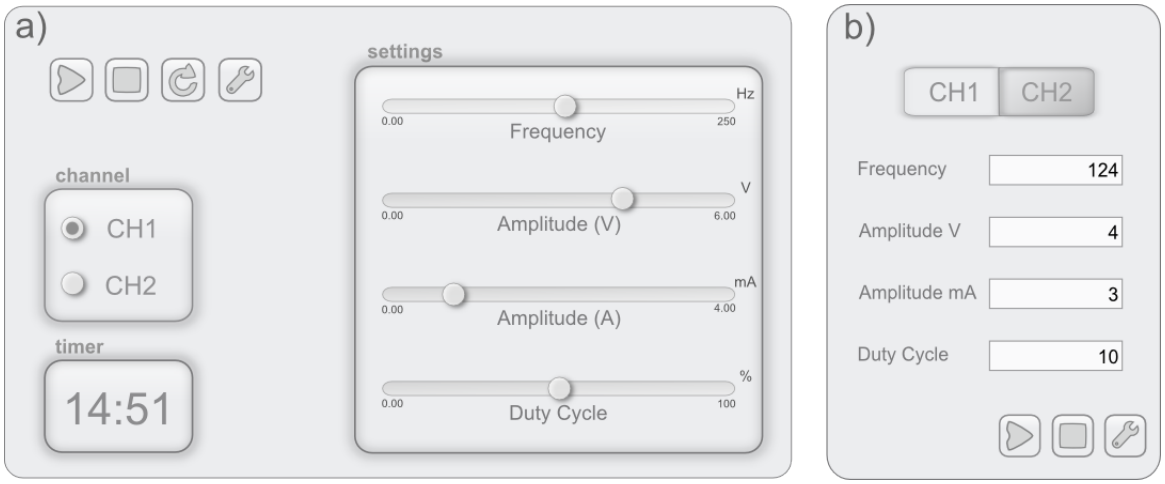

Figure 4.4: First layout interface used for real time calibrations and thresholds definition, before application of protocol: a) Computer based layout; b) Android based layout.

to the peroneal nerve until the current intensity necessary to perform supra-maximum contraction was selected.

The force analysis was divided into two components: one that evaluates the relation of stimulation frequency with generated torque/force and another in which the relation is between torque and the angle of the rat paw.

1. Torque - Stimulation frequency:
    - Place the pedal at 90° in isometric mode;
    - Apply pulse trains with the supra-maximum current intensity reached, 400 ms of duration, varying the stimulation frequency (1 - 200 Hz, 10 Hz step) with rest intervals of 45s;
    - Record torque;
2. Torque - Paw Angle:
    - Place the pedal at 120° in isometric mode;
    - Apply pulse trains with supra-maximum current intensity, frequency of 150 Hz, 400 ms of duration;
    - Rotate the pedal to -10° relative to the previous position;
    - Repeat the second and third points until the pedal is rotated in 20°, with 45s rest intervals;
    - Record torque and angle from the encoder.

4.2.5 Outcomes

Variation of torque with stimulation frequency:

The signals collected were individually computed for each animal and the outcomes are presented as the example of Figure 4.5. The variation of torque with the stimulation frequency was analyzed in order to find specific patterns for each Group, regarding different outcomes from different training strategies. In this specific case, as example, it is possible to note high frequency muscle fatigue on the final contractions, belonging to higher stimulation frequencies.

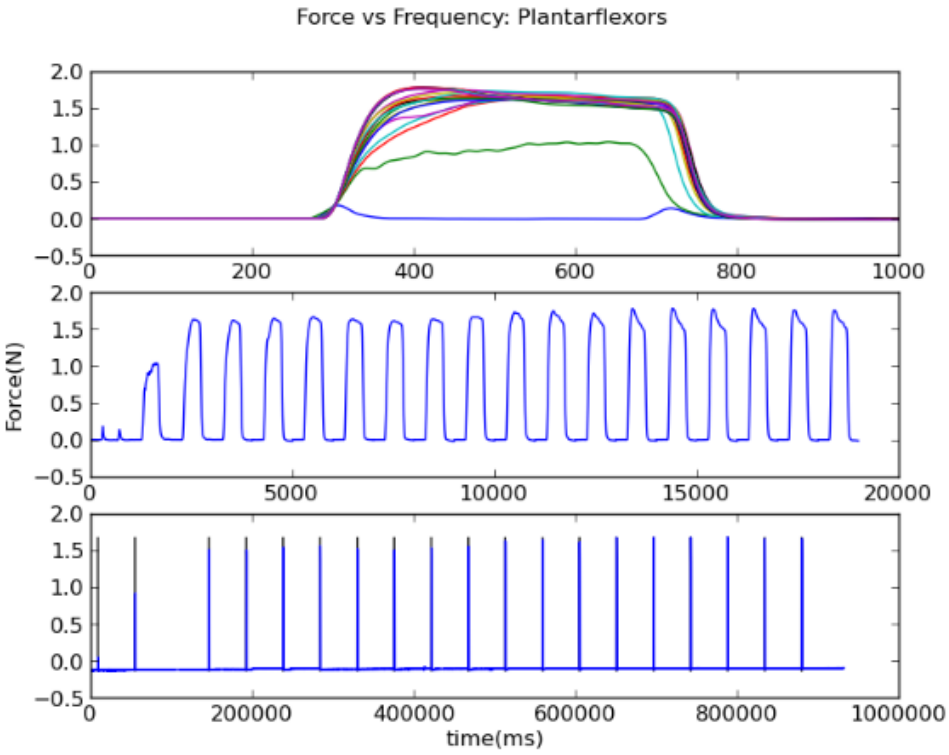

Figure 4.5: Variation of force with stimulation frequency. a) Force curves for different frequencies overlapped; b) Sequence of force curves for 10-200Hz frequencies; c) raw signal.

Variation of torque with pedal angle:

The same approach of results exposition was applied in the data concerning the variation of torque with the angle of the rat paw. One example of the analysed data is presented in Figure 4.6. As it would be expected due to the binary-joint relation, the generated force decreases with the decrease of the pedal angle.

This study contributed with several inputs to the methodologies developed in this PhD. The main contribution concerns the implementation of firmware that enables simultaneously control of several variables: i) invasive electrical stimulation: frequency,

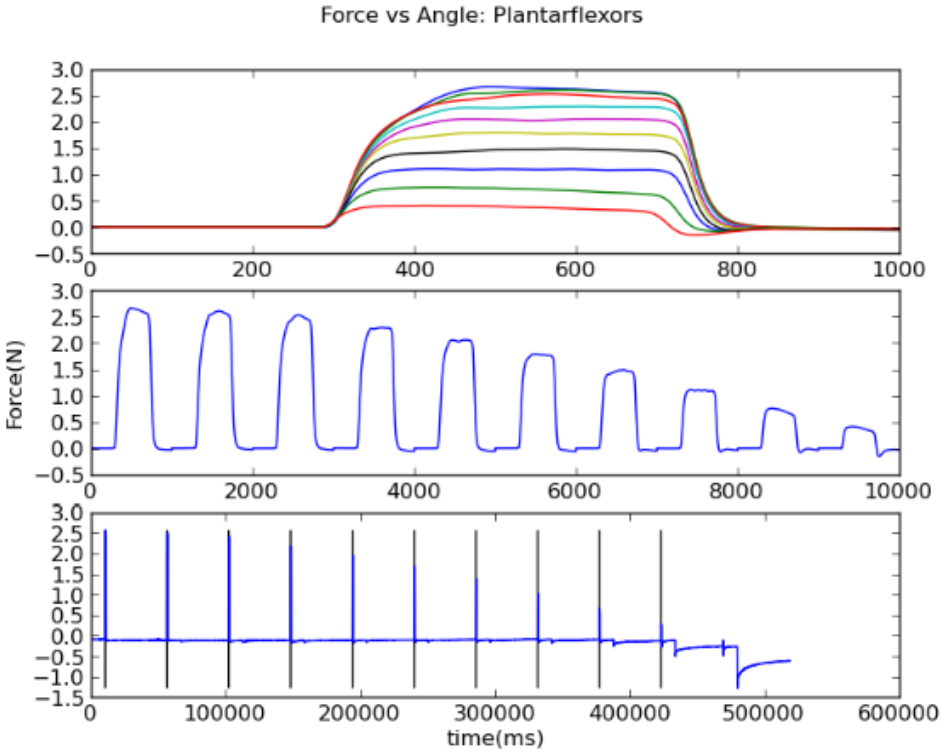

Figure 4.6: Variation of force with ankle angle: a) Force curves acquired for different angle positions overlapped; b) Sequence of force curves from 120-20°; c) raw signal.

amplitude, time on, burst duration, amongst others; ii) The servomotor control: speed, angle, force sustained; iii) The acquisition of the force signal applied by the rat's paw; and finally iv) Access the information of the optical encoder to acquire rotational information. These technological challenges strengthened the necessity of a session architecture and other features like the possibility to include on the device drivers to control an external system.

4.2.6 Real-time stimulation impact on the ANS

In the second scientific study the methodologies were validated through the evaluation of electrical stimulation influence on the Autonomic Nervous System (ANS) of human subjects. Despite all the studies, there has always been a gap in understanding both the immediate collateral effects of electrical stimulation on human physiology and there are very few studies on its impact on the ANS [164][53]. One way to have a direct pointer of ANS management is through the analysis of EDA [188]. EDA or galvanic skin response acquisition involves measuring the conductance of the skin which depends on the amount of sweat produced by eccrine glands, regulated by the sympathetic nervous system. This signal has been reported as a potential non-invasive marker for sympathetic activity, and has been used recently in psycho-physiological research. Another way to evaluate compensations of ANS is through Heart Rate (HR) and Heart Rate Variability (HRV)

analysis [188]. The sympathetic and parasympathetic neurons, which are linked to the sinoatrial node in the heart, have a major contribution to changes in its beating rate. Through the analysis of the latency associated to successive heart beat intervals it is possible to obtain a measure of the sympathetic and parasympathetic vagal activity [45]. From the Blood Volume Pulse (BVP) acquisition signal it is possible to extract HR and HRV. With the cardiac pulse, erythrocytes will change the spatial alignment and this will affect the blood's opacity. The BVP sensor makes use of opacity variations from the tip of the finger to gather the cardiac pulse on a certain instant.

4.2.6.1 Instrumentation

This study was held during the development of the final PCB release (v1.1). A biosignalsplux unit was used to acquire EDA and BVP. The synchronization with the biosignal acquisition system was done connecting the optical decoupling system developed to the stimulator device. The biosignals were acquired at a 2000Hz sampling rate and 12 bits of resolution. Stimuli were applied through two pre-gelled disposable 30x24mm electrodes on the median nerve of the left wrist. EDA self-adhesive pre-gelled Ag/AgCl, 24x24mm round reusable electrodes were placed on the abductor pollicis muscle and on the 3rd palmar interosseous muscle of the right hand. An oximeter was also placed on the index finger of the right hand to measure the BVP of the subjects.

A total of 10 healthy subjects, composed of 5 males and 5 females, mean (SD) age of 24.10 (2.38) years volunteered to participate in the acquisition protocol. All of the subjects were healthy, with no known physical or neurophysiological disorders. The subjects were seated on a comfortable chair with both arms relaxed. Earmuffs were placed on the subjects' ears to prevent any noise distraction. The room was kept silent during the acquisition and the subjects were asked to remain relaxed until the end of the protocol.

4.2.6.2 Protocol

The first stage of the acquisition protocol consisted in the acquisition of four minutes of basal BVP and EDA, without any external stimuli to posterior comparison with the responses during stimulation.

The second segment featured the application of the electrical stimulation. A standard square wave was used for the electrical current pulse. This segment consisted in applying 6 bursts of increasing intensities with 20 repetitive stimuli each. The bursts intensities ranged from 5 to 30 mA with a 5 mA step. In each burst, the interval between stimuli was 0.9 seconds and the time interval between bursts was 10 seconds.

The final segment of the acquisition was similar to the first one: a four minute acquisition without external stimulation, to record the subjects' recovery after the application of stimuli.

Figure 4.7 exemplifies the steps and segments for the acquisition protocol.

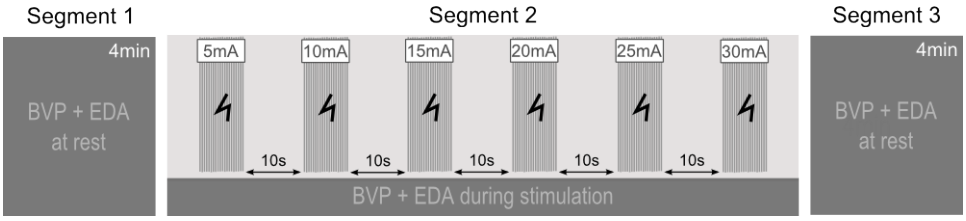

Figure 4.7: Illustration of the steps followed in the acquisition protocol.

4.2.6.3 Data Processing

To study the effect of electrical stimulation filtered from external environmental stimulus and normal basal activity, it was necessary to choose objective parameters from the biosignals acquired. For the BVP signal, absolute amplitude was analyzed in each segment. After a qualitative and subjective analysis, the HR and HRV of each segment was quantified (before, during and after stimulus). The following steps were considered:

1. Detection of maximum peaks in the BVP signal, for all segments;
2. Computation of maximum peak values for each segment;
3. Computation of HR and HRV for each segment, through the difference of peak instants.

For the EDA signal, a qualitative analysis was also made previously, to understand which parameters were influenced by the stimulation. The first stage of parametrization is the extraction of phasic and tonic values from the recorded signal [121][28]. EDA is decomposed into two components: i) the baseline, present in the basal state and ii) a phase level, which emerges as a response to external stimuli. Although, in some cases, it is considered to be constant, EDA baseline reveals a slight rise tendency and the phase level reflects the arousal of the sympathetic nervous system [54]. Figure 4.8 represents a generic EDA signal with events. The parameters analyzed are comprised in this figure: time latency, response rise time and re-adaptation slope.

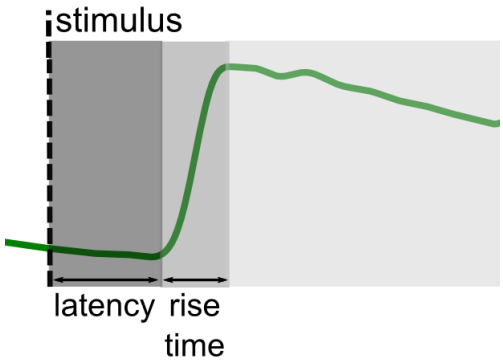

Figure 4.8: Example of an EDA event and possible extracted parameters.

Considering the EDA parameters, the procedure was the following:

1. Event onset detection by calculation of baseline variation;
2. Detection of the plateau phase after the event triggers;
3. Computation of latency and rise time by measuring the timing from the stimulus to the onset (1.) and from the onset to the beginning of the plateau (2.), respectively;
4. Computation of re-adaptation slope, by computing the slope originated from the stabilization of the event until it reaches its baseline value.

4.2.6.4 Outcomes

The EDA signal in its absolute value has high inter-subject variability, which makes it difficult to establish a measurement range capable of comprising significant population [102]. To overcome this effect, it is mandatory to establish amplitude / gain independent objective parameters. In this study, only 7/10 subjects revealed significant responses of sympathetic nervous system to the electrical stimulation.

Figure 4.9 shows the EDA signal during segment 1 and segment 2 for all subjects.

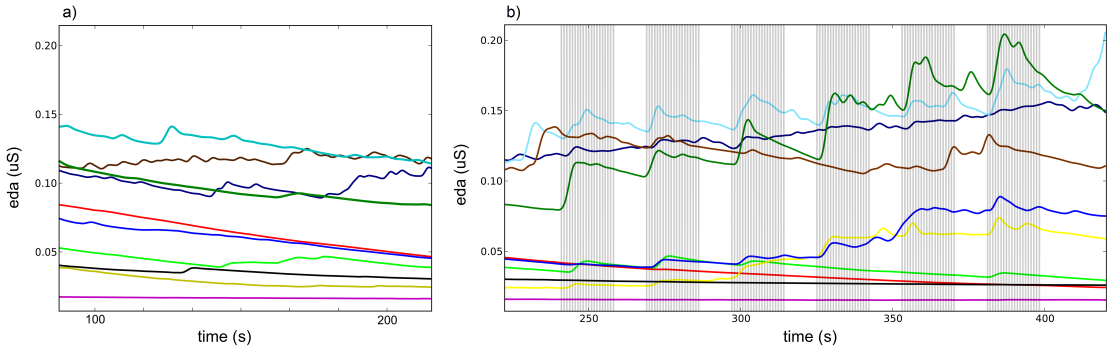

Figure 4.9: EDA signals obtained for all subjects: a) Example window obtained from segment 1 of the acquisition protocol (basal activity); b) Signal obtained from segment 2 of the acquisition protocol (six bursts of electrical stimulation).

Regarding the subject's EDA from segment 1, analysis of the results showed that prior to the application of the stimuli small oscillations were detected but deemed of low importance. In general, for this segment, a continuous smooth descent tendency was noticed for all subjects. For segment 3, the behavior was the same as presented in Figure 4.9 a). The EDA signals from all subjects during segment 2 of the acquisition protocol are presented in Figure 4.9 a). For segment 2, EDA results presented, for most of the subjects, some events in response to the electric stimulus (Figure 4.9 b). This allows the analysis of the time latency between the stimulus reception by the median nerve and the ANS reaction to it.

Another pointer for the ANS management used in this work was the analysis of BVP signal. Figure 4.10 shows an example of the BVP reaction to stimulation for one subject.

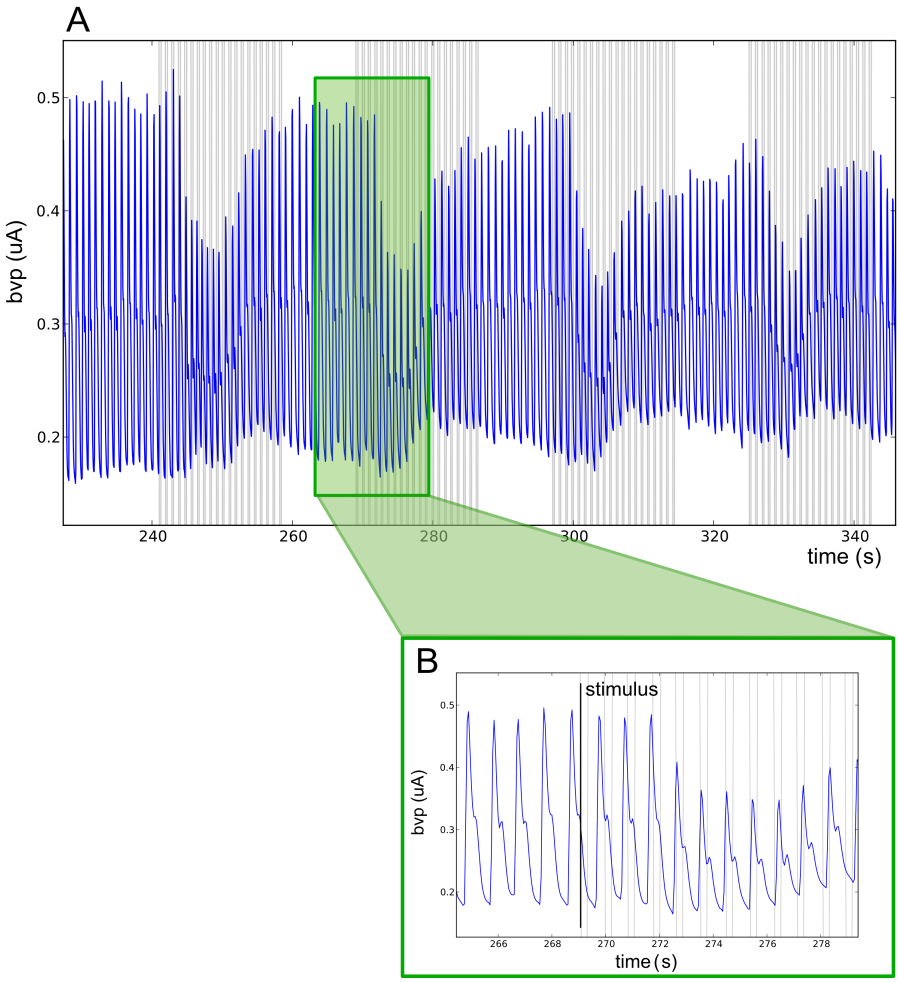

Figure 4.10: Example of the BVP signal from one subject during the segment 2 of the acquisition protocol: a) Example window showing 4 of the 6 bursts of acquisition with electrical stimulation; b) Zoomed window of one burst, enhancing the stimulus instant and signal amplitude decrease afterwords.

The BVP signal of 5/10 subjects showed an amplitude decreasing with the beginning of the electrical stimulation. This is justified by a vasoconstriction effect caused by adaptations of the ANS to the electrical stimulation. Vasoconstriction of the blood vessels increases the spatial density and consequent alignment of erythrocytes. This fact will increase the opacity of the finger, leading to lower signal detection by the sensor used for the detection of the BVP signal.
Concerning the HR and HRV analysis, contrary from what would be expected, half of the subjects (5/10) showed a decrease of these parameters during segment 2. The other half did not show significant changes. In segment 3, HR and HRV returned to the same basal values presented on stage 1, as it can be seen on Table 4.4.

Table 4.4: Mean values and respective standard deviation error for the heart rate (in beats per minute) obtained during segments 1, 2 and 3.

Heart Rate (bpm)						
	Segment 1		Segment 2		Segment 3	
	Mean	*(SD)*	*Mean*	*(SD)*	*Mean*	*(SD)*
Subject 1	80.3	(8.79)	81.6	(8.24)	79.0	(8.26)
Subject 2	66.6	(7.99)	64.9	(5.91)	67.0	(8.24)
Subject 3	69.5	(2.89)	71.9	(3.81)	69.3	(3.25)
Subject 4	64.3	(5.57)	61.1	(4.15)	64.5	(5.44)
Subject 5	70.1	(5.62)	64.4	(4.88)	69.8	(5.38)
Subject 6	72.4	(5.68)	69.8	(3.72)	72.1	(4.66)
Subject 7	67.1	(4.40)	71.0	(6.43)	65.5	(4.85)
Subject 8	83.2	(5.53)	83.9	(5.86)	83.2	(5.97)
Subject 9	61.9	(6.32)	61.7	(5.01)	60.6	(6.36)
Subject 10	63.2	(4.22)	62.4	(3.22)	63.2	(3.68)

This study's main goal was to evaluate if electrical stimulation has a direct influence into several parameters of the ANS, which were obtained from EDA and BVP signals. Electrical stimulation revealed to clearly influence several parameters of ANS as the EDA arousals, the BVP amplitude and HRV changes.

Besides the scientific results reached, the importance of this study is primarily related with its application in a real case scenario and the feedback retrieved from the usage of the implemented methodologies. The precision of synchronization between stimuli and reflex events was a parameter optimized after the feedback of this second validation study. This study also allowed to evaluate the device usability and intrusiveness in a real context with human test subjects.

The validation studies presented in the previous pages were relevant contributes to empower the device features during the development stage and assess its scientific applicability.

CHAPTER 5

APPLICATION TO NEUROPLASTICITY OF TETRAPLEGIC SUBJECTS

The motivation for the development of the electrical stimulator device consisted in the belief of its added value in varied research contexts. In this chapter, an application of the developed technology is presented, in the context of rehabilitation of severe Spinal Cord Injury (SCI) patients. An analysis and correlation of the Interlimb Reflexes (ILR) process was performed, using a standard methodology for both healthy and tetraplegic patients. This chapter provides an insight on SCI neuroplasticity, as an introduction to this specific study. After this introduction, the parametrization methods for the stimulation procedure and EMG acquisition are described. The results and comparison between healthy subjects and SCI patients are discussed by the end of the chapter.

5.1 Introduction

Neuroplasticity is the central nervous system ability to adapt when exposed to changes. It presents itself in varied situations, from memory processes to recovery from injuries [35][36]. Dynamic changes associated with recovery may be observed in a diversity of complementary diagnostic tests. Imaging studies, such as computerized tomography and nuclear magnetic resonance imaging, do not correlate directly to the clinical status of subjects and provide less functional information regarding the sometimes subtle recovery of the patients. On the other hand, studies with EMG, evoked potentials and ILR are better suited to assess the physiology of specific neural pathway [2]. Studies on ILR have gained importance over the past years. ILR pathway represents an interconnection between upper and lower limbs. Thus, stimuli applied on cutaneous nerves of the upper limb can evoke motor response on contralateral lower limb, and vice-versa. Although there are still few studies on the matter, some authors have found ILR in healthy subjects and correlated it

with bipedal gait and spatial orientation [73][159][72][105]. Other studies claim that the ILR found in SCI patients are due exclusively to cellular modifications on the injury level and a new propriospinal pathway [34][37], which may suggest a regeneration process. Recent studies have identified its existence, but have not yet established objective measures of the ILR. In the present study, two groups of SCI patients and one healthy control group are analyzed for a better understanding of ILR, in an attempt to establish objective parameters for future use in the evaluation of inter and intra subject clinical evolution. Objective analysis of the propriospinal pathway responsible for the ILR may present the possibility of interlimb recovery therapy, in which stimulation of lower limbs could help improve upper limbs functionality and vice-versa, leading to new therapeutic options for SCI patients. In tetraplegic patients, increased functionality of upper limbs plays a fundamental role on a better quality of life, increasing also the subject's independence regarding routine activities and self-esteem.

5.2 Methods

5.2.1 Subjects

In this study a total of twenty five subjects were analyzed and divided in three groups. Group 1 was composed of 6 male tetraplegic patients with sensory level 10 between C1 and C4 (Asia Impairment Scale AIS [97] - Appendix E - A n=5, AIS - B n=1) with mean (SD) age at lesion of 25.2 (4.16) years, range from 20-31 years and chronic traumatic lesion for mean 12.0 (4.29) years, range from 7 to 17 years. Group 2 was composed of 9 male tetraplegic patients with sensory level between C5 and C8 (AIS - A n=7, AIS - B n=1 and AIS - C n=1), with mean age at lesion of 26.4 (6.07) years, range from 19-34 years and chronic traumatic lesion for mean 10.6 (2.92) years, range from 6 to 14 years. Finally, the control group was composed of 10 healthy subjects (8 males and 2 females), mean age of 22.0 (1.58) years, range from 22-26 years, without clinical history on neurologic disorders. Exclusion criteria for Group 1 and 2 was a time since traumatic injury less than 1.50 years, for properly Central Nervous System (CNS) adaptation [36]. For the control group, the exclusion criterion was the existence of a previous diagnostic of neurological or degenerative disease[1].

[1] All experiments were approved by the Research Ethics Committee of the *Hospital de Clínicas da Universidade Estadual de Campinas*. The study here described was first published concerning the analysis of healthy subjects, and after extending also to SCI patients:
[7]: Araújo, T., Brandão, A., Didier, T., Bracco, B., Gamboa, H. and Cliquet, A. *Analysis of Inter-Subjects Variability of Contralateral Interlimb Electrophysiological Reflexes.* In Proceedings of American Spinal Injury Association Annual Meeting (ASIA 2014). San Antonio - Texas, USA.
[6]: Araújo, T., Brandão, A., Didier, T., Bracco, B., Gamboa, H. and Cliquet, A. *Analysis of descriptive electrophysiological parameters in contralateral interlimb reflexes on tetraplegic patients.* Spinal Cord, Nature, advanced online publication 7 October 2014; doi: 10.1038/sc.2014.169

5.2.2 Procedure

To explore both directions of the interlimb contralateral pathway, two tests were performed:

- In **Test 1**, the stimulus was applied at the radial nerve on the right arm surface and the EMG signal collected in contralateral left leg anterior tibial muscle surface.
- In **Test 2**, the stimulus was applied at the fibular nerve surface on the left leg fibula head and EMG signal was collected in surface of contralateral limb biceps brachii, exploring the opposite direction of the pathway.

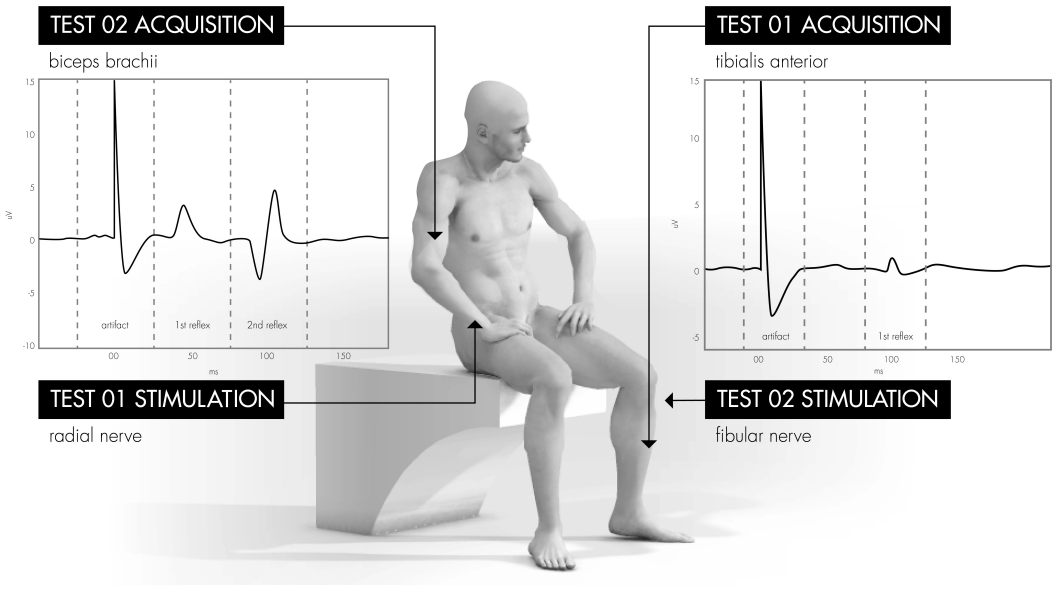

Figure 5.1: Illustration of Test 1 and Test 2 stimulation electrodes positioning and respective evaluated muscles through EMG acquisition. In the graphics, the black line represents the averaging wave of reflexes from 40 sweeps on biceps brachii for Test 2 and tibialis anterior for Test 1.

Figure 5.1 illustrates the procedure for EMG acquisition and electrical stimulation.

In both tests, the subjects were relaxed and seated while stimulated with intensities from 5-30 mA (5 mA step), with 40 sweeps of 500 μs current modulated single pulses, for each current increment. To properly cancel noise and mechanical artifacts, the pulses were randomly distributed in frequencies from 1.8 - 2.2Hz. The entire procedure was repeated 3 times per patient, each repetition using a different single pulse stimulation waveform [155], called mode. A standard square wave was applied in mode 1, a triangular wave in mode 2 and a quadratic wave in mode 3. In all 3 modes, monophasic single pulses with the same intensity steps and the same duration (500μs) were used. Figure 5.2 provides an illustrative schematics of the stimulation and acquisition procedure.

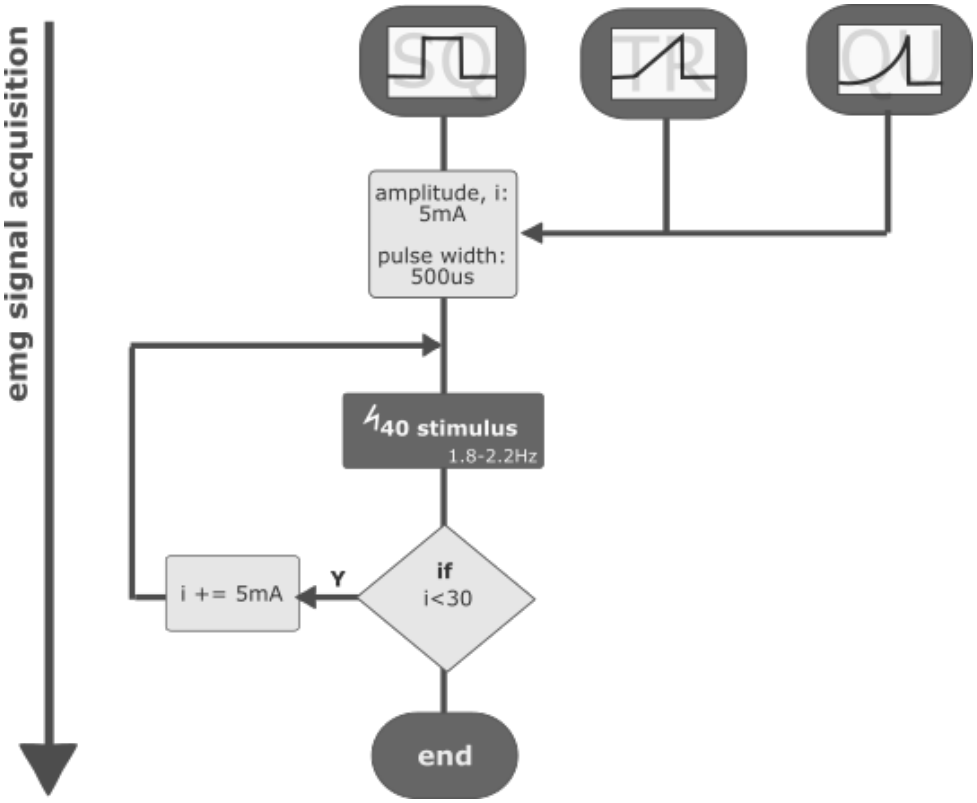

Figure 5.2: Illustrative schematics for the stimulation and acquisition protocol.

EMG signal was acquired at a 2000Hz sampling frequency, amplified with a gain of 1000, 12 bits of resolution and bandpass filtered from 25 to 550Hz. Self-adhesive pre-gelled Ag/AgCl electrodes were used for EMG acquisition and peripheral nerve stimulation. The acquisition electrodes were placed according to SENIAM standards [77] and the ground electrode was placed at the radius styloid apophysis.

The application of the developed methodology enables the exploration of new descriptive parameters for the evaluation of the interlimb propriospinal pathway.

5.2.3 Data analysis

The first step of data analysis was to automatically detect the incidence of ILR in all subjects. After automatic detection, all the ILR sweeps were still visually validated individually by 4 M.D. specialists. For the subjects with ILR incidence, in the EMG signal, the peak reflex amplitude values were automatically withdrawn. Only the first reflex after stimulus was considered to explore the shortest possible pathway for interlimb reflexes. The electromyographic signal was acquired and stored continuously. Each EMG sweep was then stored in an individual vector for posterior averaging with a time window from -50ms to 250ms (considering 0ms as the stimulus instant).

Reflexes were extracted from the averaging of the 40 EMG sweeps, acquired in each stimulation intensity (5-30mA pulses with 5mA step). Peak-to-peak amplitudes and

latencies were computed from the resulting mean wave. For amplitude, the absolute difference between maximum and minimum values of the first reflex was considered. For latency, the time distance between stimuli and reflex first peak point (maximum or minimum) was considered. The mean and standard deviation value for amplitudes and latencies, in each intensity step, was computed for Group 1, 2 and Control.

Since all pulse waveforms were applied in each step with the same amplitude and duration, the current charge between the three pulses differed. The current charge difference was taken into account in the data analysis. The stimulation charge was computed accordingly to the stimulation intensity and waveform, with equation 5.1.

$$Q = \int_{t1}^{t2} I dt \tag{5.1}$$

Where I represents the current intensity, and t1 to t2 is the stimulus time, which in this case is a constant (500μs).

5.3 Results

Each Group was analyzed concerning the reflexes incidence, amplitude and latency. The inter-subject incidence of ILR enables the analysis of the number of subjects that elicited significant reflexes in comparison with the total number, n, of the analyzed population. Table 5.1 provides the results for the inter-subject incidence of reflexes for the three groups, different stimulation modes and tests. The incidence was approximately 50% for both tests and groups. Test 2 generally elicited more reflex occurrences.

Table 5.1: Number of subjects per group that elicited significant reflexes in the three stimulation modes versus the total number of subjects analyzed.

Group		**Test 1**	**Test 2**
G1 (C1-C4)	*n=6*	3	4
G2 (C5-C8)	*n=9*	4	6
Control	*n=10*	5	5

Figure 5.3 presents the mean values of the reflexes peak-to-peak amplitudes from each group related to the stimulation intensities applied in all participants. This Figure was compiled with results from Test 1 and mode 1, but this effect was found to be consistent with both tests and stimulation modes. The reflexes peak-to-peak amplitude remains almost constant with the different stimulation intensities for all three groups. However, there is a distinct difference among each group regarding its base amplitude value.

Figure 5.4 present an EMG signal, acquired in each intensity step (from 5mA to 30mA), from one healthy and one SCI subject. Figure 5.4 a) concerns an example subject from Control group, and Figure 5.4 b) is representative of the findings in both SCI groups (G1/G2) and tests, meaning that the behavior found was equal for both groups. Comparing the results of both figures, a different behavior in the Control group versus the SCI groups was found: while the reflex latency, for the healthy subjects, remains almost unaltered

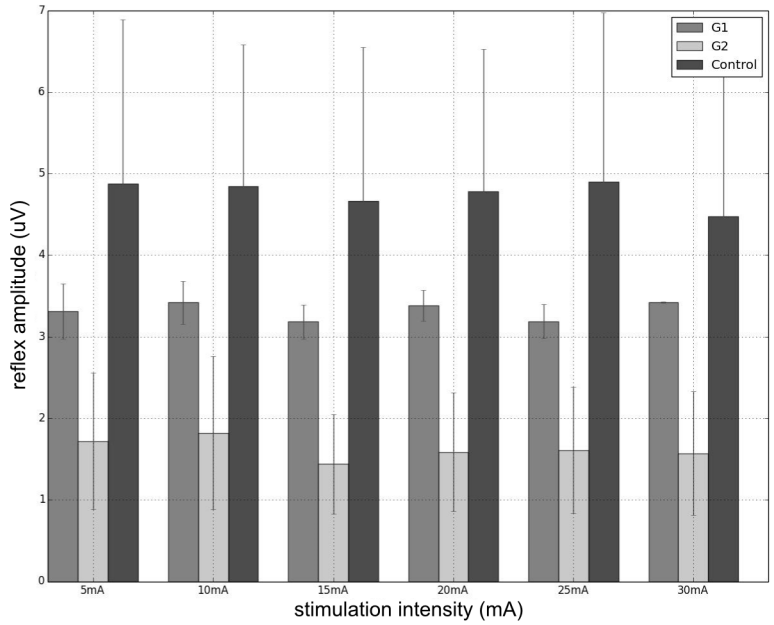

Figure 5.3: Reflexes mean peak-to-peak amplitude in μV (with SD error bars) related to the stimulation intensity for Test 1 and three groups.

with the increase of stimulation intensity, in the SCI groups the latency shows a notorious rise tendency pattern.

As differences were found between groups regarding the reflex latency, a deeper analysis on this parameter was compiled in Figure 5.5. This Figure presents the results of the mean reflexes latency from each group related to the stimulation charge for Test 1 and 2. The reflex latency shows different behaviors regarding each group and, unlike the reflex amplitude, is correlated with the stimulation charge, showing different increase tendencies for each group. Table 5.2 compiles the linear tendency equations and R^2 for each group between stimulation charge and latency response.

Table 5.2: Linear tendency equations and correspondent R^2 of latency vs charge for all groups and tests.

Group	**Test 1**	**Test 2**
G1 (C1-C4)	y = 3.64x + 42.4	y = 6.10x + 82.8
	$R^2 = 0,961$	$R^2 = 0,982$
G2 (C5-C8)	y = 8.19x + 23.1	y = 7.49x + 76.9
	$R^2 = 0.998$	$R^2 = 0.997$
Control	y = 1.04x + 39.3	y = 0.356x + 41.0
	$R^2 = 0.751$	$R^2 = 0.345$

In some patients (n=2 from Group 1), during the acquisition procedure, it was also verified a prominent twitch-like movement of the upper contralateral limb, following the stimulation frequency.

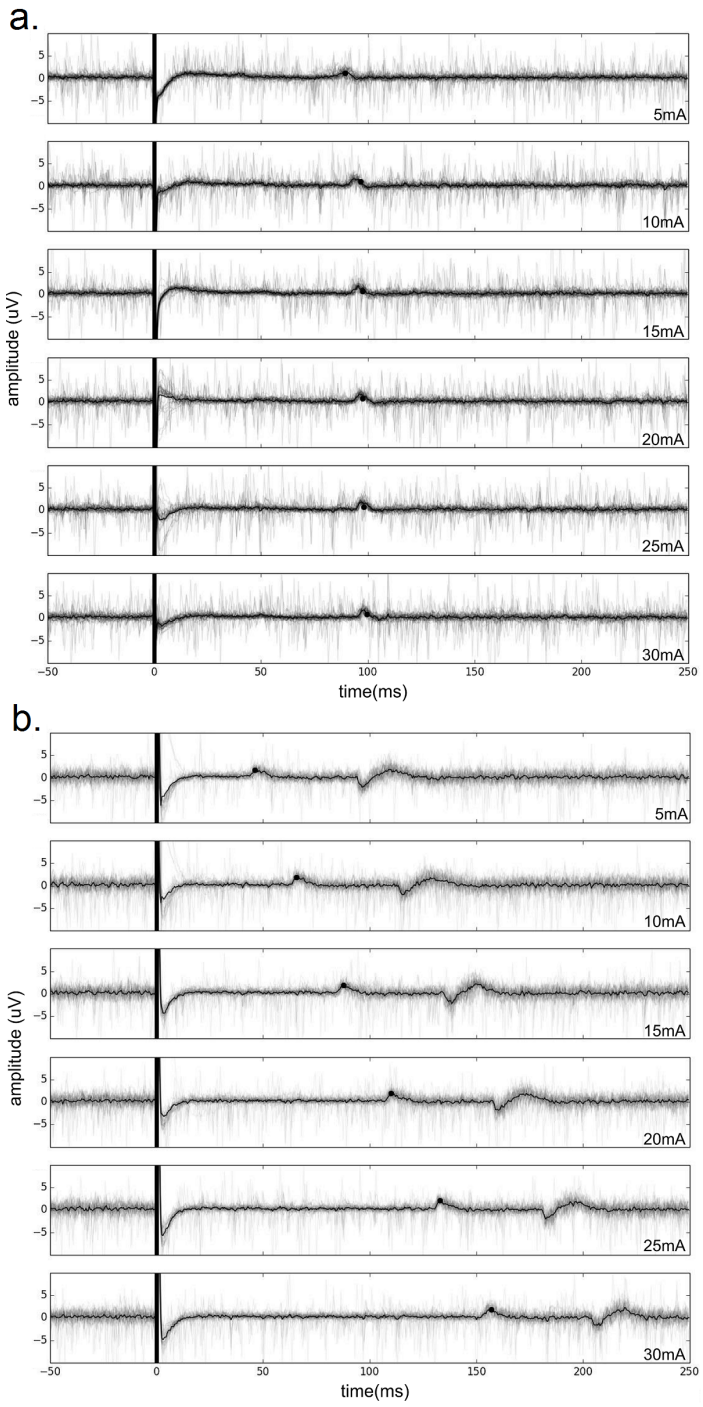

Figure 5.4: Results of ILR elicited with different stimulation intensities for Test 1 in: a) healthy subjects (example from one subject of Control Group); b) SCI subjects (representative example from one subject of Group 1). The black line represents the averaging of the 40 EMG responses to the stimulation. Background lines are the 40 responses overlapped and black dot notes the automatic peak and latency detection. The thick vertical black line marks the stimulation instant, covering the stimulation artifact.

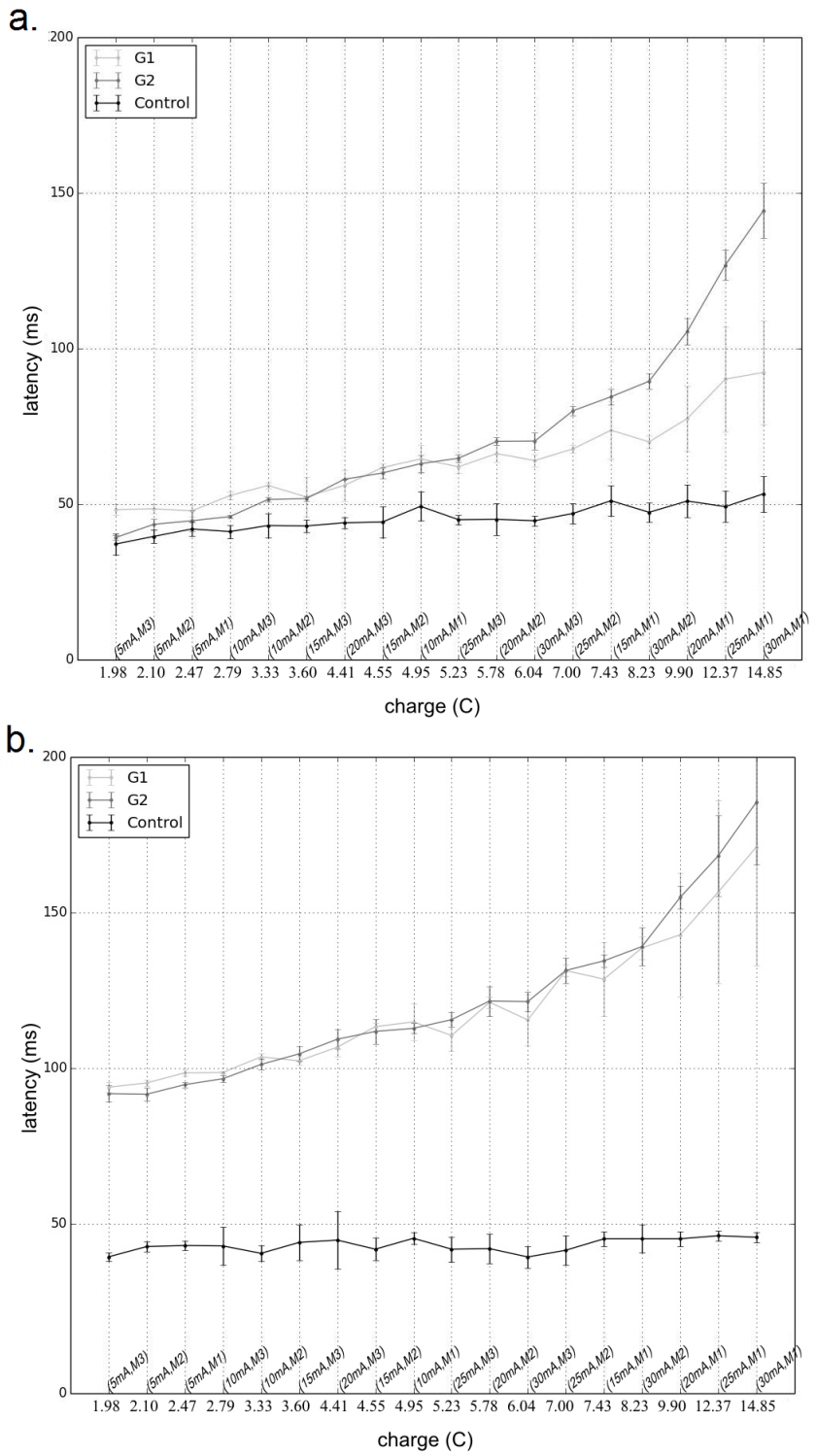

Figure 5.5: Mean values (and SD error bars) for the reflexes latency related to the stimulation charge for: a) Test 1 and b) Test 2. The stimulation charge is complemented by the indication of the mode and intensity of the original electrical pulse.

5.4 Discussion

With the results obtained, it is possible to derive conclusions regarding the incidence, amplitude and latency of the ILR when comparing the three different groups analyzed.

Incidence

The inter-subject incidence of ILR, either in healthy subjects and in patients with SCI, is involved in scientific controversy [73][159][72][105]. This study evaluates the ILR incidence in healthy subjects and SCI subjects through the same methodology, for a proper discussion. Although, for this analysis, the sample is not sufficiently significant, since in this study the inter-subject incidence was revealed to be uncorrelated to the clinical condition of the patient or stimulation charge. These results support the latest works exploring interlimb reflexes on healthy subjects [73][159][72][105] and SCI patients [36]. It was verified that the inter-subject incidence is always higher for Test 2, with the stimulation on fibular nerve and acquisition at biceps brachii, than for Test 1. These results suggest a higher excitability of this pathway than in the opposite direction.

Amplitude

Previous works with healthy subjects analyzed the ILR amplitude of each subject, normalizing the amplitude with their maximum voluntary contraction [73][159][72][105]. Due to the clinical condition of the SCI patients, a different normalization process needs to be implemented. For reliable comparison between different groups, the ILR amplitude was analyzed referring to the absolute value in micro Volt (μV) measured. Although the amplitude of the ILR measured from the EMG signal can be highly correlated with external factors, some conclusions are prominent. A correlation between the ILR amplitude and the clinical condition of the patient is verified. In this case, healthy subjects generally produce ILR with higher amplitudes than the SCI subjects. This fact was expected since the SCI patients can have compromised nerve conductivity. With the ILR subjects, the highest injury group, Group 1, shows amplitudes above the lowest injury level group, Group 2. This is possibly explained by the higher proximity between the interlimb connection level and the lesion level for the lowest injury group (Group 2 C5-C8). It was also found that the amplitude of the responses analyzed does not expose an obvious correlation with the amplitude/charge of stimulation.

Latency

Concerning the ILR latency on healthy subjects it is verified that there is a small correlation between stimulation intensity or charge with the reflex latency. In Test 1 the latency was stable, with a very low linear uprising tendency between [40:60] ms. In Test 2, for the same group, the latency was approximately 40 ms independently of the stimulation intensity or charge. These results are in accordance with the standards for the healthy nerve conduction speed [139]. A strong correlation of the ILR latency with the electrical pulse charge is

verified in SCI patients. As it can be seen in a more prominent way in the Test 2 (Figure 5.5 b)), the latency evolves with stimulation charge, independently of the injury level. The linear equations and R^2 present in Table 2 show a stronger correlation for Group 2 and 1 than for the Control Group. In Test 1, Group 1, the rise tendency is influenced by one SCI subject outlier (AIS = A) that revealed a different behavior with no latency response increase (Figure 5.6). This pattern was previously reported by McNulty [124], where the only patient analyzed showed a similar response. However, even with this outlier subject, the rising pattern is still linear and with a R^2 value of 0.96. Analyzing ILR latency referent to the first stimulation charge (base latency) in Test 1 and Test 2, some differences emerge. Whereas in Test 1 the base latency is identical in both SCI (G1/G2) and Control groups (Mean (SD) = 44.318 (3.466) ms; n = 10), in Test 2 the SCI subject's latency start with an offset. The lowest latency for SCI subjects in Test 2 is around 90ms (Mean (SD) = 96.389 (2.132) ms; n = 9) while for the control group is in 40ms (Mean (SD) = 43.000 (1.414) ms; n = 3). All these facts strongly suggest different pathways between SCI and healthy subjects.

Supporting theories

ILR have been previously explored in healthy subjects and are hypothesized to facilitate a reciprocal gait coordination mechanism for bipedal locomotion that is mediated by long propriospinal fibers [73][159][72][105]. However, Calancie [36] states that the ILR arise through an exclusive SCI patients' pathway, emerging from a regenerative sprouting process of ascending afferent fibers, which do not reconnect again into the original target populations. It is assumed that this process is triggered after denervation of the spinal tract caused by the injury and that this new pathway, generated only 6 months after injury, is strengthened over time. Calancie has not verified the existence of ILR in healthy subjects and states some inconsistency of the ILR mechanism studied in healthy subjects by Zehr [195] in comparison to the reported mechanism in SCI patients. In this study, the same methodology was applied for the first time to both healthy and SCI subjects. The results are consistent with the previous studies that reported the presence of ILR in healthy subjects. The comparison conducted in this study also supports the idea of a different ILR transmission mechanism between healthy and SCI subjects, strongly reinforcing the hypothesis of nerve regeneration after acute spinal cord injury. This is concluded mainly due to the differences in latency response to stimulation charge (Figure 5.4, and Figure 5.5).

This study evaluated the ILR transmission mechanism in SCI and compared them with a healthy control group. It was possible to establish descriptive parameters for the ILR cortico-spinal pathway characterization. With these results the ILR pathway can now be explored from the functional interlimb rehabilitation and training perspective for tetraplegic patients.

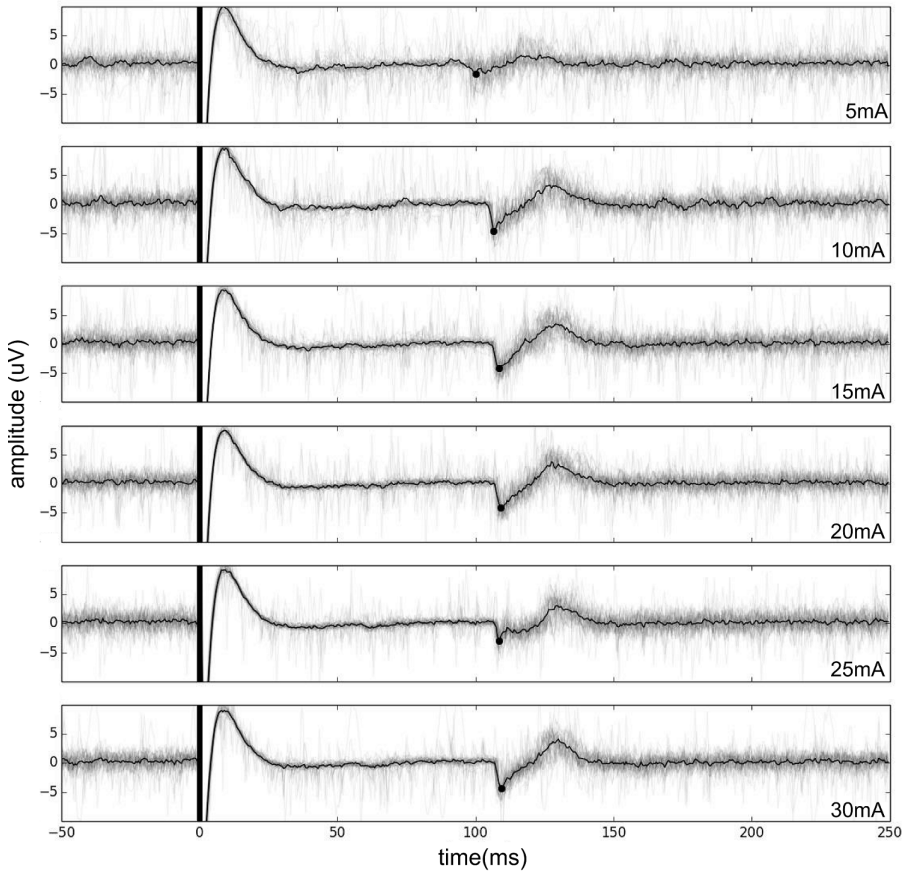

Figure 5.6: Results of EMG response with different stimulation intensities of the Test 2 from the unique patient that exposed a different rise pattern of ILR latency related to the stimulation charge. The black line represents the averaging of the 40 EMG responses to the stimulation. Background lines are the 40 responses overlapped and black dot notes the automatic peak and latency detection. The thick vertical black line marks the stimulation instant, partially covering the stimulation artifact.

CHAPTER 6

APPLICATION TO THE WAVEFORM CONTROL ON CMAP SCAN

One of the first challenges, with the end of the development stage, was to evaluate what could be revealed by the application of this new parametrization freedom in current electrical stimulation methodologies. Compound Muscle Action Potential (CMAP) scan is a non-invasive promissory technique recently applied on neurodegenerative pathologies diagnosis. In this chapter new CMAP scan protocols were implemented using different single pulses waveforms, understanding the influence of electrical pulse waveform on transcutaneous peripheral nerve excitability.

6.1 Introduction

Nowadays, CMAP scan is applied as diagnosis technique for neurodegenerative pathologies, such as ALS. It allows a quick analysis of the muscle action potentials in response to motor nerve stimulation, by electrical stimulation applied on the surface of the motor nerve and response evaluation by surface EMG at muscle level. Because they are at different distances and depths, each Motor Unit (MU) will be activated with different Stimulus Intensity (SI). Varying the intensity of the stimuli applied, gradually increasing from subthreshold to supramaximal values, will sequentially activate all MUs in the muscle. This way, it is possible to obtain a graphical representation of the evoked action potentials amplitude in the muscle versus the stimulation intensity. This record will show a sigmoid tendency which is called the CMAP scan [112][113][114]. Henderson [76] examined the variability of the CMAP scan between healthy and ALS subjects. It was showed that there is a significant difference in relation to CMAP scan evolution, number of steps (visible jumps in CMAP amplitude within consecutive stimuli) and size, since ALS patients present more and larger steps on the stimulus-response curve than healthy

subjects. Figure 6.1 presents a CMAP scan of an healthy individual opposed to one of a ALS patient. A healthy CMAP scan has traditionally a sigmoid tendency curve for the Motor Unit Action Potential (MUAP) amplitude in response to a linear increase of current intensity.

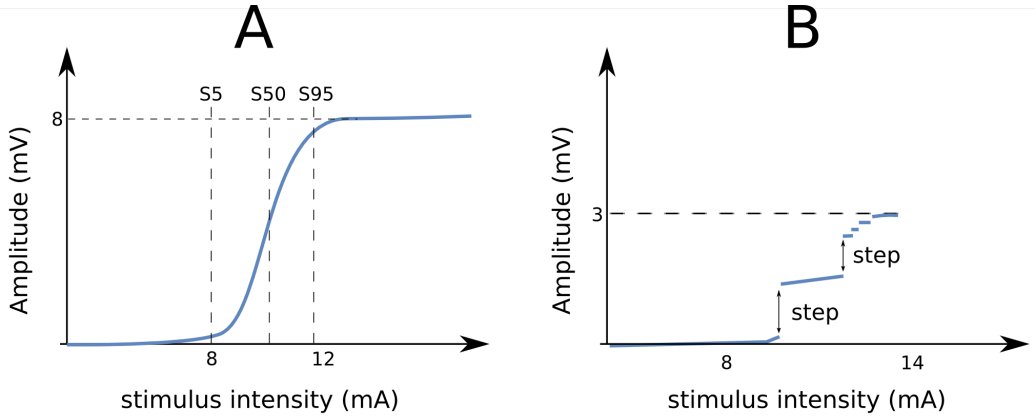

Figure 6.1: Representations of CMAP scans. A) From an healthy individual. The horizontal line indicates the CMAP maximum amplitude while the vertical lines refer to S5, S50 and S95 (stimulus intensity that elicited 5%, 50% and 95% of the maximum CMAP, respectively). B) From an ALS patient. Differences in the CMAP scan between the healthy and the ALS patient are visible because of several steps observed in the ALS CMAP scan and also the decrement in maximum amplitude. Adapted from Henderson et al. [76].

This technique provides clinically relevant information about re-innervation processes, number and size of functional motor units and neuromuscular activity/excitability. Moreover, CMAP amplitude has significant correlation with muscle strength, motor unit number estimation and functional disability in ALS [42]. To be used as a clinical tool, stimulation parameters must be standardized and quantified in order to enable uniform data collection and comparison. Several studies have been developed recently to verify the potentiality of this technique, investigating the influence of different parameters in the quality of the CMAP scan [112]. A consensual method is based on the analysis of key points like the maximum CMAP, S5, S50, S95 (the stimulus intensity that elicited 5%, 50% and 95% of the maximum CMAP, respectively), SI range (the difference between S95 and S5) and step percentage [112]. Despite that, the physiological influence of different order stimulation parameters like waveform and polarity on the CMAP scan remains unknown. This chapter's study aims to evaluate the influence of different pulse modulated waveforms in peripheral nerve excitability, by CMAP scan technique, on healthy subjects for future comparison with ALS patients. To accomplish that, an electrical stimulation protocol was developed, and biosignals from healthy subjects were acquired, analyzed and processed, in order to extract features for the analysis of the different waveforms' influence in the stimulation of the peripheral nerve. The waveforms tested in the stimulation protocol were monophasic square, triangular and quadratic waves and also a biphasic square wave.

6.2 Methods

6.2.1 Subjects

In this study a total of 13 healthy subjects were submitted to the same test. This group was composed of 7 males and 6 females, mean (SD) age of 26.00 (3.63) years, range from 20-36 years, without clinical history on neurologic disorders. All subjects with predisposition to peripheral nerve problems were excluded from the study.

6.2.2 Instrumentation

The stimuli were applied in the median nerve on the right wrist and EMG signal collected on the Abductor Pollicis Brevis muscle surface on the right thumb. Self-adhesive pre-gelled Ag/AgCl, 30x24mm disposable electrodes were attached to the skin for acquisition and stimulation, placed according to SENIAM [77] standards. The ground electrode was placed on the left wrist ulnar styloid process. During the test, the subjects were seated, motionless and relaxed, with thumb fixation to minimize movement artifacts. Figure 6.2 illustrates the equipment and electrodes placement for the protocol applied.

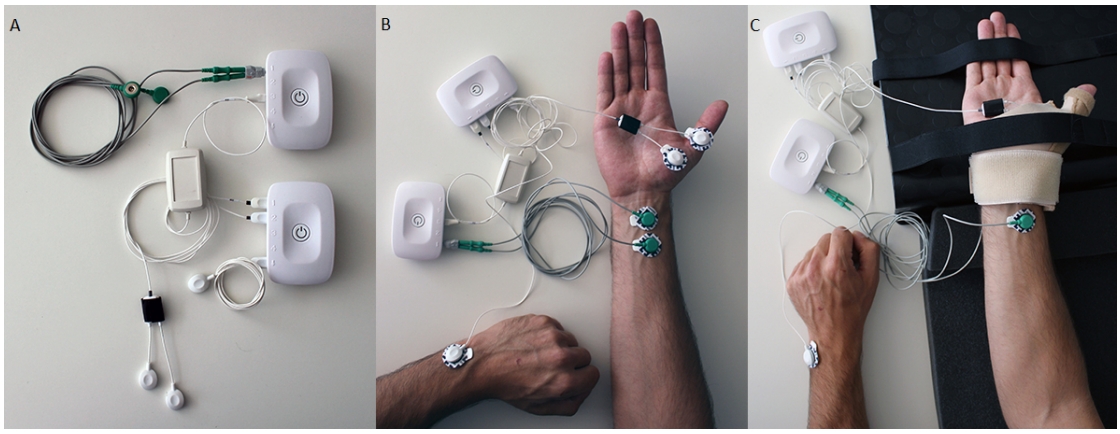

Figure 6.2: Illustration of the equipment used and electrodes placement. A) The electrical stimulator and biosignal acquisition unit. B) Electrodes placement: stimulation electrodes on the median nerve, surface EMG electrodes on the thumb and ground electrode on the wrist. C) Hand fixation for the test.

6.2.3 Stimulation and acquisition

Stimulation was performed with increasing intensities range from 4 to 30 mA. Different number of stimuli and current increment steps were tested in order to have a stimulation protocol that would allow obtaining a curve with enough resolution and not excessive test duration. After extensive testing, it was perceived that only 3 stimuli *per* step were sufficient to have high resolution in the CMAP. Regarding the steps, it was decided that in the beginning (4 to 6mA) and end (25 to 30mA) the current increment would be of 1mA for each step. From 6 to 25mA the increment was 0.5mA, to have a higher definition in

that zone that usually contains the slope of the sigmoid. To properly cancel noise and mechanical artifacts, the pulses were randomly distributed in frequencies from 1.8-2.2 Hz. The EMG signal was acquired with a 3000Hz sampling frequency, amplified with a gain of 201 and 12bits of resolution. The stimulation and acquisition protocol is illustrated in Figure 6.3.

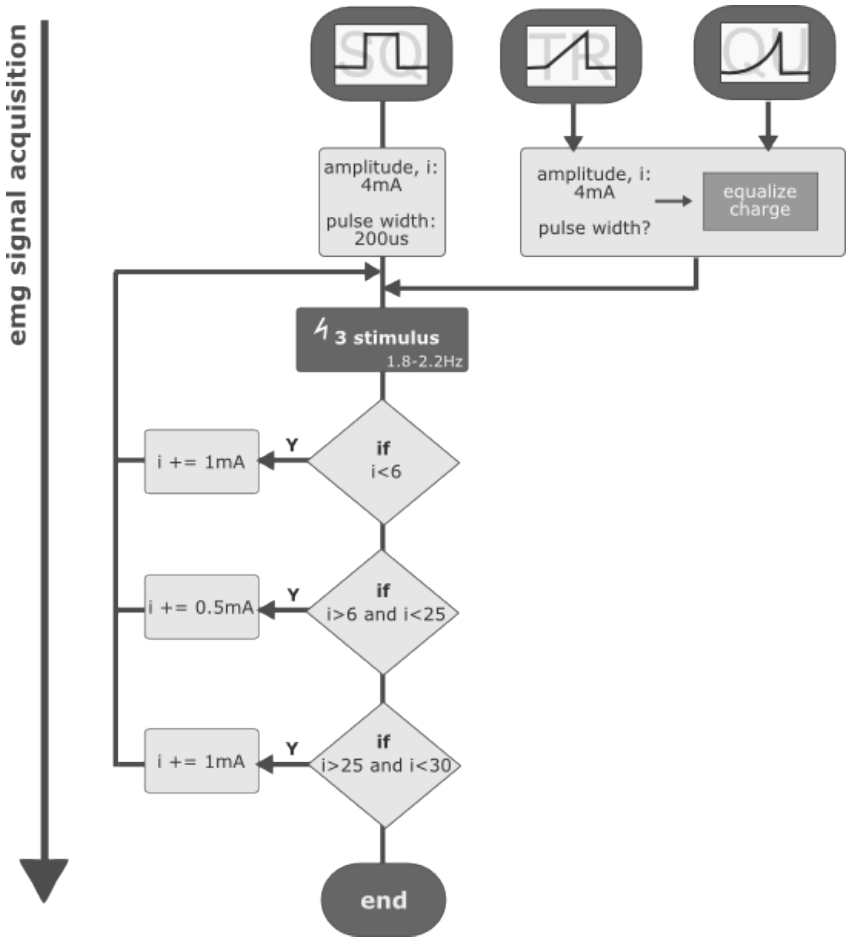

Figure 6.3: Illustrative schematics for the stimulation and acquisition protocol.

The procedure was repeated 4 times per subject, each repetition using a different single pulse stimulation waveform. A standard square wave was applied in mode 1, a triangular wave in mode 2 and a quadratic wave in mode 3. In all these 3 protocols, monophasic single pulses were used with the same intensities. A fourth mode was tested with a biphasic single pulse square wave, with the same intensities of the other tests.

The current charge difference from each waveform was taken into account in the data analysis. The stimulation charge was computed using the equation 5.1 already presented in Chapter 5.

The different single pulses total charge have been equalized for each current intensity, maintaining the amplitude and varying the pulse-width time. From the theory, the total charge of the electrical impulse is the most reliable measurement of the biological reaction

to the electrical stimulation [154]. Figure 6.4 presents an illustration of the pulses tested. The four different waveform single pulses present the charge equalization using a fixed amplitude and a varying pulse-width. To note that the biphasic pulse is equalized, but considering the absolute value of the negative phase.

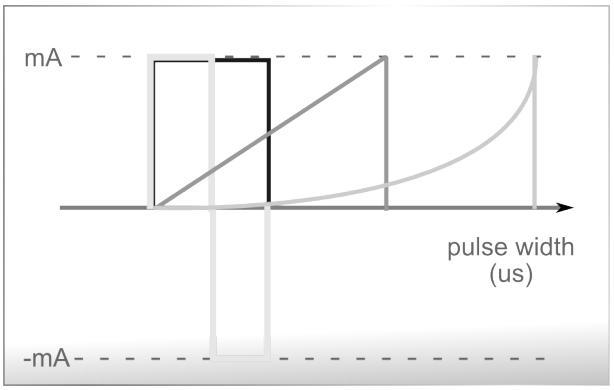

Figure 6.4: Example of the charge equalization of the four different pulse waveforms. Maintaining the amplitude and the area of the pulse, the only variable parameter is the pulse-width, to equalize the charge.

6.2.4 Processing

After acquisition, the collected biosignals were processed and features were extracted, according to the following steps:

1. Detection of the peak-to-peak amplitude of the stimulus response M-wave;
2. CMAP scan composition via interpolation;
3. Extraction of S5, S50, S95, SI range and stimulus-response amplitude elicited by these parameters;
4. Detection of the beginning, final and slope of the resulting sigmoid;
5. Calculus of the mean and standard deviation of the computed parameters;
6. Analysis of the differences in the computed parameters regarding each waveform.

These steps were repeated for each waveform type and all subjects. All results had posterior visual validation by two specialists.

6.3 Results and Discussion

There are several theoretical models to describe the electrical properties of the biological tissue. However, there are also several constraints which cannot be simulated, like the patient comfort to some type of stimulation, the nervous fiber fatigue associated with

Table 6.1: S95 response amplitudes. SQ corresponds to the monophasic square pulse, TR to monophasic triangular pulse, QU to monophasic quadratic pulse and BSQ to the biphasic square pulse.

Amplitude (mV)	S95 SQ	S95 TR	S95 QU	S95 BSQ
Subject 1	4.59	4.46	4.43	5.39
Subject 2	10.0	9.99	9.95	9.82
Subject 3	6.25	6.20	6.63	6.37
Subject 4	5.11	4.97	4.91	5.22
Subject 5	9.91	9.88	9.94	9.93
Subject 6	5.91	5.90	6.05	6.06
Subject 7	6.03	6.05	5.97	5.99
Subject 8	7.35	7.36	7.27	6.31
Subject 9	9.67	9.45	9.41	9.17
Subject 10	7.01	7.02	7.03	6.73
Subject 11	7.86	8.07	8.06	8.06
Subject 12	4.65	4.63	4.71	4.58
Subject 13	5.75	5.78	5.72	5.95

the habituation to the electrical pulse or the possible changes of tissue impedance during stimulation (increase of temperature, increase of skin sudation, micro-irritations to the tissue after consecutive stimulus application, etc). There are also effects impossible to contemplate in a theoretical model, such as the study in injured patients or early prospecting/diagnosed for that. Peripheral nerve stimulation is influenced by external variables that are hard to control, like the adipose tissue layer that the electrical current has to pass, the distance between the stimulation electrodes and the nerve to be stimulated, among other body inhomogeneities. Taking this into consideration, the analyzed parameters were chosen to allow a more objective assessment of the considered effects among different subjects.

Each subject was analyzed regarding the maximum CMAP amplitudes, the excitability parameters (S5, S50, S95 - stimulus current intensity in mA that elicited a correspondent response amplitude in mV), the sigmoid slope and current intensity differences of the CMAP scan, between each different waveform.

Table 6.1 presents S95's stimulus-response amplitude (the amplitude of the pulse stimulus that elicited a response of 95% of the maximum CMAP amplitude) taken from the CMAP scan of all subjects. For each subject, as expected, the variability for each waveform is very low - with all the waveforms it was reached the maximum response amplitude. Although, it is possible to observe that the variability inter-subject is high, and therefore the analysis regarding response amplitudes should be normalized in some way.

Figure 6.5 presents a CMAP wave elicited by the four different waveforms with the same pulse amplitude (10.5mA). Differences in the responses' peak-to-peak amplitude can be observed, using the same current intensity and charge. Figure 6.6 shows four CMAP scans generated with the waveforms. Differences between the waveforms in the stimulation intensities to generate the same response amplitude can also be observed.

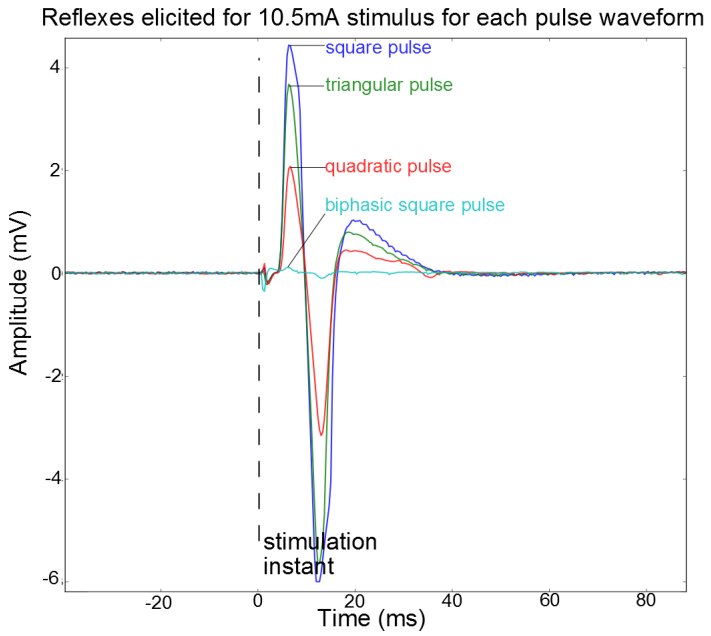

Figure 6.5: CMAPs acquired in a fixed intensity step for each waveform: 10.5mA. Differences in the waves' amplitude, with the same intensity stimulation, can be observed.

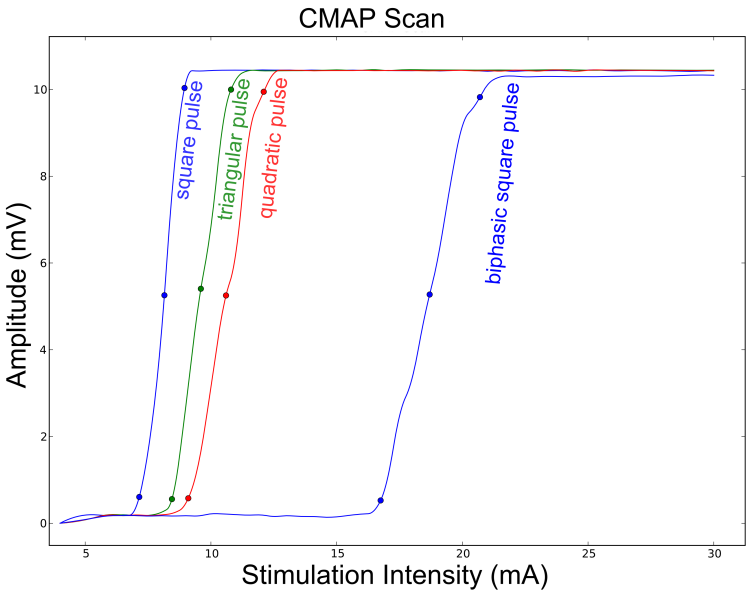

Figure 6.6: Four CMAP scans generated with four waveforms, for one example subject.

Table 6.2 presents the mean CMAP scan sigmoid slope differences between the different waveforms and relative to the square wave. The value is given in percentage, assuming

that the sigmoid slope of the square wave is 100%.

Table 6.2: Mean CMAP scan slope differences between the different types of waveforms. SQ corresponds to the monophasic square pulse, TR to monophasic triangular pulse, QU to monophasic quadratic pulse and BSQ to the biphasic square pulse.

Slope differences	Mean	SD
SQ - TR	81.0%	11.0%
SQ - QU	67.0%	11.0%
SQ - BSQ	44.0%	19.0%

The results show that the square pulse, besides needing less current intensity to generate the same response amplitude as the other waves, it is also the one that presents a steeper curve slope. This means that, for the square wave, the intensities range between the beginning and end of the CMAP scan are usually shorter than for the other waves.

Table 6.3 presents the differences between each waveform to generate the same response amplitude, for all subjects. In this Table it is shown the stimulation threshold for S5 (the stimulation pulse intensity, in mA, that elicited 5% of the CMAP scan maximum amplitude) for the different subjects and waveforms. In Table 6.3 it is presented the mean intensity differences regarding the stimulation parameters S5, S50 and S95 between each waveform and the Square wave. As the stimulation parameters increase in amplitude (from S5 to S50 and S50 to S95), the difference between each wave (from Square to Triangular, Triangular to Quadratic and Quadratic to Biphasic Square) also increases. This is highly correlated with the slope of each wave.

Table 6.3: S5 current intensities. SQ corresponds to the monophasic square pulse, TR to monophasic triangular pulse, QU to monophasic quadratic pulse and BSQ to the biphasic square pulse.

S5 (mA)	SQ	TR	QU	BSQ
Subject 1	5.10	6.10	6.45	8.10
Subject 2	7.10	8.35	9.05	16.8
Subject 3	4.45	5.35	6.10	8.25
Subject 4	4.85	5.10	5.55	8.35
Subject 5	7.80	8.70	9.55	16.6
Subject 6	5.10	6.40	7.15	10.7
Subject 7	6.05	7.20	8.10	10.7
Subject 8	5.30	7.05	8.25	10.1
Subject 9	7.70	9.10	9.90	14.2
Subject 10	8.80	10.6	11.6	17.7
Subject 11	4.15	4.40	4.45	5.45
Subject 12	6.20	7.80	8.35	9.95
Subject 13	7.00	8.50	9.50	13.0

The quadratic wave, among the monophasic waves group, represents the stimulation pulse that needs a larger current intensity to elicit the same response amplitude in comparison with the other waves. This fact consequently translates to an inferior sigmoid slope.

Table 6.4: Current intensity differences for each waveform relative to the square wave. SQ corresponds to the monophasic square pulse, TR to monophasic triangular pulse, QU to monophasic quadratic pulse and BSQ to the biphasic square pulse.

Intensity differences (mA)	S5 Mean (SD)	S50 Mean (SD)	S95 Mean (SD)
TR - SQ	1.22 (0.570)	1.60 (0.630)	1.92 (0.890)
QU - SQ	1.82 (0.700)	2.44 (0.500)	3.01 (0.810)
BSQ - SQ	5.39 (2.41)	7.48 (2.27)	8.62 (2.79)

This happens possibly due to nervous fiber sensibility to charge transfer rate, since in the used setup all single pulses have the total charge equalized. Concerning the biphasic square pulse it is possible to verify that it has a distinct behavior from the monophasic pulses, with activation intensities of the response levels S5, S50 and S95 quite superior and also a rather inferior sigmoid slope, possibly indicating that only one of the flanks of the biphasic waveform is activating the nerve fibers. The monophasic waveforms have a more linear behavior, while the biphasic waveform shows a more unstable behavior with greater variations.

In the context of the nerves' excitability, new effects were revealed with the analysis of the pulse waveform influence in peripheral nerve stimulation. By changing this parameter, the stimulus-response curve slope varies accordingly.

State-of-the-art electrophysiology studies reveal significant differences between healthy subjects and neurodegenerative patients. Upon this, introducing a variable that is able to change the sensibility of the CMAP stimulus-response curve, opens new possibilities of neurodegenerative disorders monitoring and diagnostic. Some questions raise: Will this variable have the same behavior when evaluating patients? Is it possible that subjects with a pathology or propensity to develop will show differences in the sensibility to the electrical charge? These are the relevant questions that this work starts to address, studying the effect on control group composed by healthy subjects. The evaluation of new wave parametrizations in healthy subjects, in addition to being a basis for comparison for future patients evaluation, also represents a contribution to research associated with the CMAP scan methodology and a step forward for understanding electrical pulse waveform influence on peripheral nerve excitability.

CHAPTER 7

APPLICATION TO THE WAVEFORM EFFECT ON FATIGUE AND COMFORT

As referred on the first chapter, fatigue induction is one of the main drawbacks transverse to most of the electrical stimulation applications. The main goal of the following study was to determine the impact of the pulse current waveform on muscle fatigue onset. While the previous studies concerned the peripheral nerve stimulation context, in this study the methodology is applied on the NMES context, requiring special care on the protocol design.

7.1 Introduction

As introduced before, neuromuscular electrical stimulation is a commonly used tool by physical therapists in sports and clinical conditions characterized by motor impairments such as stroke, cerebral palsy, and spinal cord injury [117][170][61][132][174]. The common neuromuscular changes that characterize the aforementioned conditions are muscle weakness and atrophy resulting from disuse or neurological injury [170][116]. However, during electrical stimulation, skeletal muscles fatigue more rapidly than during voluntary contractions [153][187]. Muscle fatigue is an important factor limiting the clinical use of NMES [60]. Researchers have attempted to identify preferred stimulation settings in terms of force contraction [55][106], fatigue [22][65][96] and comfort [91]. The stimulation variables that are thought to have the greatest impact on muscle fatigue include pulse amplitude and duration and pulse train frequency [55][22]. However, because the number of factors considered in the different studies is extremely variable, it is difficult to conclude about the optimal settings that can elicit the strongest contractions with minimal fatigue. The independent effects of these 3 parameters on muscle fatigue are still controversial. Conflicting results exist on the role of current amplitude on muscle fatigue: for instance,

while some authors demonstrate fatigue increasing with current intensity [23], others show no change in fatigue induction with increasing stimulation amplitude [167]. The pulse frequency has been shown to accelerate muscle fatigue [65][108]. Nonetheless, a full understanding of the role of pulse duration on muscle fatigue has not been reached. Gorgey et al. [65] concluded that changing the pulse duration does not appear to influence fatigue in NMES.

Compared to the influence of current amplitude, frequency and pulse duration, the role of single pulse waveform on muscle fatigue is even less well established.

According to the literature, square shape waveform is the most widespread and, for some authors, the most efficient [154]. However, if the pulse duration is sufficiently short (250 μs or less), the triangular shape waveforms are functionally equivalent to square waves [154]. Studies in theoretical models reached promising conclusions about the decrease of the impulse total charge, optimizing the waveform, as a measure to reduce the fatigue induction [84][85][86]. However, as referred previously on Chapter 1, studies with practical implementations passed through methodological barriers that undermine the practical results.

Another factor to take into consideration during NMES is the subjective comfort of stimulation. Many previous studies attempted to determine waveform parameters or combination of parameters which caused less discomfort [51][15]. The results did not show evidences that one waveform was more comfortable than the others [51].

The main aim of this study was to investigate the impact of shape waveform on quadriceps muscle fatigue with three different electric current waveforms, in individuals without impairments. A second purpose was to determine whether changing the waveform could improve the comfort level of subjects.

7.2 Methods

7.2.1 Subjects

A total of 12 healthy subjects, six female and six male, mean (SD) age of 25.0 (2.80) years, volunteered to participate in the study. All subjects reported having no known neuromuscular, skeletal, vascular or dermatological impairment. Each one received a detailed explanation of the study and gave informed consent prior to participation. The Scientific Committee of Health School of Technology of Lisbon approved the present study.

7.2.2 Instrumentation

A isokinetic dynamometer (Biodex) [24] synchronized with the developed stimulation device was used to assess the torque generated by the right quadriceps muscle group during Maximum Voluntary Isometric Contraction (MVIC) and during the electrically induced muscle contractions protocols. The reliability of the Biodex system dynamometers

for knee extensors and knee flexors peak torque measurements in isometric, concentric and eccentric tests is already well established. Inter.class correlation coefficients indicated high to very high reproducibility for isometric, concentric and eccentric peak torques (0.880-0.920), and moderate to high reliability for agonist-antagonist strength ratios (0.620-0.730) [3].

Each subject's right thigh was cleaned with alcohol and two 10 x 5 cm rectangular, reusable, self-adhering electrodes were used for the neuromuscular electrical stimulation. The distal electrode was placed on the vastus medialis approximately 5 to 7 inches from the top margin of the patella; the proximal electrode was placed on the lateral border of the femoral rectus muscle approximately 2/3 of its length above the top edge of the patella, as seen in Figure 7.1.

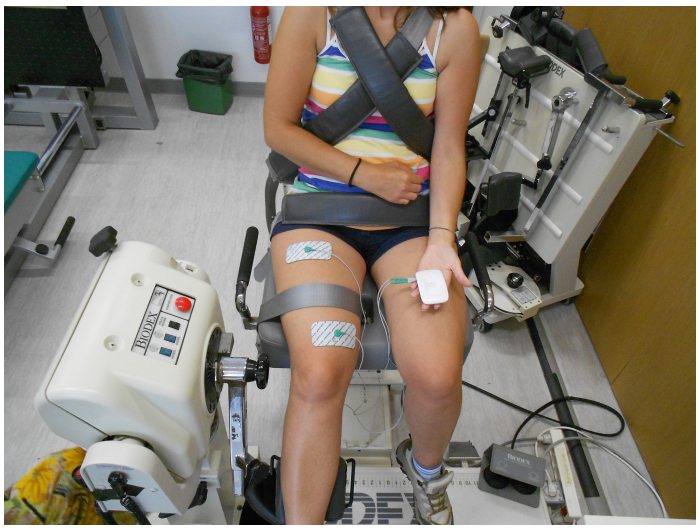

Figure 7.1: Subject prepared to be evaluated by the Biodex system and electrical stimulator. Two electrodes are positioned over vastus medialis and on the lateral border of the femoral rectus. The stimulated limb is maintained in isometric conditions.

The electrical stimulator was connected to the Biodex system through its digital port. Table 7.1 summarizes the electrical stimulation settings used.

Table 7.1: Summary of stimulation characteristics for 3 waveforms. SQ - Square waveform; TR - Triangular waveform; QU - Quadratic waveform.

Stimulation parameters	**SQ**	**TR**	**QU**
Type of Waveform	Monophasic	Monophasic	Monophasic
Pulse width (μs)	175	375	500
Frequency (Hz)	50	50	50
Maximal peak intensity (mA)	100	100	100

7.2.3 Protocol

Each subject participated in 3 sessions, separated by at least 48 hours. Subjects were assigned to 1 of 3 groups, determining the order in which they were tested using 3 different electrical stimulation waveforms. Group assignment was random and participants were not informed of the waveform being used during each testing session. Table 7.2 presents the group division and presents some demographic variables of each.

Table 7.2: Demographic variables (Sex, Age, BMI, Dominant leg, Exercise practice) for 3 groups. Group 1: SQ, TR and QU; Group 2: QU, SQ and TR; Group 3: TR, QU and SQ. *Data presented in form of mean (SD).

Variables	Group 1 (n=4)	Group 2 (n=4)	Group 3 (n=4)
Sex			
- Female	2.0	2.0	2.0
- Male	2.0	2.0	2.0
Age*	22(3.2)	25(1.3)	27(2.7)
BMI*	21(2.8)	22(2.0)	19(0.8)
Dominant leg			
- Right	4.0	4.0	4.0
- Left	0.0	0.0	0.0
Exercise practice			
- Yes	3.0	3.0	2.0
- No	1.0	1.0	2.0

All the tests were performed using the right quadriceps muscle and the MVIC was measured only in the first session. This measurement was followed by determination of the electrical stimulation current amplitude required to elicit 50% of the MVIC and after by a fatigue test using 1 of the 3 shape waveforms. The procedure for each ensuing sessions was similar to the initial procedure except for the MVIC protocol which was determined at the initial session only; the pulse waveform to be used for the electrical stimulation was determined by group assignment. Testing was carried out at the FMH Exercise Physiology Laboratory.

MVIC test: The Biodex system was used to measure MVIC at a 60 degree knee flexion. Subjects' leg, thigh, and pelvis were stabilized by seating system pads and belts. Backrest was set at 110 degree posterior inclination. The fulcrum of the lever arm was aligned with the most inferior aspect of the lateral epicondyle of the right femur. The inferior portion of the shin pad was adjusted superior to the medial malleolus. Before the test, participants warmed up and then stretched the major muscle groups of the lower extremity, holding each stretch for 15 seconds. Subjects did three consecutive 5-second MVIC trials of the right quadriceps muscle group, with 60 seconds of rest between trials. They were asked to keep their arms crossed over their chest and to contract knee extensors as fast and forcefully as possible, while verbal encouragement was provided. Participants were not allowed to view the measurements on the computer screen. The highest measured torque

was used to calculate 50% of the MVIC level. Figure 7.2 provides an illustrative schematics of this MVIC protocol.

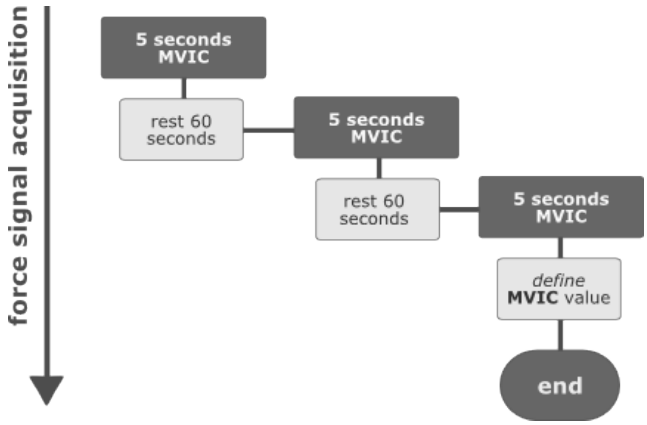

Figure 7.2: Illustrative schematics for the MVIC test acquisition protocol.

Amplitude required to elicit 50% of the MVIC: A five minute rest period was allowed between the MVIC test and the determination current amplitude required to elicit 50% of the MVIC value. The current amplitude was determined by delivering three second trains of progressively greater amplitude. At least one minute separated each train. Three to four trials per participant were performed to determine the amplitude of the current in milliamps (mA).

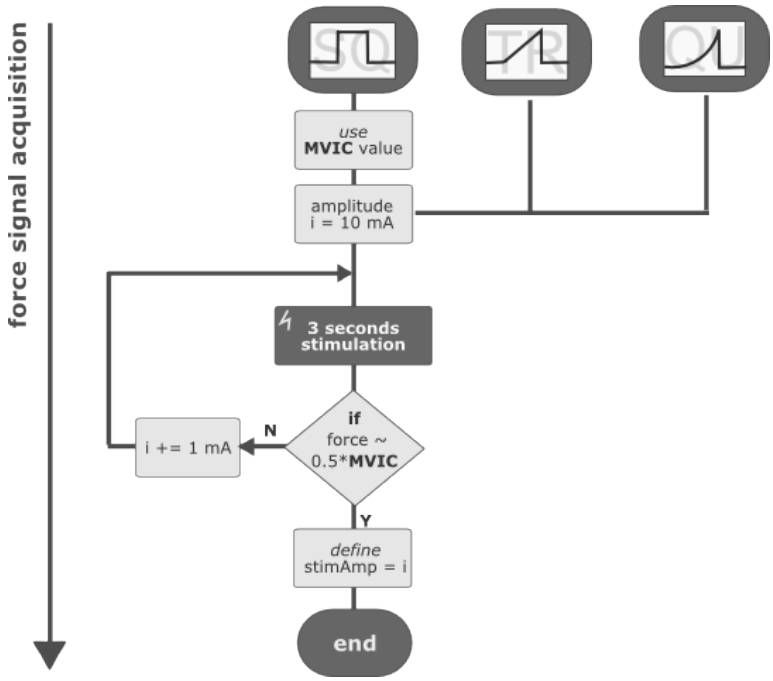

Figure 7.3: Illustrative schematics of the acquisition and stimulation protocol defined to determine the amplitude required to elicit 50% of MVIC.

Figure 7.3 provides an illustrative schematics of the acquisition and stimulation protocol defined to determine the necessary amplitude to be used in the fatigue test.

Fatigue test: After a fifteen minute rest period, to ensure muscle recovery, the fatigue component of the protocol was performed, using the current amplitude previously identified and an identical positioning in the Biodex. The fatigue test consisted in nineteen three-second contractions (work-to-rest cycle of 3 seconds on and 3 seconds off).

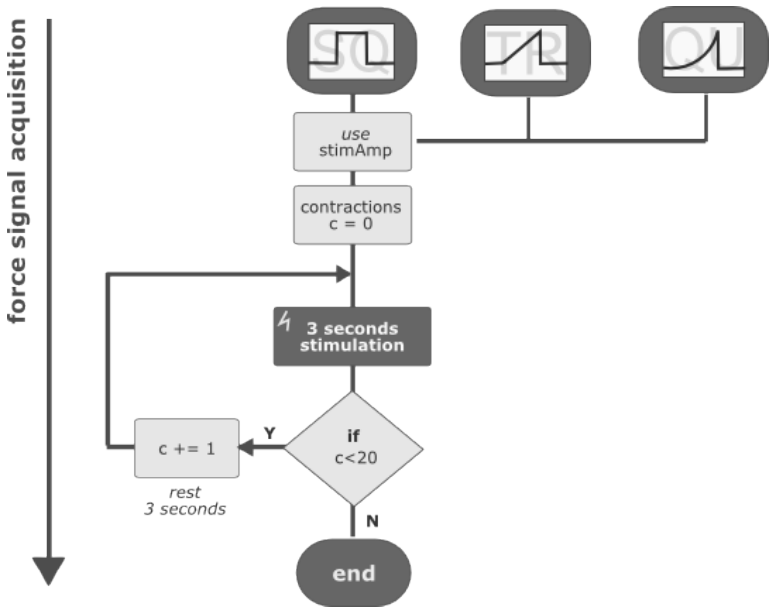

Figure 7.4: Illustrative schematics of the acquisition and stimulation fatigue protocol.

Figure 7.4 provides an illustrative schematics of the acquisition protocol defined to study the fatigue induced by stimulation with each pulse waveform.

The fatigue index (F_index) was measured and reflects the difference between the torques of the initial (T_i) and final (T_f) contractions divided by the torque of the initial contraction, as expressed in equation 7.1.

$$F_index = \frac{T_f - T_i}{T_i} \tag{7.1}$$

An example of the torque signal obtained through the Biodex system for this fatigue test is present in Figure 7.5.

As in other portions of the study, subjects were instructed to keep their arms crossed over their chest and to try to relax during the electrically stimulated muscle contractions. They were not able to view the torque measurements displayed on the computer screen. The study of the fatigue induction was parallel to the comfort evaluation. The subjects were asked to express their pain/discomfort on a Visual Analogue Scale (VAS), a 10 cm long straight line marked at each end with labels which anchor the scale. At the left extreme was the "maximum discomfort" label and, at the right extreme, the "no discomfort" label. VAS has been reported to be accurate, sensitive, and reproducible instruments for patients to report the degree of pain they are experiencing [95]. After the three first contractions,

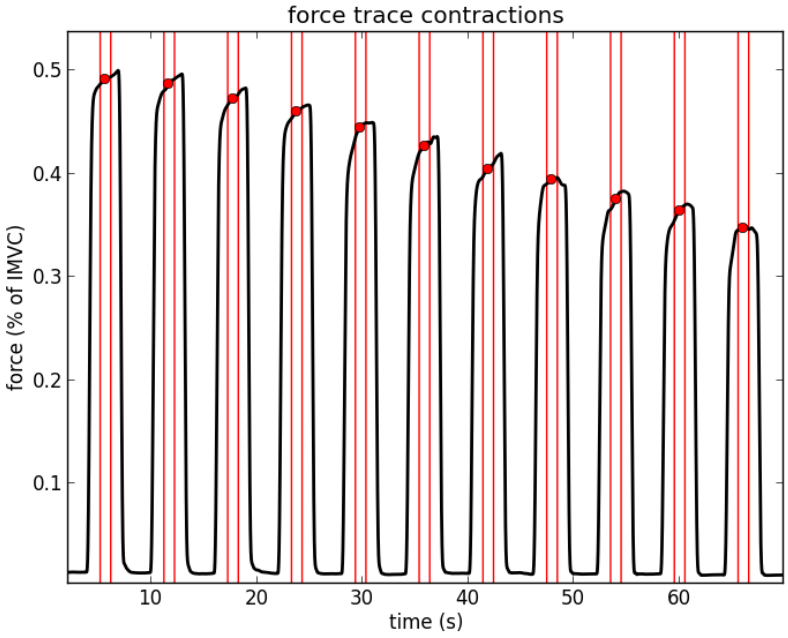

Figure 7.5: Example of the declining torque of a subject during fatigue test with SQ shape waveform. Vertical lines mark the portion where force was evaluated. The red dot marks the force value extracted on each contraction.

the subjects were asked to express their perceived discomfort placing a mark on the line at a point representing the severity of their pain [190]. Scores were noted in millimeters thus giving a total score range of 0-100 millimeters.

7.2.4 Data analysis

The mean value of each contraction was extracted for all subjects and for all the signals resulting from the different waveforms. For that, we computed the mean and standard deviation value of the contraction above 90% of its maximum value. The results were extracted automatically and visually validated by two experts. Descriptive analysis was performed. Frequency, means and standard deviations were calculated for each of the demographic variables. To check if the variables approached a normal distribution the Shapiro-Wilk test was used. The level of significance used was $\alpha = 0.01$. To compare groups in age, Body Mass Index (BMI), discomfort and fatigue percentage the data was analyzed using One-way ANOVA. If the assumption of normality or homogeneity was not verified, Kruskal-Wallis test was used. To examine the effects of the three different shape waveforms on muscle fatigue and discomfort the ANOVA Friedman test was used. The independent variables were the shape waveforms (SQ, TR and QU) and the contraction number (1, 9, 13, 19). The dependent variables were the peak value of force, perceived discomfort and fatigue percentage. Post-hoc tests were used after the identification of differences. The level of significance used to inferential statistics was $\alpha = 0.01$.

7.3 Results

Of the 12 subjects who participated, two of them have not reached values close to 50% MVIC with TR and QU shape waveforms. There were no differences between the 3 groups in age ($F_{2,9}$ = 5.42, $p = 0.029$), BMI ($X^2_{kw}(2)$ = 3.500, $p = 0.174$) and sex (Table 7.2). The groups are also similar in physical exercise practice, although the intensity of the exercise was not discriminated.

Table 7.3: Mean (SD) amplitude and charge values obtained for all subjects.

Shape waveforms	Amplitude (mA)	Charge (μC)
SQ	77.5 (10.6)	13.6 (1.85)
TR	92.5 (7.27)	17.8 (1.51)
QU	98.3 (2.60)	17.1 (0.421)

The mean current amplitudes used for SQ, TR and QU shape waveforms were 77.5 mA, 92.5 mA and 98.3 mA, respectively, as exposed in Table 7.3. Regarding the mean charge, it is verified that TR and QU waves require an higher value than the standard SQ to elicit similar muscle recruitment levels. The SQ, TR and QU waveforms evoked mean (SD) percents of MVIC of 50.5 (2.40)%, 47.2 (11.1)% and 45.6 (10.1)%, respectively. The SQ wave generates higher percent of MVIC than the others with lower current amplitudes. Friedman's test did not reveal statistical difference between evoked percentage of MVIC by the three shape waveforms in the first contraction of the fatigue test ($X^2_{AF}(2)$ = 3.362, $p = 0.186$).

The One-way ANOVA did not reveal significant differences in fatigue percent for SQ ($F_{2,9}$ = 1.063, $p = 0.385$), TR ($F_{2,9}$ = 0.201, $p = 0.821$) and QU ($F_{2,9}$ = 0.317, $p = 0.736$) waveform amongst the three groups. This result ensures that the stimulation order, which was different for each group, didn't interfere with the single effect of the waveform.

Comfort perception score of SQ ($F_{2,9}$ = 0.66, $p = 0.537$), TR ($F_{2,9}$ = 1.725, $p = 0.232$) and QU ($F_{2,9}$ = 2.189, $p = 0.168$) protocols, amongst the three groups, also suggests that the sequence of pulse waves assigned to each stimulation session does not interfere with the results.

Figure 7.6 illustrates the decline in the evoked torque for the three shape waveforms. For all waveforms, there was significant reduction in torque from the initial contraction ($F_{3,2}$ = 189, $p = 0.00$; $X^2_{AF}(3)$ = 32.7, $p = 0.00$; $X^2_{AF}(3)$ = 32.5, $p = 0.00$ for SQ, TR and QU waveform, respectively). No significant differences were observed in fatigue percentage amongst the three shape waveforms ($F_{2,2}$ = 2.68, $p = 0.091$). Despite not statistically significant, the TR wave resulted in a lower fatigue induction when compared to the other two shape waveforms (mean (SD) fatigue percentage 34.8 (12.4)% versus 40.3 (5.50)% and 41.9 (9.30)%).

Relative to comfort score there were significant differences in the results obtained for the three pulse waveforms (X^2_{AF} = 9.50 , $p = 0.009$). On Table 7.4 it is verified that SQ wave differs significantly from TR wave ($p = 0.007$). The most comfortable shape waveform was

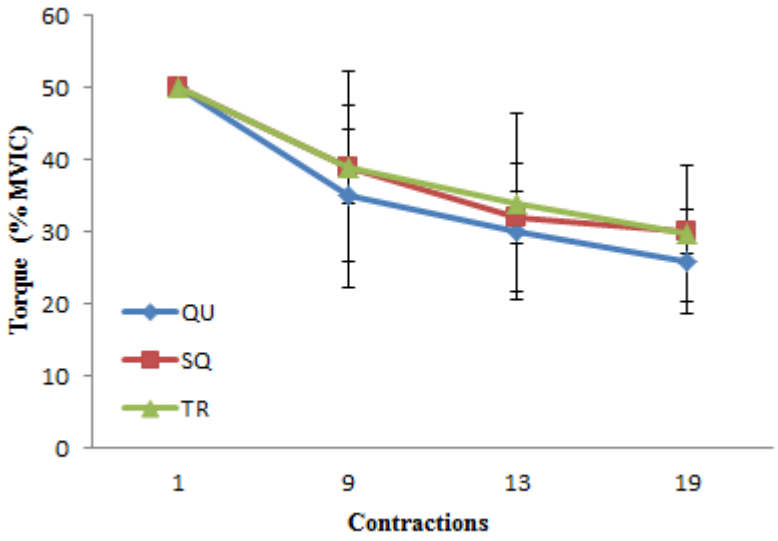

Figure 7.6: Decline in percentage of the MVIC over repeated contractions for QU, SQ and TR (mean (SD)). No significant differences between QU, SQ and TR (P > 0.05).

the TR wave - mean 5.00 (2.50) -, then the QU wave - mean 5.60 (2.90) -, and finally the SQ shape waveform - mean 6.70 (2.70).

Table 7.4: Pairwise comparisons amongst waveforms, relative comfort scores. F: Value of ANOVA Friedman test. *Significantly different $p < 0.05$

Shape waveforms	Value test	P
SQ vs TR	9.50	0.007*
SQ vs QU	9.50	0.662
QU vs TR	9.50	0.199

7.4 Discussion

The current study investigated the influence of the waveform (SQ, TR and QU) on muscle fatigue, during NMES. A second purpose was to determine how the wave shape could alter subject comfort level during stimulation.

It is relevant to mention that there are few works that study the effect of the waveform on muscle fatigue and the independent study of the effect of NMES parameters (frequency, pulse duration and amplitude) on fatigue was made using only the standard SQ wave, which may condition on whether generalizations can be made for other waves. It is also important to mention that, for this first study, the sample size was 12 subjects and more studies with bigger population are necessary to confirm our pilot hypothesis.

Although not statistically significant, the TR wave, mean 34.8 (12.4)%, has shown lowest percentage of fatigue than the standard wave SQ, mean 40.3 (5.50)%, and the QU waveform, mean 41.9 (9.30)%. The three variables considered to have the greatest effect on

muscle fatigue (frequency, electrical charge and time on-off ratios) were controlled in all protocols [55][22].

Previous studies showed that increasing the current amplitude and pulse duration while keeping other NMES parameters constant modestly increased motor unit activation, higher energy demand and thus leading to faster muscle fatigue [51][64][63]. However, as reported before, the nervous fiber is also sensitive to the current transfer rate, showing an accommodation effect on the excitability threshold. Possibly, the TR wave has the best commitment between current transfer rate and total pulse charge.

The TR waveform, as used in our study, had higher amplitude, pulse duration and charge than the SQ wave, but evoked lower percent of MVIC. According to clinical research [111], a good balance between stimulation efficiency and comfort to the patient is reached using pulse durations within the interval 200-400 μs, in which the triangular wave used in this study is included. Relatively to the comfort level, and concerning the sample size, results indicate that the TR wave (mean (SD) of 5.00 (2.50) on VAS score) is significantly more comfortable than the standard SQ wave (mean (SD) of 6.70 (2.70), on VAS score). The statistics applied suggest that the order of waves administration do not interfere with comfort perception.

The best results of the TR wave compared to the SQ wave, at the level of muscle fatigue (although not statistically significant) and mostly at the level of comfort, can be quite relevant for clinical practice. Literature indicates that more efficient stimulation of the nerve fiber is made using the square wave, with pulse durations of less than 250s, but these results show that the triangular wave provides improved comfort and reduced fatigue levels for patients. This confirms and extends the results published before [154].

CHAPTER 8

CONCLUSIONS

The use, manipulation and application of electric currents in biological tissue, as a controlled interference mechanism in the complex system of the human body, is currently a strong source of motivation to researchers around the world. This thesis concerns the creation of tools to address electrical stimulation disadvantages through electrical pulse parametrization. The scientific application of the developed methodologies reveals important conclusions about the fundamental electrophysiology of the human body.

In this chapter, the developed work is summarized, presenting an overall view of what was accomplished. The application scenarios derived from the results are described and all contributions are clarified. Future goals and work guidelines are presented as next research steps. Future implications of the attained advances in the particular field of electrical stimulation, where the thesis' contributions have focused, are discussed.

8.1 Overall Results

The work underlying this PhD rises from the need of new transcutaneous electrical stimulation methodologies, to address the following scientific questions:

- What is the physiological effect of the electric pulse parametrization concerning charge, waveform and polarity? Does the effect change with the clinical condition of the subjects?
- The parametrization influence on muscle recruitment can retard fatigue onset?
- Can parametrization enable fiber selectivity, optimizing the motor fibers recruitment rather than the nervous fibers, reducing contraction discomfort?

The first step to achieve that goal was to carefully go through the theoretical background and state-of-the-art of general electrophysiology and electrical stimulation. A

survey was done covering the basic physiological processes associated with electrical stimulation and the current circuit topologies used. When addressing the electrical stimulation state-of-the-art technology, the degrees of freedom allowed by the current devices are still insufficient concerning mainly the current parametrization control, biosignal acquisition synchronism and usability. A survey exposed in Chapter 2 enlightens how the challenges raised by our scientific questions are inaccessible with current market technology.

After the identification and analysis of the gaps in the available solutions, requirements for a new platform were compiled to guide the technical design and implementation phase (Chapter 3). High freedom of stimulus control concerning parameters like frequency, amplitude, pulse-width and non-standard parameters like the charge, polarity, waveform and automation of a stimulation sequence/session were identified. Envisioning the performance of the device on the clinical and research fields, characteristics such as portability, low intrusiveness, high usability, miniaturization and energy efficiency were also addressed in the requirements.

After the objective requirement definition stage, took place the dimensioning and development of the electrical stimulator and signal acquisition synchronization hardware.

The design and implementation of a high performance circuit given the voltage levels, portability, low consumption and miniaturization of the projected device, required special care from the early phase of components dimensioning to the final PCB layout. Due to the usability and ergonomic specifications of the system, a specific enclosure casing was also developed. The final solution was completed with software architectures required to configure and control the electrical stimulator. A communication layer between the firmware and the user-interface, called API, was created. With this generic API it is possible to consider a vast set of platform-independent applications, from generic to user-specific.

The developed device fulfills all requirements to address the scientific questions of this project. By the end of the development stage, extensive characterization and production tests to the device were executed. After these tests, the device was also applied as a methodological base for two validation studies: i) Nerve regeneration on mice and ii) Real-time stimulation impact on the ANS. These studies, although performed still during the development phase of this PhD, were important contributes to assess and validate the device specifications, as well as its scientific applicability.

Looking for objective answers to the initial questions, three application studies were conducted. The first one focused on the analysis of Interlimb Reflexes (ILR) of tetraplegic and healthy subjects. By controlling the electrical pulse charge and evaluating faithfully the stimulus-response, it was possible to establish descriptive parameters for the ILR cortico-spinal pathway. It was found that the stimulus-response latency is correlated with the pulse electrical charge when analyzing tetraplegic patients. However, the same relation does not appear in control subjects, which corroborates the hypothesis of nerve regeneration after spinal cord injury.

The second study concerns the analysis of the pulse waveform's influence on the transcutaneous peripheral nerve stimulation in the Compound Muscle Action Potential

(CMAP) scan context. CMAP is a non-invasive promissory technique for neurodegenerative pathologies diagnosis. In this study, new CMAP scan protocols were implemented to analyze the influence of electrical pulse waveform on peripheral nerve excitability. A standard electrical stimulation procedure was applied using four different single pulse waveforms: square, triangular and quadratic monophasic waves and a biphasic square wave. Different waveforms elicit different intensity-response amplitude curves. The square pulse needs less current to generate the same response amplitude regarding the other waves and this effect gradually decreases for the triangular, quadratic and biphasic pulse, respectively. The biphasic square pulse shows a distinct behavior from the monophasic pulses, with superior activation intensities and also a rather inferior sigmoid slope. This fact prominently indicates that only one of the flanks of the biphasic waveform is activating the nerve fibers. The stimulation waveform has a direct influence on the stimulus-response slope and consequently on the motoneurons transcutaneous excitability.

The last study evaluates the comfort and fatigue induction of three different Neuromuscular Electrical Stimulation (NMES) waveforms. NMES is a technique widely used by physical therapists in the clinic but its efficacy is limited by the rapid onset of muscle fatigue. Maximal Voluntary Isometric Contraction (MVIC) was measured during the first session. A fatigue electrical stimulation protocol was applied with amplitude required to elicit 50% of the MVIC. Contraction torques and comfort levels were measured and percent fatigue was calculated after the fatigue protocol. An analysis of variance tests for dependent samples was used to determine the effect of shape waveform on muscle fatigue and comfort scores. The results show that the triangular waveform provides more comfort than the standard square waveform. Although not statistically significant, the triangular wave also shows better results concerning fatigue induction. This could be relevant for clinical practice suggesting that waveform parametrization may lead to fiber selectivity, optimizing the motor fibers recruitment rather than the nervous fibers. Due to the low number of analyzed subjects and the subjective nature of pain evaluation these conclusions should be further and deeply studied.

Figure 8.1 complements the questions asked in Chapter 1, showing their correlation with each study performed.

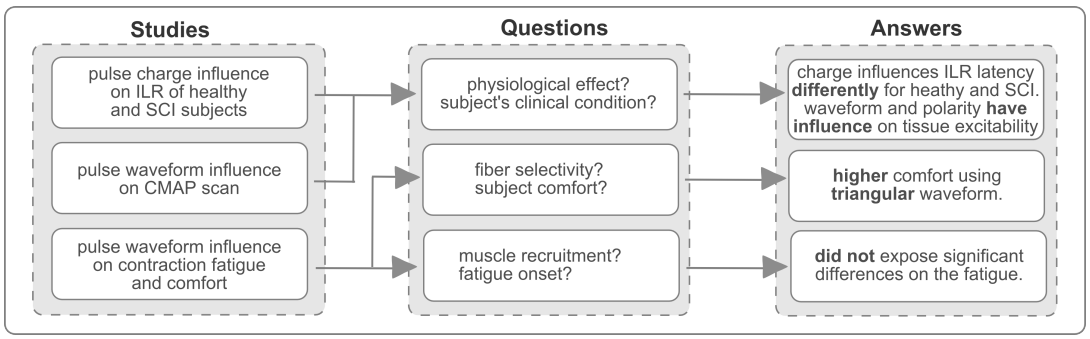

Figure 8.1: Illustration of the final scientific and methodological conclusions of this work. The studies implemented, the scientific questions and the answer for those questions.

Compiling the main pointers from each study a key note emerges: The core concept to control and understand the current-tissue interaction resides in the concept of tissue excitability and its two main concepts: chronaxie and rheobase, as already introduced in Chapter 2. Thenceforth, these two excitability values have been extensively studied in a wide variety of excitable tissues. Current studies establish that these excitability pointers, which are inherent to the tissue type, have high inter-subject variability and high dependency of the clinical condition of the subject [59]. This knowledge about current-tissue interaction has not been contemplated in the context of transcutaneous electrical stimulation in which researchers end up evaluating the relation of parametrization with stimulus response in purely empirical terms. Recently, authors corroborate the claim that the excitability is a parameter that should be taken into account for each patient to improve the clinical efficiency in the application of transcutaneous electrical stimulation [125].

This is, undoubtedly, the key to a new approach in parametrization of electrical pulses. An objective personalization of the stimuli, according to the specific tissue, subject's characteristics and final goal, will lead to a more effective stimulation. For that to be viable and feasible, a reliable device, with high usability and freedom of parametrization, such as the one developed, is needed. Scanning the stimulation amplitude or pulse-width (among other aspects) and respective EMG evaluation, enables a real time measure of tissue excitability. The developed system can contain a set of pre-loaded excitability evaluation protocols and therefore optimize and personalize the electrical stimulation parametrization.

8.2 Contributions

Today's electrical stimulation challenges require innovative solutions. In general, technological development is defined by market demand and characteristics such as portability, usability and integration flexibility are expensive details that the research field usually does not support. However, the intrusiveness of the system can have the same negative influence on the research results as a poor quality signal acquisition (for example, low signal-to-noise ratio, movement artifacts, amongst others). The study performed with tetraplegic patients in this thesis corroborates this affirmation. The ease of use of the miniaturized and wireless system allows a wider coverage both in subjects' number and data reliability due to the low intrusiveness for the patient.

Several subjective experiences highly influenced by emotional, cognitive and contextual factors, use electrical stimulation to assess the impact of psychological manipulations on pain perception [191][151]. For example, in a recent study that aimed to assess the impact of social distress on pain, electrical stimuli were applied while participants were excluded from a virtual ball tossing game. It was found that participants more sensitive to social distress were also more sensitive to physical pain [40]. In these experimental settings a complex apparatus of cables and heavy instrumentation may induce higher anxiety in

the participant, thus artificially heightening the relevance of the anxiety variable. This compromises the laboratory results' applicability when used in more naturalistic settings.

Reliability both in the applied stimuli, concerning the current effective control, and in the biosignals acquired, concerning its quality, signal-to-noise ratio and resolution is another valuable feature for research purposes. On the other hand, the possibility of parametrization is relevant for therapists, who can set parameters and design customized electrical stimulation programs targeted at each patient.

Table 8.1 summarizes the device's features that were differentiating factors and catalyzers in each case study performed. Concerning the evaluation of ILR in healthy and SCI subjects, described in Chapter 5, transcutaneous peripheral nerve stimulation was applied with three different monophasic pulse waveforms. The ILR were evaluated through surface EMG, synchronized with the stimulation protocol. This study required the application of a stimulation session which scanned a range of increasing amplitudes in specific timings. Regarding the application of CMAP scan protocol, described in Chapter 6, transcutaneous peripheral nerve stimulation was applied with four different monophasic and one biphasic pulse waveform. Surface EMG was also used to acquire the CMAP signal. This study was only possible due to the automation of the stimulation session, like in the previous study, although with different intensity ranges, steps, timings and charge equalization. In the fatigue and comfort evaluation study, described in the previous chapter, a *multi* waveform NMES protocol was implemented with specific parametrizations for fatigue induction. Fatigue was evaluated by the decrease in the muscle force acquired through a Biodex system synchronized with the stimulation unit.

Table 8.1: Summary of the stimulator features that were a differentiating factor in each scientific study.

Features	Studies		
	ILR in SCI	CMAP scan	Fatigue
Type	TENS	TENS	NMES
Polarity	Monophasic	Monophasic + Biphasic	Monophasic
Charge Equalization	NO	YES	YES
Biosignals	EMG	EMG	FORCE
Session Driving	YES	YES	NO

The hardware developments in the scope of this thesis were initially reported in the validation stage [4] and the final solution is being disseminated under intellectual property patent process. Still in the methodological context, the configuration of electrical pulses and real time synchronization with physiological data was also reported [46][47].

There were also contributions in the human electrophysiology field, answering the scientific questions previously raised, which are listed in the following paragraphs.

- An extensive survey on the physiological impact of electrical stimulation parameters and current circuit topologies was done. This review summarizes the actual paradigm of surface electrical stimulation.

- The study of descriptive electrophysiological parameters in contralateral interlimb reflexes was performed in *Hospital de Clínicas da Universidade Estadual de Campinas*, Brasil, first concerning the analysis of healthy subjects [7], and after extending to SCI patients [6]. The achieved results empowered new rehabilitation pathways for tetraplegic patients.

- Transcutaneous nerve excitability was evaluated through the implementation of new CMAP scan protocols with current modulated waveforms [41].

- Quadriceps muscle fatigue and comfort were addressed through a novel NMES protocol using with current modulated waveforms [9].

During this PhD, the methodologies developed were applied in a set of collateral contributions not focused on electrical stimulation. Despite this, they are worth noting:

- **EMG Onset:** In both ILR and CMAP processing studies (from Chapters 5 and 6), algorithms for event detection (in this case, EMG reflexes), were implemented. Given its high performance, the event detection algorithms were also applied in the context of EMG contractions onset detection [58]. The muscle activation study has proven to be a key element in the comprehension of the motor strategies underlying human kinetics. EMG has been widely selected in the investigation of these strategies. The accurate onset measuring of EMG activity enables the motor strategies and physiological information assessment. In order to validate and evaluate the algorithm operational performance, the methodology was tested in synthetic and acquired EMG signals. The algorithm revealed high immunity to noise and sensitivity to morphological signal modifications. The methodology was implemented in a real time EMG acquisition context, being the base to the development of new tools in assistive technology designed for persons with disabilities like Cerebral Palsy [110]. The EMG onset detection toolkit was also necessary to enhance the development of a occupational biomechanical exposure platform based on the EMG analysis and accelerometry [134].

- **Coherence on ALS:** EMG coherence analysis was addressed as a prognostic factor for ALS patients [38], driven from algorithmic methodologies developed during this work. Both the algorithms for event detection and the knowledge for characterization and processing of EMG reflexes, were applied in the study of Coherence and Phase Locking Disruption evaluation in electromyograms of patients with amyotrophic lateral sclerosis (ALS) [38]. In motor neuron disease, the aim of therapy is to prevent or slow neuronal degeneration and early diagnosis is essential. Hypothesising that beta-band (15-30 Hz) is a measure of pathways integrity as shown in literature, coherence and Phase Locking Factor (PLF) could be used as an electrophysiological indicator of upper and lower neuron integrity in patients with ALS. Coherence and

PLF analysis were computed for EMG signals registered from 2 groups: control subjects and ALS patients. The data was recorded during instants of steady contraction for both contra and ipsilateral acquisitions. Overall results allowed to conclude that contralateral coherence is not a good measure of corticospinal pathways integrity, however, ipsilateral acquisitions show promising results and it is possible to affirm that ipsilateral measurements may reflect neuronal degeneration.

- **Biometry Algorithm:** In this PhD, EMG reflexes are acquired and its morphology analyzed. CMAP and ILR reflexes are analyzed concerning amplitude, latency, waveform, amongst others. This morphological analysis is relevant in the contemporary context of biometry [5][8]. Two studies were implemented exposing the implementation and test of a biometric identification procedure based on ECG signal morphology. For those studies, 63 subjects were analyzed in two data-recording sessions separated by six months (Time Instance 1, T1, and Time Instance 2, T2). Two tests were performed aiming at subject identification, using a distance-based method with the heartbeat patterns. The accuracy achieved was 95.2% for the first test and 90.5% for the second. These results were achieved with the optimization of crucial parameters with impact in a real time identification problem, like the length of ECG signal needed to perform an accurate decision. Those studies show the potential of ECG signal morphology as a valid parameter for classification in biometric applications.

8.3 Future Work

This project research leaves a few aspects unfinished and raises new questions for which additional research effort should be devoted in the future. Concerning this work's applications, the future improvements can be divided into three aspects:

1. Extend the research:
    - The CMAP scan study has already started with ALS patients. In the next stage, the methodology will be extended to other neurodegenerative pathologies.
    - Study the effect of new waveforms, particularly the biphasic waves, in muscle fatigue and comfort.
2. Apply clinical methodologies:
    - Implement new mechanisms of interlimb rehabilitation for tetraplegic patients;
    - Apply, in current NMES, TENS and PNS therapies, electrical stimulus customizations, according to the real tissue excitability conditions, patient conditions and final therapy objectives.

3. Commercialization:

    - Integrate the device in the current platform for biofeedback rehabilitation from PLUX, the physioplux system, opening new doors for psycho-motor rehabilitation;
    - The protection of the intellectual property by patenting the device is already in process;
    - It is also our intention to obtain the mandatory conformity marking for certain products sold within the European economic area, the CE Marking.

APPENDIX A

LIST OF PUBLICATIONS

A.1 Book Chapters

- *Generic biometry algorithm based on signal morphology information: application in the electrocardiogram signal.*
  Araújo, T., Nunes, N., Gamboa, H. and Fred, A. In Pattern Recognition Applications and Methods, Edited by Ana Fred, Maria De Marsico, 11/2014: pages 301-310; Springer International Publishing, 2014.

- *Knowledge Acquisition System Based on JSON Schema for Electrophysiological Actuation.*
  Costa, N., **Araújo, T.**, Nunes, N. Gamboa, H. E-Business and Telecommunications, vol. 455, pp. 284-302, 12 Sep 2014, Springer Berlin Heidelberg, 2014.

- *Enhancing Interaction of Persons with Cerebral Palsy using Biosignals Detection.*
  Londral, A., Sousa, J., **Araújo, T.** and Silva, H. Assistive Technology Research Series, vol. 33, pp. 1051-1055, IOS Press Ebooks, 2013.

- *Time Series Clustering Algorithm for Two-Modes Cyclic Biosignals.*
  Nunes, N., **Araújo, T.** and Gamboa, H. In A. Fred, J. Filipe, and H. Gamboa (Eds.): BIOSTEC 2011, CCIS 273, pp. 233–245. Springer, Heidelberg, 2012.

A.2 Journal Papers

- *Analysis of descriptive electrophysiological parameters in contralateral interlimb reflexes on tetraplegic patients.*
  Araújo, T., Brandão, A., Didier, T., Bracco, B., Gamboa, H. and Cliquet, A. Spinal Cord, Nature, Advance online publication 7 October 2014; doi: 10.1038/sc.2014.169

- *Wireless Platform for Ergonomics Evaluation of Occupational Biomechanical Exposure.*
  Nunes, N., Carnide, F., Batista, N., **Araújo, T.**, Martins, G., Vieira, F., Veloso, A. and Gamboa, H. Journal of Biomechanics, vol. 45, Supplement 1, pp. S506, 2012.

- *Electromyography onset detection: new methodology.*
  Gamboa, H., Matias, R., **Araújo, T.** and Veloso, A. Journal of Biomechanics Vol. 45 Supplement 1, Page S49, 2012.

A.3 Conference Proceedings

- *Quadriceps muscle fatigue and comfort generated by neuromuscular electrical stimulation with current modulated waveforms.*
  Araújo, T., Anjos, A., Nunes, N., Rebelo, P. and Gamboa, H. In Proceedings of 8th International Joint Conference on Biomedical Engineering Systems and Technologies, Lisbon, Portugal, 2015.

- *Multi-biosignals analysis: The effect of peripheral nerve stimulation on skin conductance and heart rate variability.*
  Araújo, T., Dias, P., Nunes, N. and Gamboa, H. In Proceedings of 8th International Joint Conference on Biomedical Engineering Systems and Technologies, Lisbon, Portugal, 2015.

- *Analysis of inter-subjects variability of contralateral interlimb electrophysiological reflexes.*
  Araújo, T., Brandão, A., Didier, T., Bracco, B., Gamboa, H. and Cliquet, A. American Spinal Injury Association Annual Meeting (ASIA 2014), San Antonio, Texas, USA, 2014.

- *Coherence and Phase Locking Disruption in Electromyograms of Patients with Amyotrophic Lateral Sclerosis.*
  Camara, M., Carvalho, M., **Araújo, T.**, Gamboa, H. and Quintão, C. In Proceedings of Biosignals – International Conference on Bio-Inspired Systems and Signal Processing (BIOSIGNALS 2014), Paris, France, 2014.

- *Multi-purpose Electrostimulator Software.*
  Costa, N., **Araújo, T.**, Nunes, N., Gamboa, H. In Proceedings of Biodevices - International Conference on Biomedical Electronics and Devices (BIOSTEC), Barcelona, Spain, 2013.

- *Distance-based algorithm for biometric applications in meanwaves of subject's heartbeats.*
  Araújo, T., Nunes, N., Gamboa, H. and Fred, A. In Proceedings of International Special Session on Biometrics: Technologies, Systems and Applications (BTSA), Barcelona, Spain, 2013.

- *A New Tool for the Analysis of Heart Rate Variability of Long Duration Records.*
  Chorão, R., Sousa, J., **Araújo, T.**, Gamboa, H. In Proceedings of the 10th International

Conference on Wireless Information Networks and Systems (ICETE WINSYS), Rome, Italy, 2012.

- *Miniaturized Wireless Controlled Electrostimulator.*
  Araújo, T., Nunes, N., and Gamboa, H. In Proceedings of Biodevices - International Conference on Biomedical Electronics and Devices (BIOSTEC), Vilamoura, Portugal, 2012.

- *Localized Electroencephalography Sensor and Detection of Evoked Potentials.*
  Araújo, T., Nunes, N., Quintão, C. and Gamboa, H. In Proceedings of MindCare 2012, 2nd International Workshop on Computing Paradigms for Mental Health (BIOSTEC), Vilamoura, Portugal, 2012.

- *Two-Modes Cyclic Biosignal Clustering based on Time Series Analysis.*
  Nunes, N., **Araújo, T.** and Gamboa, H. In Proceedings of Biosignals - International Conference on Bio-inspired Systems and Signal Processing (BIOSTEC), Rome, Italy, 2011.

- *Comparison between the Standard Average muscle Activation with The Use of Snorkel and Without Snorkel in Breastroke Technique*
  Conceição, A., Gamboa, H., Palma, S., **Araújo, T.**, Nunes, N., Marinho, D., Costa, A., Silva, A. and Louro, H. In: Kjendlie, P.; Stallman, R.; Cabri, J. (Eds), Book of Abstracts of the 7688 XIth International Symposium for Biomechanics and Medicine in Swimming. Oslo, 2010.

- *Alpha rhythm onset detector based on localized EEG sensor.*
  Araújo, T., Nunes, N., Palma, S. and Gamboa, H. In Proceedings of 7th ESBME - European Symposium on Biomedical Engineering, Chalkidiki, Greece, 2010.

A.4 Oral Communications

- "*Quadriceps muscle fatigue and comfort generated by neuromuscular electrical stimulation with current modulated waveforms*", Paper presentation, 9th International Conference on Biomedical Electronics and Devices (BIOSTEC), Lisbon, Portugal, 2015.

- "*Analysis of Inter-Subjects Variability of Contralateral Interlimb Electrophysiological Reflexes*", Paper presentation, American Spinal Injury Association, Annual Meeting, San Antonio, Texas, USA, 2014.

- "*Detecção de instantes de activação muscular, novas metodologias e aplicações*", Lecture, Doctoral Program, FCT-UNL, Caparica, Portugal, 2013.

- "*Detecção de instantes de activação muscular, novas metodologias e aplicações*", Lecture, Debates series, IPS, Setúbal, Portugal, 2012.

- "*Electromyography Onset Detection: New Methodology*", Paper presentation, 18th congress of European Society of Biomechanics (ESB), Lisbon, Portugal, 2012.
- "*Knowledge Acquisition System Based on JSON Schema*", Paper presentation, International Conference on Wireless Information Networks and Systems, Rome, Italy, 2012.
- "*A New Tool for the Analysis of Heart Rate Variability of Long Duration Records*", Paper presentation, International Conference on Signal Processing and Multimedia Applications, Rome, Italy, 2012.
- "*Localized Electroencephalography Sensor and detection of evoked potentials*", Paper presentation, MindCare, Rome, Italy, 2012.

APPENDIX B

TOOLS

The work underlying the current thesis was developed using a set of tools needed during the implementation of the electrical stimulator and for writing the thesis document. Most of the used tools are Open Source applications and these lines express the gratitude to the community that provided means for scientific production in an open environment, better suited for the aim of Science.

B.1 Stimulator Development

The Integrated Development Environment (IDE) for AVR microcontrollers programming used was *AVR Studio*, in C/C++, with the GCC GNU Compiler. This IDE was used to develop, compile and implement all the firmware described in this thesis.

The electrical stimulator schematics and synchronization cable circuit were drawn using *Eagle*. This tool was also used for the PCB layout design.

Visual Studio 2011 was used to develop and compile the API in C/C++.

Teraterm and *Termite* were the applications used for the communication tests when implementing the firmware.

All the design and structure implementation of the final device enclosure box was done using *Solid Works*.

B.2 Scientific Computation

To control and configure the electrical stimulator, generic control interfaces were made. One interface was developed using *Java* and the *Android Software Development Kit (SDK)* for smartphone and tablet usage. The generic computer-based interface for both synchronization and biosignals acquisition used a server-client web-based architecture, with *Python* as a server and *Javascript*, *HTML* and *CSS* for the front-end presentation.

For the specific cases in study, custom scripts were developed. The development was based on data acquisition, preparation of stimulation protocols, posterior data processing, visualization and analysis. The selected coding platform was the *Python* environment given that a set of scientific tools are available for numerical manipulation and visualization [186]. Without entering into too much detail, the *Python* tools used in the project were: *numpy* [137], *scipy* [136] and *matplotlib* [81]. For an IDE that has a good support of *Python* development, *Eclipse* was used, with the *PyDev* plugin [186].

All the signals acquired were stored in *Dropbox* that worked as a data repository, enabling remote access to the data.

B.3 Thesis Document

For the support of the writing and composition of the thesis document, the *LATEX* environment was used, with *Miktex* distribution. *TeXnicCenter* was the editor used for writing and compiling the document. All the research publications produced during the thesis development were also created with *LATEX*.

For research purposes we extensively used a set of websites. The *Wikipedia* site, both the Portuguese and English versions, was useful to find primary general information on most of the studied topics. Some contributions to the pages related to areas studied in the present research were made. *Citeseer* has an extended library of open access research papers, with direct access to related citations, being useful for the following related research themes and to extract bibliographic data in the bibtex format.

All the diagrams present in this document were supported by *Inkscape*. Most of the images were also graphically created or processed in *Inkscape* or *Gimp*.

APPENDIX C

BROCHURE

The following page presents a brochure for the electrical stimulation device developed, in which all technical features are summarized. Also presented are illustrations of the device and correspondent accessories for peripheral nerve and muscular stimulation.

TOTAL STIMULATION CONTROL & SYNCHRONIZATION WITH BIOSIGNALS

DESCRIPTION electrical stimulation portable device for electrotherapy or research, with the capability of working as a neuromuscular electrical stimulator (NMES) or a transcutaneous electrical nerve stimulator (TENS).

it allows a precise adjustment of the stimulation parameters like frequency, pulse, on-off cicle, current and introduces a new feature to modulate the stimulus waveform (square, triangular, sinusoidal waves).

With this device it is possible to create and store personalized sessions for each subject. Each session is composed with different modes (different waveforms, amplitudes, durations and frequencies) which are also personalized and stored into the device.

STIMFORM CONTROL DRAW STIMULATION WAVEFORMS

SPECIFICATIONS

- CURRENT MODULATED [-100 : 100 mA] WITH RESOLUTION OF 25uA
- FREQUENCY RANGE [0 : 200 Hz] WITH RESOLUTION OF 1Hz
- PULSE WIDTH RANGE [5 : 500 us] WITH RESOLUTION OF 5us
- MULTIPLE WAVEFORM SELECTION
- BLUETOOTH ® CONNECTIVITY
- 1 DIGITAL I / O PORT 1BIT / I^2C
- BIOSIGNALS ACQUISITION HUB REAL TIME SYNCHRONIZATION
- SESSION AND MODES PROGRAMMING

peripheral nerve stimulation electrodes

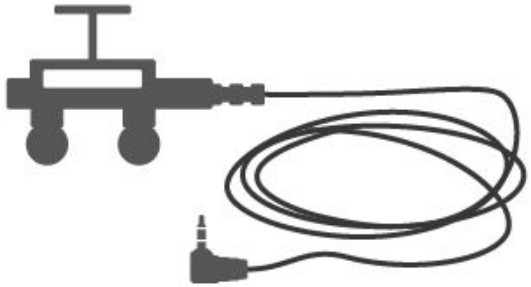

muscle stimulation electrodes

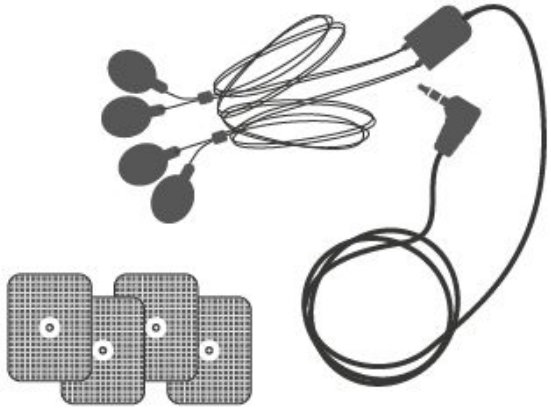

APPENDIX D

TEST PROTOCOL

The following pages present a template for the test protocol implemented after the validation stage of this PhD.

Electrical Stimulator
Caracterization tests

03/01/2012

Electrical Stimulator
Test Protocols

nº doc: EE2013/001

título: Test Protocol

projecto: EE

Autores				
Versão	Nome	Funções	Alterações	Data
1	Tiago Araújo	Eng. Hardware and PhD student	Issue Document	03/01/12

Aprovação				
Versão	Nome	Funções	Data	Assinatura

PLUX - wireless biosignals
Lisbon Office
Av. 5 de Outubro, nº 70 - 6º | 1050-059 Lisboa - Portugal
Tel.. +351 211 956 542 | Fax. +351 211 956 531

Covilhã Office
Parkurbis | 6200-865 Covilhã | Portugal
Tel.. +351 275 957 029 | Fax. +351 275 957 005

www.plux.info

Introduction

This document presents the test protocols applied to the electrical stimulator device. Thus it is intended to systematize the testing process and to facilitate detection of any problems, errors or unexpected behavior of the system in its final stage of development. In addition to the topics above, this document will also serve as a record of actions taken.

Version record of tested equipment

Hardware version (PCB)	
API version	
Firmware version	

Executed by Date	

Test protocols

Hardware test cases				
Nº	Description	Initial condition	Expected result (s)	State (Y/N)
1	Communication			
1,1	Keep continuously bluetooth communication for an extended time period. Minimum of 4h.	EE in stimulation mode; Running test script1 for continuous communication test (start/stop stimulation cycle);	EE remains in communication throughout the script. **Interval tested:** 4 h **Battery state:** Unknown	
1,2	Communication stress test	EE in stimulation mode; Run HeavyLoad software to overload the CPU performance	EE remains in communication throughout the script. **Interval tested:** 4 h **Battery state:** Unknown	
1,3	EE losing range with Continuous running if no network on	EE in stimulation mode; Continuous running if no network on (1);	The device should remains in stimulation throughout the session or mode pre-programed.	
1,4	EE losing range with Continuous running if no network off	EE in stimulation mode; Continuous running if no network off (0);	The device should stop the stimulation and pass to the idle mode.	
2	Battery and charge management			
2,1	Autonomy with standard battery (3.7V 700mAh)	Device with full battery. Setup and start the autonomy standard test session *	**Time to discharge:** 5 h	
2,3	Medical class power supply	Medical class power supply	The medical grade charger	

			meets all required specifications or safety standards of medical device.	
2,4	Battery charge and time to charge.	Device with discharged battery Medical class power supply	The device charge without any problem. It is expected some heating. **Time to charge:** 1.2 h	
2,5	Device states on charge modes	Device with discharged battery Medical class power supply	When charging the device enter in idle and stimulation mode.	
2,6	Low bat state when the device is in stimulation mode.	Device with low battery Device in stimulation mode	Led green off Led red blink 2 time/s	
2,7	Low bat state when the device is in idle mode.	Device with low battery and idle state	Led green off Led red blink 1 time/s	
2,8	Discharged battery state	Device with discharged battery	The device shut down independently of the state that it remain before discharge.	
2,9	Connect the charger during stimulation mode	Device in stimulation mode Medical class power supply	The device blinks with the same led but with inverted duty cycle	

3	Control			
3,1	• Set Wave on mode • Set frequency on mode • Start mode • Stimulation Stop	Device in idle mode; 1- Set and start the zero wave on mode 1 with 0Hz; 2- Set and start the 30mA quadratic (monophasic) wave on mode 1 with 120Hz and 500us of pulse-width;	1 - The device don't drive current 2 - The device drives the quadratic wave. Oscilloscope in run mode visualize the wave on a 400 ohm resistor.	
3,2	Drive a Stimulation Session: • Set time on state • Set mode on state • Set next state on state • Set maximum state changes • Stimulation session start	Device in idle mode; 1- Set 3s to state 0, 5s to state 1, 3s to state 2 and 5s to state 3; 2- Configure mode 0 with zero wave, configure mode 1 with the quadratic monophasic wave 30mA, configure mode 2 with square wave biphasic with 60mA. Set mode 0 to state 0, mode 1 to state 1, mode 0 to state 2 and mode 2 to state 3; 3- set next state (NS) 1 to state 0, NS 2 to state 1, NS 3 to state 2 and NS 0 to state 3; 4- set maximum state changes equal to 8 5- start the session	With the Oscilloscope in run mode visualize the wave on a 400 ohm resistor. Evaluate if the session correspond with the configuration done. 5- EE ends the idle mode and starts the stimulation mode (green led with 2 blinks/s).	
3,9	Unitary stimuli drive	Device in idle mode; Drive a unit pusle of mode 2	With the Oscilloscope in single mode visualize the wave on a 400 ohm resistor.	
3,10	Stimulation Stop	Device in idle mode;	EE ends the stimulation mode mode and starts the idle mode (idle mode – green led with 1 blink/s);.	
3,11	EE in stimulation mode and on/off button is pressed	Device in stimulation mode;	EE will pass from stimulation mode to *off.*	

APPENDIX E

CLASSIFICATION OF SPINAL CORD INJURY

A spinal cord injury is an injury to the spinal cord resulting in a change, either temporary or permanent, in the cord's normal motor, sensory, or autonomic function. The symptoms vary depending on where the spinal cord and nerve roots are damaged. Spinal cord injuries are described at various levels of 'incomplete', which can vary from having no effect on the patient to a 'complete' injury which means a total loss of function.

The American Spinal Injury Association (ASIA) first published an international classification of spinal cord injury, called the *International Standards for Neurological and Functional Classification of Spinal Cord Injury* [97]. It is a system of tests used to define and describe the extent and severity of a patient's spinal cord injury and help determine future rehabilitation and recovery needs. It is ideally completed within 72 hours after the initial injury. The patient's grade is based on how much sensation he or she can feel at multiple points on the body, as well as tests of motor function.

The grade classification exam is presented in the following pages.

Patient Name _____

Examiner Name _____ Date/Time of Exam _____

INTERNATIONAL STANDARDS FOR NEUROLOGICAL CLASSIFICATION OF SPINAL CORD INJURY

ASIA American Spinal Injury Association

ISCOS

MOTOR

KEY MUSCLES (scoring on reverse side)

	R	L	
C5	☐	☐	Elbow flexors
C6	☐	☐	Wrist extensors
C7	☐	☐	Elbow extensors
C8	☐	☐	Finger flexors (distal phalanx of middle finger)
T1	☐	☐	Finger abductors (little finger)

UPPER LIMB TOTAL (MAXIMUM) ☐ + ☐ = ☐ (25) (25) (50)

Comments:

L2	☐	☐	Hip flexors
L3	☐	☐	Knee extensors
L4	☐	☐	Ankle dorsiflexors
L5	☐	☐	Long toe extensors
S1	☐	☐	Ankle plantar flexors

(VAC) Voluntary anal contraction (Yes/No) ☐

LOWER LIMB TOTAL (MAXIMUM) ☐ + ☐ = ☐ (25) (25) (50)

	LIGHT TOUCH R	LIGHT TOUCH L	PIN PRICK R	PIN PRICK L
C2				
C3				
C4				
C5				
C6				
C7				
C8				
T1				
T2				
T3				
T4				
T5				
T6				
T7				
T8				
T9				
T10				
T11				
T12				
L1				
L2				
L3				
L4				
L5				
S1				
S2				
S3				
S4-5				
TOTALS (MAXIMUM)	☐ + (56)	☐ (56)	☐ + (56)	☐ = (56)

SENSORY

KEY SENSORY POINTS

0 = absent
1 = altered
2 = normal
NT = not testable

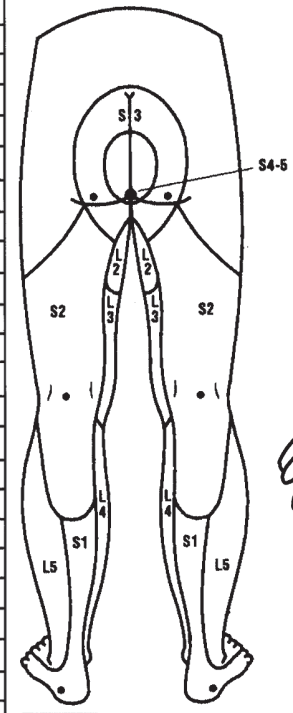

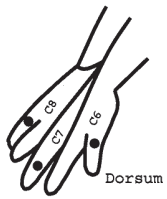

• Key Sensory Points

☐ (DAP) Deep anal pressure (yes/No)

☐ PIN PRICK SCORE (max: 112)

☐ LIGHT TOUCH SCORE (max: 112)

NEUROLOGICAL LEVEL *The most caudal segment with normal function*

	R	L
SENSORY	☐	☐
MOTOR	☐	☐

SINGLE NEUROLOGICAL LEVEL ☐

COMPLETE OR INCOMPLETE? ☐
Incomplete = Any sensory or motor function in S4-S5

ASIA IMPAIRMENT SCALE (AIS) ☐

(In complete injuries only)
ZONE OF PARTIAL PRESERVATION
Most caudal level with any innervation

	R	L
SENSORY	☐	☐
MOTOR	☐	☐

REV 04/11

Muscle Function Grading

0 = total paralysis

1 = palpable or visible contraction

2 = active movement, full range of motion (ROM) with gravity eliminated

3 = active movement, full ROM against gravity

4 = active movement, full ROM against gravity and moderate resistance in a muscle specific position.

5 = (normal) active movement, full ROM against gravity and full resistance in a muscle specific position expected from an otherwise unimpaired peson.

5* = (normal) active movement, full ROM against gravity and sufficient resistance to be considered normal if identified inhibiting factors (i.e. pain, disuse) were not present.

NT= not testable (i.e. due to immobilization, severe pain such that the patient cannot be graded, amputation of limb, or contracture of >50% of the range of motion).

ASIA Impairment (AIS) Scale

☐ **A = Complete.** No sensory or motor function is preserved in the sacral segments S4-S5.

☐ **B = Sensory Incomplete.** Sensory but not motor function is preserved below the neurological level and includes the sacral segments S4-S5 (light touch, pin prick at S4-S5: or deep anal pressure (DAP)), AND no motor function is preserved more than three levels below the motor level on either side of the body.

☐ **C = Motor Incomplete.** Motor function is preserved below the neurological level**, and more than half of key muscle functions below the single neurological level of injury (NLI) have a muscle grade less than 3 (Grades 0-2).

☐ **D = Motor Incomplete.** Motor function is preserved below the neurological level**, and <u>at least half</u> (half or more) of key muscle functions below the NLI have a muscle grade $\geq$ 3.

☐ **E = Normal.** If sensation and motor function as tested with the ISNCSCI are graded as normal in all segments, and the patient had prior deficits, then the AIS grade is E. Someone without an initial SCI does not receive an AIS grade.

**For an individual to receive a grade of C or D, i.e. motor incomplete status, they must have either (1) voluntary anal sphincter contraction or (2) sacral sensory sparing <u>with</u> sparing of motor function more than three levels below the motor level for that side of the body. The Standards at this time allows even non-key muscle function more than 3 levels below the motor level to be used in determining motor incomplete status (AIS B versus C).

NOTE: When assessing the extent of motor sparing below the level for distinguishing between AIS B and C, the ***motor level*** on each side is used; whereas to differentiate between AIS C and D (based on proportion of key muscle functions with strength grade 3 or greater) the ***single neurological level*** is used.

Steps in Classification

The following order is recommended in determining the classification of individuals with SCI.

1. Determine sensory levels for right and left sides.
2. Determine motor levels for right and left sides.
   Note: in regions where there is no myotome to test, the motor level is presumed to be the same as the sensory level, if testable motor function above that level is also normal.
3. Determine the single neurological level.
   This is the lowest segment where motor and sensory function is normal on both sides, and is the most cephalad of the sensory and motor levels determined in steps 1 and 2.
4. Determine whether the injury is Complete or Incomplete. (i.e. absence or presence of sacral sparing)
   If voluntary anal contraction = **No** *AND all S4-5 sensory scores =* **0** *AND deep anal pressure =* **No,** *then injury is COMPLETE. Otherwise, injury is incomplete.*
5. Determine ASIA Impairment Scale (AIS) Grade:

Is injury <u>Complete?</u> If **YES,** AIS=A and can record ZPP (lowest dermatome or myotome on each side with some preservation)

NO ↓

Is injury motor <u>Incomplete?</u> If **NO**, AIS=B (Yes=voluntary anal contraction OR motor function more than three levels below the motor level on a given side, if the patient has sensory incomplete classification)

YES ↓

Are <u>at least</u> half of the key muscles below the single <u>neurological</u> level graded 3 or better?

NO ↓ AIS=C

YES ↓ AIS=D

If sensation and motor function is normal in all segments, AIS=E
Note: AIS E is used in follow-up testing when an individual with a documented SCI has recovered normal function. If at initial testing no deficits are found, the individual is neurologically intact; the ASIA Impairment Scale does not apply.

BIBLIOGRAPHY

[1] G. Alon, C. Kantor, and H. Ho. "Effects of electrode size on basic excitatory responses and on selected stimulus parameters." In: *J Orthop Sports Phys Ther.* 20 (1994), pp. 29–35.

[2] K. Alonso, E. Azevedo, F. Beinotti, R. Maria, and A. Cliquet. "Electromyographic assessment of the tetraplegic upper limb during functional movement". In: *Journal of the Neurological Sciences, Elsevier* 333 (2008), e564–e564.

[3] J. Araújo, R. Rodrigues, R. Azevedo, B. Silva, R. Pinto, M. Vaz, and B. Baroni. "Inter-machine reliability of the Biodex and Cybex isokinetic dynamometers for knee flexor/extensor isometric, concentric and eccentric tests". In: *Phys Ther Sport.* 15 (2014), pp. 131–216.

[4] T. Araújo, N. Nunes, and H. Gamboa. "Miniaturized Wireless Controlled Electrostimulator." In: *In Proceedings of Biodevices - International Conference on Biomedical Electronics and Devices, Vilamoura, Portugal.* (2012).

[5] T. Araújo, N. Nunes, H. Gamboa, and A. Fred. "Distance-based algorithm for biometric applications in meanwaves of subject's heartbeats". In: *Proceedings of International Special Session on Biometrics: Technologies, Systems and Applications*. BTSA 2013. Barcelona, Spain, 2013.

[6] T. Araújo, A. Brandão, T. Didier, B. Bracco, H. Gamboa, and A. Cliquet. "Analysis of descriptive electrophysiological parameters in contralateral interlimb reflexes on tetraplegic patients." In: *Spinal Cord, Nature* advanced online publication 7 October 2014; doi: 10.1038/sc.2014.169. (2014).

[7] T. Araújo, A. Brandão, T. Didier, B. Bracco, H. Gamboa, and A. Cliquet. "Analysis of Inter-Subjects Variability of Contralateral Interlimb Electrophysiological Reflexes." In: *In Proceedings of American Spinal Injury Association Annual Meeting (ASIA 2014)*. San Antonio, Texas, United States of America, 2014.

[8] T. Araújo, N. Nunes, H. Gamboa, and A. Fred. *Generic biometry algorithm based on signal morphology information: application in the electrocardiogram signal*. Maria De Marsico and Ana Fred (Eds): PATTERN RECOGNITION APPLICATIONS AND METHODS. Vol. 318. Springer-Verlag, 2014.

[9] T. Araújo, A. Anjos, N. Nunes, P. Rebelo, and H. Gamboa. "Quadriceps muscle fatigue and comfort generated by neuromuscular electrical stimulation with current modulated waveforms". In: *Proceedings of Biosignals – International Conference on Bio-Inspired Systems and Signal Processing*. BIOSTEC 15. Lisbon, Portugal, 2015.

[10] Z. Ashley, H. Sutherland, H. Lanmuller, E. Unger, F. Li, W. Mayr, H. Kern, J. Jarvis, and S. Salmons. "Determination of the Chronaxie and Rheobase of Denervated Limb Muscles in Conscious Rabbits". In: *Artificial Organs* 29(3) (2005), p. 212.

[11] Atmel Corporation. *XMEGA A MANUAL*. 2012. URL: `http://www.atmel.com/Images/doc8077.pdf`.

[12] T Bajd, A Kralj, M Stefancic, and N Lavrac. "Use of functional electrical stimulation in the lower extremities of incomplete spinal cord injured patients." In: *Artificial Organs* 23.5 (1999), pp. 403–409. URL: `http://www.ncbi.nlm.nih.gov/pubmed/10378929`.

[13] B. A. Baker, K. M. Rao, R. R. Mercer, K. B. Geronilla, M. L. Kashon, G. R. Miller, and R. G. Cutlip. "Quantitative histology and MGF gene expression in rats following SSC exercise in vivo". In: *Med Sci Sports Exerc* 38.3 (2006), pp. 463–471.

[14] C. Baker, D. Wederich, C. McNeal, R. Newsam, and R. Waters. *Neuromuscular Electrical Stimulation: A Practical Guide.* 4th edition. Downey, CA: Los Amigos Research & Education Institute; 2000. Guidelines for adjustment of stimulation parameters., 2000.

[15] L. Baker, B. Bowman, and D. McNeal. "Effects of waveform on comfort during neuromuscular electrical stimulation." In: *Clin Orthop.* 233 (1988), 75–85.

[16] L. Baker, D. McNeal, L. Benton, B. Bowman, and R. Waters. "Neuromuscular electrical Stimulation – A Practical Conical Guide." In: *Rancho Rehabilitation Engineering Program, 3rd Edition.* (1993).

[17] P. Banerjee, B. Caulfield, L. Crowe, and A. Clark. "Prolonged electrical muscle stimulation exercise improves strength and aerobic capacity in healthy sedentary adults". In: *J. Appl. Physiol.* 99.6 (2005), pp. 2307–2311.

[18] W. Becker, L. Kleinsmith, J. Hardin, and G. Bertoni. *Signal Transduction Mechanisms: I. Electrical and Synaptic Signaling in Neurons. The world of the cell.* 7th edition. San Francisco: Pearson/Benjamin Cummings, 2009.

[19] S. Bennie, J. Petrofsky, J. Nisperos, M. Tsurudome, and M. Laymon. "Toward the optimal waveform for electrical stimulation of human muscle". In: *Eur. J. Appl. Physiol.* 88 (2002), pp. 13–19.

[20] C. Bergamini, S. Gambetti, A. Dondi, and C. Cervellati. "Oxygen, reactive oxygen species and tissue damage." In: *Current Pharmaceutical Design.* 10 (2004), pp. 1611–1626.

[21] N. Bhadra and P. Peckham. "Peripheral nerve stimulation for restoration of motor function." In: *J Clin Neurophysiol.* 14(5) (1997), 378–393.

[22] S. Binder-Macleod and L. Snyder-Mackler. "Muscle fatigue: clinical implications for fatigue assessment and neuromuscular electrical stimulation". In: *Phys Ther.* 73 (1993), pp. 902–910.

[23] S. Binder-Macleod, E. Halden, and K. Jungles. "Effects of stimulation intensity on the physiological responses of human motor units". In: *Med Sci Sports Exerc.* 27 (1995), pp. 556–565.

[24] BIODEX. *Biodex website*. 2014. URL: `http://www.biodex.com/`.

[25] R. Bogey and G. Hornby. "Gait training strategies utilized in poststroke rehabilitation: are we really making a difference?" In: *Top Stroke Rehabil.* 14(6) (2007), 1–8.

[26] V. Bolfe, S. Ribas, M. Montebelo, and R. Guirro. "Comportamento da impedância eléctrica dos tecidos biológicos durante a estimulação eléctrica transcutânea." pt. In: *Brazilian Journal of Physical Therapy* 11 (Apr. 2007), pp. 153 –159. ISSN: 1413-3555. URL: `http://www.scielo.br/scielo.php?script=sci_arttext&pid=S1413-35552007000200011&nrm=iso`.

[27] M. Bonner, J. Mortimer, and M Daroux. "Effect of pulsewidth and delay on stimulating electrode charge injection in-vitro." In: *Proc. Annu. Int. Conf. IEEE Eng. Med. Biol.* 12 (1990), pp. 1482–1483.

[28] W. Boucsein. *Electrodermal Activity.* 2nd. Elsevier, 2012.

[29] A. Bracciano. *Physical Agent Modalities.* Bethesda, MD: AOTA Press, 2008.

[30] K. Bray, D. Newgreen, R. Small, J. Southerton, S. Taylor, S. Weir, and A. Weston. "Evidence that the mechanism of the inhibitory action of pinacidil in rat and guinea-pig smooth muscle differs from that of glyceryl trinitrate." In: *Br. J. Pharmacol.* (1987), pp. 421–429.

[31] P. Breen, G. Corley, D. O'Keeffe, R. Conway, and G. Ólaighin. "A programmable and portable NMES device for drop foot correction and blood flow assist applications." In: *Medical Engineering & Physics* 31 (2009), pp. 400–408.

[32] B. Broderick, P. Breen, and G. ÓLaighin. "Electronic stimulators for surface neural prosthesis." In: *Journal of Automatic Control* 18 (2 2008), pp. 25–33.

[33] J. Burridge, I. Swain, and P. Taylor. "Functional electrical stimulation: a review of the literature published on common peroneal nerve stimulation for the correction of dropped foot." In: *Reviews in Clinical Gerontology* 8 (1998), pp. 155–161.

[34] B. Calancie. "Interlimb reflexes following cervical spinal cord injury in man." In: *Experimental brain research* 85(2) (1991), pp. 458–469.

[35] B. Calancie, S. Lutton, and J. Broton. "Central nervous system plasticity after spinal cord injury in man: interlimb reflexes and the influence of cutaneous stimulation." In: *Electroencephalography and Clinical Neurophysiology / Electromyography and Motor Control* 101(4) (1996), pp. 304–315.

[36] B. Calancie, M. Molano, and J. Broton. "Interlimb reflexes and synaptic plasticity become evident months after human spinal cord injury." In: *Brain* 125(5) (2002), pp. 1150–1161.

[37] B. Calancie, N. Alexeeva, J. Broton, and M. Molano. "Interlimb reflex activity after spinal cord injury in man: strengthening response patterns are consistent with ongoing synaptic plasticity." In: *Clinical Neurophysiology* 116(1) (2005), pp. 75–86.

[38] M. Camara, M. Carvalho, T. Araújo, H. Gamboa, and C. Quintão. "Coherence and Phase Locking Disruption in Electromyograms of Patients with Amyotrophic Lateral Sclerosis". In: *Proceedings of Biosignals – International Conference on Bio-Inspired Systems and Signal Processing*. BIOSTEC 2014. Paris, France, 2014.

[39] N. Cambridge. "Electrical apparatus used in medicine before 1900". In: *Proc R Soc Med.* 70 (9) (1997), 635–641.

[40] R. Canaipa, R. Treister, J. Moreira, and A. Castro-Caldas. "Feeling hurt: pain sensitivity is correlated with and modulated by social rejection". In: *submitted* (2014).

[41] R. Candeias, T. Araújo, N. Nunes, and H. Gamboa. "Evaluation of motor neuron excitability by CMAP scanning with modulated current". In: *Proceedings of Biosignals – International Conference on Bio-Inspired Systems and Signal Processing*. BIOSTEC 15. Lisbon, Portugal, 2015.

[42] M. Carvalho, A. Chio, R. Dengler, M. Hecht, M. Weber, and M. Swash. "Neurophysiological measures in amyotrophic lateral sclerosis: markers of progression in clinical trials." In: *Muscle & Nerve* 34 (2012), pp. 34–43.

[43] M. Chan, R. Tong, and K. Chung. "Bilateral upper limb training with functional electric stimulation in patients with chronic stroke." In: *Neurorehabil Neural Repair.* 23(4) (2009), p. 357.

[44] K. Cheng, L. Yan, T. Kai-Yu, A. Rad, D. Chow, and D. Sutanto. "Development of a circuit for functional electrical stimulation." In: *IEEE Transactions on Neural Systems and Rehabilitation Engineering* 12 (2004), pp. 43–47.

[45] G. Clifford and L. Tarassenko. "Signal Processing methods for Heart Rate Variability". In: *Department of Engineering Science, University of Oxford* (2002).

[46] N. Costa, T. Araújo, N. Nunes, and H. Gamboa. "Knowledge Acquisition System based on JSON Schema - Implementation of a HCI for Actuation of Biosignals Acquisition Systems". In: *SIGMAP*. 2012, pp. 255–262.

[47] N. Costa, T. Araújo, N. Nunes, and H. Gamboa. "Multi-purpose Electrostimulator Software." In: *Biodevices - International Conference on Biomedical Electronics and Devices (BIOSTEC 2013), Barcelona, Spain*. 2013.

[48] T. Davis and D. Durlin. *Bootloaders 101: making your embedded design future proof.* 2013. URL: http://www.embedded.com/design/prototyping-and-development/4410233/Bootloaders-101--making-your-embedded-design-future-proof.

[49] P. Dehail, C. Duclos, and M. Barat. "Electrical stimulation and muscle strengthening". In: *Annales de Readaptation et de Medecine Physique, Science Direct* 51 (2008), pp. 441–451.

[50] J. DeKroon, M. IJzerman, J. Chae, G. Lankhorst, and G. Zilvold. "Relation between stimulation characteristics and clinical outcome in studies using electrical stimulation to improve motor control of the upper extremity in stroke." In: *J Rehabil Med.* 37(2) (2005), 65–74.

[51] A. Delitto and S. J. Rose. "Comparative Comfort of Three Waveforms Used in Electrically Eliciting Quadriceps Femoris Muscle Contractions". In: *Physical Therapy* 66.11 (1986), pp. 1704–1707. eprint: http://ptjournal.apta.org/content/66/11/1704.full.pdf+html. URL: http://ptjournal.apta.org/content/66/11/1704.abstract.

[52] R. Deyo, N. Walsh, D. Martin, L. Schoenfeld, and S. Ramamurthy. "A controlled trial of transcutaneous electrical nerve stimulation (TENS) and exercise for chronic low back pain." In: *New Engl J Med.* 322(23) (1990), 1627–1634.

[53] M. Dimitrijevic. "Clinical practice of functional electrical stimulation: from 'Yesterday' to 'Today'." In: *Artif Organs.* 32(8) (2008), pp. 577–580.

[54] B. Dominik, F. Guillaume, K. Friston, and R. Dolan. "Modulating event-related skin responses". In: *University College London, United Kingdom* (2010).

[55] D. Doucet, A. Lam, and L. Griffin. "Neuromuscular electrical stimulation for skeletal muscle function". In: *Yale J Bio Med.* 85 (2012), pp. 201–215.

[56] D. Durand. *Electric Stimulation of Excitable Tissue.* 2nd edition. The Biomedical Engineering Handbook. Ed. Joseph D. Bronzino Boca Raton: CRC Press LLC, 2000.

[57] P. Eser, N. Donaldson, H. Knecht, and E. Stussi. "Influence of different stimulation frequencies on power output and fatigue during FES-cycling in recently injured SCI people." In: *IEEE Trans Neural Syst Rehabil Eng.* 11(3) (2003), pp. 236–240.

[58] H. Gamboa, R. Matias, T. Araújo, and A. Veloso. "Electromyography onset detection: new methodology". In: *Journal of Biomechanics* 45(1) (2012), S494.

[59] L. Geddes. "Accuracy limitations of chronaxie values". In: *IEEE Transactions on Biomedical Engineering* 51(1) (2004).

[60] H. Gerrits, M. Hopman, C. Offringa, B. Engelen, A. Sargeant, D. Jones, and A. Haan. "Variability in fibre properties in paralysed human quadriceps muscles and effects of training". In: *Pflugers Arch* 443 (2003), pp. 734–740.

[61] J. Glinsky, L. Harvey, and E. Van. "Efficacy of electrical stimulation to increase muscle strength in people with neurological conditions: a systematic review". In: *Physiotherapy Research International* 12 (2007), pp. 175–194.

[62] J. Gondin, P. Cozzone, and D. Bendahan. "Is high-frequency neuromuscular electrical stimulation a suitable tool for muscle performance improvement in both healthy humans and athletes?" In: *Eur J Appl Physiol.* 111(10) (2011), 2473–2487.

[63] A. Gorgey and G. Dudley. "The role of pulse duration and stimulation duration in maximizing the normalized torque during neuromuscular electrical stimulation". In: *J Orthop Sports Phys Ther.* 38 (2008), pp. 508–516.

[64] A. Gorgey, E. Mahoney, T. Kendall, and G. Dudley. "Effects of neuromuscular electrical stimulation parameters on specific tension". In: *Eur J Appl Physiol.* 97 (2006), pp. 737–744.

[65] A. Gorgey, C. Black, C. Elder, and G. Dudley. "Effects of electrical parameters on fatigue in skeletal muscle". In: *J Orthop Sports* 39(9) (2009), pp. 684–692.

[66] F. Gracanin and A. Trnkoczy. "Optimal stimulus parameters for minimum pain in the chronic stimulation of innervated muscle." In: *Arch Phys Med Rehabil.* 56(6) (1975), 243–249.

[67] W. Grill and J. Mortimer. "The effect of stimulus pulse duration on selectivity of neural stimulation." In: *IEEE Trans Biomed Eng.* 43(2) (1996), pp. 161–166.

[68] A. Guyton and J. Hall. "Textbook of Medical Physiology." In: *Philadelphia, Pennsylvania, Elsevier Inc* (2006).

[69] B. Halliwell. "Reactive Oxygen species and the central nervous system". In: *Journal of Neurochemistry* 59 (2006), pp. 1609–1623.

[70] S. Hamid and R. Hayek. "Role of electrical stimulation for rehabilitation and regeneration after spinal cord injury: an overview." In: *Eur Spine J.* 17(9) (2008), 1256–1269.

[71] K. Hardy, K. Suever, A. Sprague, V. Hermann, P. Levine, and S. Page. "Combined Bracing, Electrical Stimulation, and Functional Practice for Chronic, Upper-Extremity Spasticity." In: *Am J Occup Ther.* 64(5) (2010), 720–726.

[72] C. Haridas and E. Zehr. "Coordinated interlimb compensatory responses to electrical stimulation of cutaneous nerves in the hand and foot during walking." In: *Journal of Neurophisiology* 90(5) (2003), pp. 2850–2861.

[73] C. Haridas, E. Zehr, and J. Misiaszek. "Context-dependent modulation of interlimb cutaneous reflexes in arm muscles as a function of stability threat during walking." In: *Journal of Neurophisiology* 96(6) (2006), pp. 3096–3103.

[74] R. Hart, K. Kilgore, and P. Peckham. "A comparison between control methods for implanted FES hand-grasp systems". In: *Rehabilitation Engineering, IEEE Transactions on* 6.2 (Jun), pp. 208–218. ISSN: 1063-6528. DOI: 10.1109/86.681187.

[75] T. Hemnani and M. Parihar. "Reactive oxygen species and oxidative DNA damage." In: *Indian Journal of Physiology and Pharmacology* 42 (1998), p. 440.

[76] R. Henderson, A. Ridall GR. Pettitt, P. McCombe, and J. Daube. "The stimulus-response curve and motor unit variability in normal subjects and subjects with amyotrophic lateral sclerosis." In: *Muscle & Nerve* 34 (2012), pp. 34–43.

[77] H. Hermens, B. Freriks, R. Merletti, G. Hagg, D. Stegeman, and J. Blok. "SENIAM 8: European recommendations for surface electromyography". In: *ISBN: 90-75452-15-2: Roessingh Research and Development bv* (1999).

[78] B. Hille. *Ionic channels of excitable membranes.* Sunderland, Massachusetts: Sinauer Associates Inc., 2009.

[79] A. Hodgkin and A. Huxley. "A quantitative description of membrane current and its application to conduction and excitation in nerve". In: *Journal of Physiology* 117 (1952), pp. 500–544.

[80] A. Holzinger and H. Leitner. "Lessons from real-life usability engineering in hospital: from software usability to total workplace usability." In: *Empowering Software Quality: How can Usability Engineering reach these goals.* (2005), pp. 153–160.

[81] J. Hunter and D. Dale. *The matplotlib tutorial*. 2002. URL: http://matplotlib.org/mpl_toolkits/mplot3d/tutorial.html.

[82] J. Imlay. "Pathways of oxidative damage". In: *Annual Reviews in Microbiology* 57 (2003), pp. 395–418.

[83] T. Janssen, M. Bakker, A. Wyngaert, K. Gerrits, and H. A. "Effects of stimulation pattern on electrical stimulation-induced leg cycling performance." In: *Artif Organs.* 29(6) (2005), pp. 453–458.

[84] S. Jezernik and M. Morari. "Energy-Optimal Electrical Excitation of Nerve Fibers". In: *IEEE Transactions on Biomedical Engineering* 52(4) (2010).

[85] S. Jezernik and T. Sinkjaer. "Finite Element Modeling Validation of Energy-Optimal Electrical Stimulation Waveform". In: *10th Annual Conference of the International FES Society, July 2005, Montreal, Canada* (2005).

[86] S. Jezernik, T. Sinkjaer, and M. Morari. "Charge and energy minimization in electrical/magnetic stimulation of nervous tissue". In: *J. Neural Eng* 7(4) (2010).

[87] M. Johnson. "Transcutaneous electrical nerve stimulation - review of effectiveness". In: *Art and Science, pain management* 28 (2014), pp. 44–53.

[88] L. Jones and M. Johnson. "Transcutaneous electrical nerve stimulation. Continuing Education in Anaesthesia." In: *Critical Care and Pain* 9 (2009), pp. 130–135. ISSN: 4.

[89] E. Kandel, J. Schwarts, T. Jessel, S. Siegelbaum, and A. Hudspeth. *Principles of Neural Science*. 5th edition. McGraw-Hill Professional, 2012.

[90] J. Kang and I. Hyong. "The Influence of Neuromuscular Electrical Stimulation on the Heart Rate Variability in Healthy Subjects." In: *J Phys Ther Sci.* 26(5) (2014), pp. 633–635.

[91] G. Kantor, G. Alon, and H. Ho. "The effects of selected stimulus waveforms on pulse and phase characteristics at sensory and motor thresholds". In: *Phys Ther.* 74 (1994), pp. 951–962.

[92] M. Kebaetse, A. Turner, and S. Binder-Macleod. "Effects of stimulation frequencies and patterns on performance of repetitive, nonisometric tasks." In: *J Appl Physiol.* 92(1) (2002), pp. 109–116.

[93] M. Kebaetse, S. Lee, T. Johnston, and S. Binder-Macleod. "Strategies that improve paralyzed human quadriceps femoris muscle performance during repetitive, nonisometric contractions." In: *Arch Phys Med Rehabil.* 86(11) (2005), pp. 2157–2164.

[94] T. Keller and A. Kuhn. "Electrodes for transcutaneous (surface) electrical stimulation." In: *Journal of Automatic Control* 18 (2008), pp. 35–45.

[95] P. Kersten. "The use of Visual Analogue Scale (VAS) in rehabilitation." In: *J Rehab Med.* 44 (2012), pp. 609–610.

[96] T. Kesar and S. Binder-Macleod. "Effect of frequency and pulse duration on human muscle fatigue during repetitive electrical stimulation." In: *Exp Physiol.* 91(6) (2006), pp. 967–976.

[97] S. Kirshblum, W. Waring, F. Biering-Sorensen, S. Burns, M. Johansen, and M. Schmidt-Read. "International Standards for Neurological Classification of Spinal Cord Injury (Revised 2011)." In: *J Spinal Cord Med* 34(6) (2011), pp. 547–554.

[98] S. Kitchen and S. Bazin. *Clayton's Electrotherapy*. 10th edition. London: WB Saunders., 1998.

[99] A. Kralj and T. Bajd. "Functional electrical stimulation: standing and walking after spinal cord injury." In: *Boca Raton, FL: CRC Press* (1989).

[100] M. Krenn, M. Haller, M. Bijak, E. Unger, C. Hofer, H. Kern, and W. Mayr. "Safe Neuromuscular Electrical Stimulator Designed for the Elderly". In: *Artificial Organs* 35 (2011), pp. 253–256.

[101] S. Kuffler and J. Nicholls. *From Neuron to Brain*. 2nd edition. Sinauer Associates, Incorporated, 1976.

[102] O. Lacey and P. Siegel. "An analysis of the unit of measurement of the galvanic skin response." In: *Journal of Experimental Psychology* 39(1) (1949), pp. 122–127.

[103] O. Lagerquist and D. Collins. "Influence of stimulus pulse width on M-waves, H-reflexes, and torque during tetanic low-intensity neuromuscular stimulation." In: *Muscle Nerve* 42(6) (2010), 886–893.

[104] D. A. Lake. "Neuromuscular electrical stimulation. An overview and its application in the treatment of sports injuries". In: *Sports Med* 13.5 (1992), pp. 320–336.

[105] E. Lamont and E. Zehr. "Earth-referenced handrail contact facilitates interlimb cutaneous reflexes during locomotion." In: *Journal of Neurophisiology* 98(1) (2007), pp. 2850–2861.

[106] Y Laufer, J. D. Ries, P. M. Leininger, and G Alon. "Quadriceps femoris muscle torques and fatigue generated by neuromuscular electrical stimulation with three different waveforms." In: *Phys Ther* 81.7 (2001), pp. 1307–16. ISSN: 0031-9023. URL: http://www.biomedsearch.com/nih/Quadriceps-femoris-muscle-torques-fatigue/11444994.html.

[107] W. Liberson, H. Holmquest, D. Scott, and M Dow. "Functional electrotherapy: stimulation of the peroneal nerve synchronized with the swing phase of the gait of hemiplegic patients". In: *Archives of physical medicine and rehabilitation* 42 (1961), pp. 202–205.

[108] R. Lieber and M. Kelly. "Torque history of electrically stimulated human quadriceps: implications for stimulation therapy". In: *J Orthop Res.* 11 (1993), pp. 131–141.

[109] L. Livshitz, J. Mizrahi, and P. Einziger. "Interaction of array of finite electrodes with layered biological tissue: effect of electrode size and configuration." In: *IEEE Trans Neural Syst Rehabil Eng.* 9(4) (2001), 355–361.

[110] A. Londral, J. Sousa, T. Araújo, and H. Silva. "Enhancing Interaction of Persons with Cerebral Palsy using Biosignals Detection". In: *Assistive Technology Research Series. Assistive Technology: From Research to Practice* (2013), pp. 1051–1055.

[111] G. Lyons, T. Sinkjær, J. Burridge, and D. Wilcox. "A review of the portable FES-based neural orthoses for the correction of drop foot." In: *IEEE Transactions on Neural Systems and Rehabilitation Engineering* 10 (2002), pp. 260–279.

[112] E. Maathuis, J. Drenthen, G. Visser, and J. Blok. "Reproducibility of the CMAP scan." In: *Journal of electromyography and kinesiology.* 21 (2011), pp. 433–437.

[113] E. Maathuis, R. Henderson, J. Drenthen, N. Hutchinson, J. Daube, J. Blok, and V. GH. "Optimal stimulation settings for CMAP scan registrations." In: *Journal of brachial plexus and peripheral nerve injury.* 7 (2012), p. 4.

[114] E. Maathuis, J. Drenthen, P. Van Doorn, G. Visser, and J. Blok. "The CMAP scan as a tool to monitor disease progression in ALS and PMA." In: *Amyotrophic lateral sclerosis and frontotemporal degeneration.* 1 (2012), pp. 1–7.

[115] N. Maffiuletti, M. Minetto, D. Farina, and R. Bottinelli. "Electrical stimulation for neuromuscular testing and training: state-of-the-art and unresolved issues". In: *European Journal of Applied Physiology* 111 (2011), pp. 2391–2397.

[116] N. Maffiuletti. "Physiological and methodological considerations for the use of neuromuscular electrical stimulation". In: *European Journal of Applied Physiology* 110 (2010), pp. 223–234.

[117] N. Maffiuletti, G. Cometti, I. Amiridis, A. Martin, M. Pousson, and J. Chatard. "The effects of electromyostimulation training and basketball practice on muscle strength and jumping ability". In: *International Journal of Sports Medicine* 21 (2000), pp. 437–443.

[118] N. Maffiuletti, N. Pensini, and A. Martin. "Activation of human plantar flexor muscles increases after electromyostimulation training." In: *J Appl Physiol.* 92(4) (2002), 1383–1392.

[119] S. Mangold, T. Keller, A. Curt, and V. Dietz. "Transcutaneous functional electrical stimulation for grasping in subjects with cervical spinal cord injury". In: *Spinal Cord.* 43(1) (2004), 1–13.

[120] F. Martini. *Fundamentals of Anatomy and Physiology*. 3rd. Pearson Education, 2004.

[121] F. Martini and E. Bartholomew. *Essentials of Anatomy and Physiology.* San Francisco: Benjamin Cummings., 2003.

[122] D. McCreery, W. Agnew, T. Yuen, and L. Bullara. "Charge density and charge per phase as cofactors in neural injury induced by electrical stimulation." In: *IEEE Trans Biomed Eng* 37 (1990), pp. 996–1001.

[123] P. A. McNulty, S. K. Jankelowitz, T. M. Wiendels, and D. Burke. "Postactivation depression of the soleus H reflex measured using threshold tracking". In: *J. Neurophysiol.* 100.6 (2008), pp. 3275–3284.

[124] P. McNulty and D. Burke. "Self-Sustained Motor Activity Triggered by Interlimb Reflexes in Chronic Spinal Cord Injury, Evidence of Functional Ascending Propriospinal Pathways." In: *PloS One* 8(8) (2013), e72725.

[125] P. Melo, J. Durigan, L. Urache, P. Silva, B. Lemos, J. Filho, V. Carvalho, T. Oliveira, G. Cipriano, and V. Silva. "The Measurement Of Chronaxie And Rheobase In Patients With Polineuromyopathy Of Critical Illness". In: *Critical Care: New care approaches* (2014).

[126] D. Merrill, M. Bikson, and J. R. "Electrical stimulation of excitable tissue: design of efficacious and safe protocols." In: *J Neurosci Methods* 141 (2005), pp. 171–198.

[127] L. Mesin, E. Merlo, R. Merletti, and C. Orizio. "Investigation of motor unit recruitment during stimulated contractions of tibialis anterior muscle." In: *J Electromyogr Kinesiol.* 20(4) (2010), 580–589.

[128] J. Millar and T. Barnett. "The Zeta pulse: a new stimulus waveform for use in electrical stimulation of the nervous system." In: *Journal of Neuroscience Methods* 77 (1997), pp. 1–8.

[129] J. Moe and H. Post. "Functional electrical stimulation for ambulation in hemiplegia." In: *The Lancet* 82 (1962), pp. 285–288.

[130] M. Mulla, F. Sepulveda, and M. Colley. "A review of non-invasive thecniques to detect and predict localized muscle fatigue." In: *Sensors* 11 (2011), pp. 3545–3594.

[131] R. H. Nathan. "Control strategies in FNS systems for the upper extremities". In: *Crit Rev Biomed Eng* 21.6 (1993), pp. 485–568.

[132] C. Newsam and L. Baker. "Effect of an electric stimulation facilitation program on quadriceps motor unit recruitment after stroke". In: *Archives of Physical Medicine and Rehabilitation* 85 (2004), pp. 2040–2045.

[133] T. Nosek. *Essentials of Human Physiology: A Multimedia Resource for Physiology and Anatomy.* Micron BioSystems, 1996.

[134] N. Nunes, F. Carnide, N. Batista, T. Araújo, G. Martins, F. Vieira, A. Veloso, and H. Gamboa. "Wireless Platform for Ergonomics Evaluation of Occupational Biomechanical Exposure". In: *Journal of Biomechanics* 45(1) (2012), S506.

[135] F. Offner and W. Liberson. *Method of muscular stimulation in human beings to aid in walking*. US Patent 3,344,792. 1965. URL: `http://www.google.com/patents/US3344792`.

[136] T. Oliphant. *Scipy Tutorial*. 2004. URL: `http://www.tau.ac.il/~kineret/amit/scipy_tutorial/`.

[137] T. Oliphant. *Guide to Numpy*. 2006. URL: `TregolPublishing`.

[138] PARASTEP. *Parastep System - Therapeutic Alliances Inc.* 2014. URL: `http://www.musclepower.com/parastep.htm`.

[139] G. Parry and J. Steinberg. "Guillain-Barr syndrome: from diagnosis to recovery." In: *Demos Medical Publishing* (2007).

[140] P. Peckham and J. Knutson. "Functional Electrical Stimulation for Neuromuscular Applications." In: *Annual Review of Biomedical Engineering* 7 (2005), pp. 327–360.

[141] D. Peters, I. A. Barash, M. Burdi, P. S. Yuan, L. Mathew, J. Friden, and R. L. Lieber. "Asynchronous functional, cellular and transcriptional changes after a bout of eccentric exercise in the rat". In: *J. Physiol. (Lond.)* 553.Pt 3 (2003), pp. 947–957.

[142] M. Piccolino. "Luigi Galvani and animal electricity: two centuries after the foundation of electrophysiology." In: *Trends Neurosci* 20.10 (1997), pp. 443–8.

[143] S. Piva, E. Goodnite, K. Azuma, J. Woollard, B. Goodpaster, and M. e. a. Wasko. "Neuromuscular electrical stimulation and volitional exercise for individuals with rheumatoid arthritis: A multiple-patient case report." In: *Phys Ther.* 87(8) (2007), 1064–1077.

[144] PLUX. *Biosignalsplux website*. 2014. URL: `http://www.biosignalsplux.com/`.

[145] PLUX. *Plux, Wireless Biosignals, SA*. 2014. URL: `www.plux.info`.

[146] D. Popovi, M. Radulovi, L. Schwirtlich, and N. Jaukovi. "Automatic vs hand-controlled walking of paraplegics". In: *Med Eng Phys* 25.1 (2003), pp. 63–73.

[147] D. Popovic, T. Sinkjær, and M. Popovic. "Electrical stimulation as a means for achieving recovery of function in stroke patients." In: *Neurorehabilitation* 25 (2009), pp. 45–58.

[148] J. Porcari, K. McLean, C. Foster, T. Kernozek, B. Crenshaw, and C. Swenson. "Effects of electrical muscle stimulation on body composition, muscle strength, and physical appearance." In: *J Strength Cond Res* 16(2) (2002), pp. 165–172.

[149] M. Prausnitz. "The effects of electric current applied to skin: A review for transdermal drug delivery." In: *Advanced Drug Delivery Reviews* 18 (1996), pp. 395–425.

[150] A. Prochazka, M. Gauthier, M. Wieler, and Z. Kenwell. "The bionic glove: an electrical stimulator garment that provides controlled grasp and hand opening in quadriplegia." In: *Archives of physical medicine and rehabilitation* 78 (6 1997), pp. 608–614.

[151] P. Rainville, G. Duncan, D. Price, B. Carrier, and M. Bushnell. "Pain affect encoded in human anterior cingulate but not somatosensory cortex". In: *Science* 277 (1997), pp. 968–971.

[152] B Reed. "The physiology of neuromuscular electrical stimulation." In: *Pediatric Physical Therapy* 9 (1997), pp. 96–102.

[153] R. Riener. "Model-based development of neuroprosthesis for paraplegic patients." In: *Philos Trans R Soc Lond B Biol Sci.* 354 (2011), pp. 877–894.

[154] V. Robertson, A. Ward, J. Low, and A. Reed. *Electrotherapy Explained: Principles and Practice*. 4th edition. Vol. 10. 2006, pp. 260–279.

[155] W. Rosellini, P. Yoo, N. Engineer, S. Armstrong, R. Weiner, C. Burress, and L. Cauller. "Voltage Controlled Capacitive Discharge Method for Electrical Activation of Peripheral Nerves." In: *Neuromodulation: Technology at the Neural Interface* 146 (2011), pp. 493–500.

[156] K. Ross. *The Basics - Microcontrollers (part 1). Encoder, The Newsletter of the Seattle Robotics Society.* 2013. URL: `http://www.seattlerobotics.org/encoder/sep97/basics.html`.

[157] S. Sabut, C. Sikdar, R. Mondal, R. Kumar, and M. Mahadevappa. "Restoration of gait and motor recovery by functional electrical stimulation therapy in persons with stroke." In: *Disabil Rehabil.* 32(19) (2010), 1594–1603.

[158] M. Sahin and Y. Tie. "Non-rectangular waveforms for neural stimulation with practical electrodes". In: *J. Neural Eng.* 4 (2007), pp. 227–233.

[159] M. Sakamoto, T. Endoh, T. Nakajima, T. Tazoe, S. Shiozawa, and T. Komiyama. "Modulations of interlimb and intralimb cutaneous reflexes during simultaneous arm and leg cycling in humans." In: *Clinical Neurophysiology* 117(6) (2006), pp. 1301–1311.

[160] D. Sarddar, M. Kumar, and K. SS. "Functional Electrical Stimulation using PIC Microcontroller." In: *International Journal of Computer Applications* 44 (2012), pp. 31–35.

[161] N. Sha, L. Kenney, B. Heller, A. Barker, D. Howard, and M. Moatamedi. "A finite element model to identify electrode influence on current distribution in the skin." In: *Artif Organs.* 32(8) (2008), 639–643.

[162] A. Shariat, P. Horan, K. Gratenstein, C McCally, and A. Frulla. "Electrical Nerve Stimulators and Localization of Peripheral Nerves". In: *Regional Anesthesia* (2013). URL: http://www.nysora.com/regional-anesthesia/3010-electrical-nerve-stimulators-and-localization-of-peripheral-nerves.html.

[163] L. Sheffler and J. Chae. "Neuromuscular electrical stimulation in neurorehabilitation". In: *Muscle & Nerve* 35 (2007), pp. 562–590.

[164] A. Shetter, G. Racz, R. Lewis, and J. Heavner. *Peripheral Nerve Stimulation, Neurosurgical Management of Pain.* Springer New York, 1997, pp. 261–270.

[165] S. Simcox, G. Davis, A. Barriskill, J. Middleton, I. Bruinsma, M. Duncan, and R. Smith. "A portable, 8-channel transcutaneous stimulator for paraplegic muscle training and mobility–a technical note". In: *Journal of Rehabilitation Research and Development* 41 (2004), pp. 41–51.

[166] T. Sinkjær and D. Popovic. "Neurorehabilitation Technologies – Present and Future Possibilities". In: *Neurorehabilitation* 25 (2009), pp. 1–3.

[167] J. Slade, C. Bickel, G. Warren, and G. Dudley. "Variable frequency trains enhance torque independent of stimulation amplitude". In: *Acta Physiol Scand.* 177 (2003), pp. 87–92.

[168] K. Sluka and D. Walsh. "Transcutaneous electrical nerve stimulation: basic science mechanisms and clinical effectiveness." In: *J Pain.* 4(3) (2003), 109–121.

[169] J. Smans, H. Korsten, J. Blom, and V. Dietz. "Optimal surface electrode positioning for reliable train of four muscle relaxation monitoring." In: *Int J Clin Monit Comput.* 13(1) (1996), 9–20.

[170] L. Snyder-Mackler, A. Delitto, S. Stralka, and S. Bailey. "Use of electrical stimulation to enhance recovery of quadriceps femoris muscle force production in patients following anterior cruciate ligament reconstruction". In: *Physical Therapy* 74 (1994), pp. 901–907.

[171] M. Solomonow, E. Aguilar, E. Reisin, R. V. Baratta, R. Best, T. Coetzee, and R. D'Ambrosia. "Reciprocating gait orthosis powered with electrical muscle stimulation (RGO II). Part I: Performance evaluation of 70 paraplegic patients". In: *Orthopedics* 20.4 (1997), pp. 315–324.

[172] SPES MEDICA. *Spes medica - the medical accessories source*. 2014. URL: http://www.spesmedica.com/br/.

[173] N. Spielholz and M. Nolan. "Conventional TENS and the phenomena of accommodation, adaptation, habituation and electrode polarization." In: *J ClinElectrophysiol.* 7 (1995), pp. 16–19.

[174] S. Stackhouse, S. Binder-Macleod, C. Stackhouse, J. McCarthy, L. Prosser, and S. Lee. "Neuro-muscular electrical stimulation versus volitional isometric strength training in children with spastic diplegic cerebral palsy: a preliminary study". In: *Neurorehabilitation and Neural Repair* 21(6) (2007), pp. 475–485.

[175] J. Stevens-Lapsley, J. Balter, P. Wolfe, D. Eckhoff, and W. Kohrt. "Early neuromuscular electrical stimulation to improve quadriceps muscle strength after total knee arthroplasty: a randomized controlled trial." In: *Phys Ther.* 92(2) (2012), 210–226.

[176] S. Stohs. "The role of free radicals in toxicity and disease." In: *Journal of Basic and Clinical Physiology and Pharmacology* 6 (2001), pp. 205–228.

[177] O. Sujith. "Functional electrical stimulation in neurological disorders." In: *Eur J Neurol* 15(5) (2008), pp. 437–444.

[178] B. Suter, T. O'Connor, V. Iyer, L. Petreanu, B. Hooks, T. Kiritani, K. Svoboda, and G. Shepherd. "Ephus: multipurpose data acquisition software for neuroscience experiments." In: *Frontiers in Neural Circuits* 4 (2010), p. 100.

[179] J. Szecsi, C. Fornusek, P. Krause, and A. Straube. "Low-frequency rectangular pulse is superior to middle frequency alternating current stimulation in cycling of people with spinal cord injury." In: *Arch Phys Med Rehabil.* 88(3) (2007), pp. 338–345.

[180] I. Tarkka and M. Kononen. "Methods to improve constraint-induced movement therapy." In: *NeuroRehabilitation* 25(1) (2009), pp. 59–68.

[181] R. Thorsen and M. Ferrarin. "Battery powered neuromuscular stimulator circuit for use during simultaneous recording of myoelectric signals". In: *Medical Engineering & Physics* 31 (2009), pp. 1032–1037.

[182] A. Thrasher, G. Graham, and M. Popovic. "Reducing muscle fatigue due to functional electrical stimulation using random modulation of stimulation parameters." In: *Artif Organs.* 29(6) (2005), pp. 453–458.

[183] T. Thrasher and M. Popovic. "Functional electrical stimulation of walking: Function, exercise and rehabilitation". In: *Annales de Readaptation et de Medecine Physique* 51.6 (2008), pp. 452 –460. ISSN: 0168-6054. DOI: 10.1016/j.annrmp.2008.05.006.

[184] A. Uranga, J. Sacristan, T. Oses, and N. Barniol. "Electrode-Tissue Impedance Measurement CMOS ASIC for Functional Electrical Stimulation Neuroprostheses." In: *IEEE Transactions on Instrumentation and Measurement* 56 (2007), pp. 2043–2050.

[185] F. Valenti. "Neuromuscular electrical stimulation in clinical practice." In: *Acta Anaesthesiol.* 15 (1964), 227–245.

[186] G. Van Rossum. *The Python Language Reference Manual*. 2003. URL: https://docs.python.org/2/reference/.LastupdatedonMar13,2015..

[187] M. Vanderthommen, S. Duteil, C. Wary, J. Raynaud, A. Leroy-Willig, J. Crielaard, and et al. "A comparison of voluntary and electrically induced contractions by interleaved 1H- and 31P-NMRS in humans." In: *J Appl Physiol.* 94 (2003), pp. 1012–1024.

[188] Z. Visnovcova, A. Calvoska, and I. Tonhajzerova. "Heart rate variability and electrodermal activity as noninvasive indices of sympathovagal balance in response to stress". In: *Comenius University, Slovak Republic.* (2013).

[189] A. Vuckovic. "Selective nerve fiber activation by anodal block. Experimental and simulation studies on charge reduction and chronic stability." In: *PhD Thesis, Center for Sensory Motor Interaction, Aalborg University, Denmark* (2004).

[190] M. Wewers and N. Lowe. "A critical review of visual analogue scales in the measurement of clinical phenomena". In: *Research in Nursing and Health* (1990), pp. 227–236.

[191] K. Wiech, M. Farias, G. Kahane, N. Shackel, W. Tiede, and I. Tracey. "An fMRI study measuring analgesia enhanced by religion as a belief system." In: *Pain* 139 (2008), pp. 467–476.

[192] Wikipedia. *Cyclic redundancy check*. 2014. URL: http://en.wikipedia.org/wiki/Cyclic_redundancy_check.

[193] H. Wu, S. Young, and T. Kuo. "A versatile multichannel direct-synthesized electrical stimulator for FES applications." In: *IEEE Transactions on Instrumentation and Measurement* 51 (2002), pp. 2–9.

[194] T. Yuen, W. Agnes, L. Bullara, S. Jacques, and D. McCreery. "Histological evaluation of neural damage from electrical stimulation: considerations for the selection of parameters for clinical application." In: *Neurosurgery* 9 (1981), pp. 292–299.

[195] P. Zehr, D. Collins, and R. Chua. "Human interlimb reflexes evoked by electrical stimulation of cutaneous nerves innervating the hand and foot." In: *Experimental brain research* 140(4) (2001), pp. 495–504.

[196] D. Zhang, T. H. Guan, F. Widjaja, and W. T. Ang. "Functional electrical stimulation in rehabilitation engineering: a survey". In: *Proceedings of the 1st international convention on Rehabilitation engineering and assistive technology: in conjunction with 1st Tan Tock Seng Hospital Neurorehabilitation Meeting*. i-CREATe 07. Singapore: ACM, 2007, pp. 221–226. ISBN: 978-1-59593-852-7. DOI: 10.1145/1328491.1328546.

[197] K. Zyp. *A JSON Media Type for Describing the Structure and Meaning of JSON Documents*. 2011. URL: http://tools.ietf.org/id/draft-zyp-json-schema-00.html.